



PB99-163180

Summary Report of Research on
Permanent Ground Anchor Walls,
Volume I: Current Practice and
Limiting Equilibrium Analyses

PUBLICATION NO. FHWA-RD-98-065

SEPTEMBER 1998



U.S. Department of Transportation
Federal Highway Administration

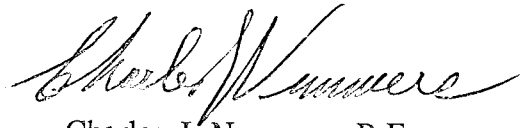
Research and Development
Turner-Fairbank Highway Research Center
6300 Georgetown Pike
McLean, VA 22101-2296

REPRODUCED BY: **NTIS**
U.S. Department of Commerce
National Technical Information Service
Springfield, Virginia 22161



FOREWORD

This report is part of a four-volume series which summarizes a comprehensive study on permanent ground anchor walls. Volume I (FHWA-RD-98-065) discusses current practice and limiting equilibrium analyses. Volume II (FHWA-RD-98-066) presents results of full-scale wall tests and a soil-structure interaction model. Volume III (FHWA-RD-98-067) covers model-scale wall tests and ground anchor tests. Volume IV (FHWA-RD-98-068) summarizes the first three volumes and presents conclusions and recommendations.



Charles J. Nemmers, P.E.
Office of Engineering
Research and Development


NOTICE

This document is disseminated under the sponsorship of the Department of Transportation in the interest of information exchange. The United States Government assumes no liability for its contents or use thereof. This report does not constitute a standard specification or regulation.

The United States Government does not endorse products or manufacturers. Trademarks or manufacturers names appear herein only because they are considered essential to the object of this document.

PROTECTED UNDER INTERNATIONAL COPYRIGHT
ALL RIGHTS RESERVED.
NATIONAL TECHNICAL INFORMATION SERVICE
U.S. DEPARTMENT OF COMMERCE

Technical Report Documentation Page

1. Report No. FHWA-RD-98-065	2. Government Accession No.	3.  PB99-163180	
4. Title and Subtitle SUMMARY REPORT OF RESEARCH ON PERMANENT GROUND ANCHOR WALLS, VOLUME I: CURRENT PRACTICE AND LIMITING EQUILIBRIUM ANALYSES		5. Report Date September 1998	6. Performing Organization Code
		7. Author(s) Long, J.H., Weatherby, D.E., and Cording, E.J.	
9. Performing Organization Name and Address Schnabel Foundation Company 45240 Business Court, Suite 250 Sterling, Virginia 20166		10. Work Unit No. (TR AIS)	11. Contract or Grant No. DTFH61-89-C-00038
		12. Sponsoring Agency Name and Address U.S. Department of Transportation Federal Highway Administration, Research and Development 6300 Georgetown Pike McLean, Virginia 22101-2296	
14. Sponsoring Agency Code		15. Supplemental Notes FHWA Contracting Officer's Technical Representative (COTR): Albert F. DiMillio, HNR-10 FHWA Technical Consultant: Richard S. Cheney, HNG-31	
		16. Abstract Research directed toward improving the design and construction of permanent ground anchor walls is presented. The research focused on tiedback soldier beam walls for highway applications. These walls are generally less than 25 ft high, and they are supported by one or two rows of permanent ground anchors. This volume is part of a four-volume report summarizing the research. It presents apparent earth pressure methods for determining the lateral earth load. Differences between anchored and braced walls are discussed. The limiting equilibrium bases for the apparent earth pressure diagrams are reviewed. Current force equilibrium methods (simple limiting equilibrium methods) for evaluating the external stability of an anchored wall are reviewed. A force equilibrium method is developed and used to illustrate how anchor position, soil strength and the location of the failure surface affect anchor load, and internal and external stability of a wall. The factor of safety inherent in the apparent earth pressure diagram is determined. Recommendations for using general purpose slope stability computer programs for determining lateral load and evaluating internal and external stability of an anchored wall are made. This volume is the first in a series. The other three volumes are entitled: FHWA-RD-98-066 Volume II Full-scale Wall Tests and a Soil-structure Interaction Model FHWA-RD-98-067 Volume III Model-scale Wall Tests and Ground Anchor Tests FHWA-RD-98-068 Volume IV Conclusions and Recommendations In addition, a manual and computer program were developed that incorporate research results. They are entitled: FHWA-RD-97-130 Design Manual for Permanent Ground Anchor Walls FHWA-RD-98-093 TB Wall — Anchored Wall Design and Analysis Program for Personal Computers	
17. Key Words Ground anchor walls, tiebacks, ground anchors, anchors, retaining walls, apparent earth pressure diagrams, limiting equilibrium.		18. Distribution Statement No restrictions. This document is available to the public through the National Technical Information Service, Springfield, Virginia 22161.	
19. Security Classif. (of this report) Unclassified	20. Security Classif. (of this page) Unclassified	21. No. of Pages 135	22. Price

SI* (MODERN METRIC) CONVERSION FACTORS

APPROXIMATE CONVERSIONS FROM SI UNITS

Symbol	When You Know	Multiply By	To Find	Symbol	When You Know	Multiply By	To Find	Symbol
LENGTH								
in	inches	25.4	millimeters	mm	mm	0.039	inches	in
ft	feet	0.305	meters	m	m	3.28	feet	ft
yd	yards	0.914	meters	m	m	1.09	yards	yd
mi	miles	1.61	kilometers	km	km	0.621	miles	mi
AREA								
in ²	square inches	645.2	square millimeters	mm ²	square millimeters	0.0016	square inches	in ²
ft ²	square feet	0.093	square meters	m ²	square meters	10.764	square feet	ft ²
yd ²	square yards	0.836	square meters	m ²	square meters	1.195	square yards	yd ²
ac	acres	0.405	hectares	ha	hectares	2.47	acres	ac
mi ²	square miles	2.59	square kilometers	km ²	square kilometers	0.386	square miles	mi ²
VOLUME								
fl oz	fluid ounces	29.57	milliliters	ml	milliliters	0.034	fluid ounces	fl oz
gal	gallons	3.785	liters	l	liters	0.264	gallons	gal
ft ³	cubic feet	0.028	cubic meters	m ³	cubic meters	35.71	cubic feet	ft ³
yd ³	cubic yards	0.765	cubic meters	m ³	cubic meters	1.307	cubic yards	yd ³
NOTE: Volumes greater than 1000 l shall be shown in m ³ .								
MASS								
oz	ounces	28.35	grams	g	grams	0.035	ounces	oz
lb	pounds	0.454	kilograms	kg	kilograms	2.202	pounds	lb
T	short tons (2000 lb)	0.907	megagrams	Mg	megagrams	1.103	short tons (2000 lb)	T
TEMPERATURE (exact)								
°F	Fahrenheit temperature	5(F-32)/9 or (F-32)/1.8	Celsius temperature	°C	Celsius temperature	1.8C + 32	Fahrenheit temperature	°F
ILLUMINATION								
fc	foot-candles	10.76	lux	lx	lux	0.0929	foot-candles	fc
fl	foot-Lamberts	3.426	candela/m ²	cd/m ²	candela/m ²	0.2919	foot-Lamberts	fl
FORCE and PRESSURE or STRESS								
lbf	poundforce	4.45	newtons	N	newtons	0.225	poundforce	lbf
psi	poundforce per square inch	6.89	kilopascals	kPa	kilopascals	0.145	poundforce per square inch	psi

* SI is the symbol for the International System of Units. Appropriate rounding should be made to comply with Section 4 of ASTM E380. (Revised August 1992)

TABLE OF CONTENTS

<u>Section</u>	<u>Page</u>
1.0 INTRODUCTION	1
2.0 BACKGROUND AND CURRENT PRACTICE	7
2.1 INTRODUCTION	7
2.2 APPARENT EARTH PRESSURE	7
2.3 EFFECT OF BEARING CAPACITY	11
2.3.1 Assessing Base Stability	11
2.3.2 Assessing Apparent Earth Pressure	13
2.4 LATERAL EARTH PRESSURE	15
2.5 ANCHORED WALL GEOMETRY	15
2.6 ANCHORED WALL STABILITY	17
2.6.1 Kranz's Method	17
2.6.1.1 Long Anchors	17
2.6.1.2 Short Anchors	18
2.6.1.3 Discussion	19
2.6.2 Ranke and Ostermayer's Method	20
2.6.3 Broms' 1968 Method	22
2.6.4 Broms' 1988 Method	25
2.7 SUMMARY	25
3.0 LIMITING EQUILIBRIUM	27
3.1 INTRODUCTION	27
3.2 PRECEDENCE FOR USING LIMITING EQUILIBRIUM PROCEDURES TO DETERMINE THE OVERALL FORCE REQUIRED FOR STABILITY	27
3.2.1 Sands	27
3.2.2 Soft to Medium Clays	29
3.2.3 Stiff Clays	33
3.2.4 Discussion	34
3.3 DEFINITION OF FACTOR OF SAFETY AND COMMON VALUES	34

TABLE OF CONTENTS

(continued)

<u>Section</u>	<u>Page</u>	
3.3.1	Factor of Safety with Respect to Strength — $FS_{strength}$	34
3.3.2	Factor of Safety with Respect to Load — $FS_{strength}$	35
3.3.3	Factor of Safety for an Example Wall	35
3.3.4	Back-calculated Values for Factor of Safety	36
3.3.4.1	Sand — Apparent Earth Pressures	36
3.3.4.2	Sand — κ_o Conditions	37
3.3.4.3	Sand — Discussion	39
3.3.4.4	Soft to Medium Clay ($\gamma H/s_u > 4$)	39
3.3.4.5	Stiff Clays ($\gamma H/s_u < 4$)	40
3.3.4.6	Interpretation of the Stiff Clay Criteria as a Frictional Soil	41
3.3.4.7	Discussion	43
3.4	SIMPLIFIED LIMITING EQUILIBRIUM APPROACH	44
3.4.1	Results for a Simple Failure Surface	46
3.4.2	Comparison with Rankine Analysis	51
3.4.2.1	Discussion of Force Equilibrium	53
3.5	USING LIMITING EQUILIBRIUM AS AN APPROACH FOR DESIGN	53
3.5.1	Simplified Approach — Internal Stability	53
3.5.1.1	Development of Equations for Determining Internal Stability	53
3.5.1.2	Evaluation of Minimum Unbonded Length	56
3.5.2	Simplified Approach — External Stability	59
3.5.2.1	Analysis for External Stability	60
3.5.2.2	Base Failures (Below the Bottom of the Cut)	63
3.5.2.3	Failures Through the Bottom of the Cut	65
3.5.3	Wall Stability — Failure Surface Passing Through Anchor	66
3.6	USE OF LIMITING EQUILIBRIUM EQUATIONS AND GENERAL PURPOSE SLOPE STABILITY COMPUTER PROGRAMS	69
4.0	USE OF GENERAL PURPOSE SLOPE STABILITY PROGRAMS	71
4.1	INTRODUCTION	71
4.2	DETAILS OF USING GPSSP FOR ANCHORED WALL ANALYSIS	71

TABLE OF CONTENTS

(continued)

<u>Section</u>	<u>Page</u>	
4.3	USE OF GPSSP FOR DETERMINING P_{reqd}	75
4.3.1	Analyses Based on the Location of the Failure Surface . . .	76
4.3.1.1	Failure Surface Passing Through the Soldier Beam at the Excavation Level	76
4.3.1.2	Failure Surface Passing Through the Soldier Beam Tip and the Bottom of the Excavation . .	77
4.3.1.3	Failure Surface Passing Below the Soldier Beam	79
4.3.2	Simplified Approach for Determining P_{reqd}	80
4.3.3	Toe Resistance	82
4.3.3.1	Failure by Soil Flowing Between the Soldier Beams	82
4.3.3.2	Failure by Exceeding the Lateral Capacity of the Soldier Beam Below the Failure Surface . .	84
4.4	USE OF GPSSP FOR DETERMINING THE POSITION FOR THE BACK OF THE ANCHOR	85
4.5	USE OF GPSSP FOR DETERMINING STABILITY FOR FAIL- URE SURFACES THROUGH THE ANCHOR BOND LENGTH . .	90
4.5.1	Assumptions Necessary for GPSSP Analyses	91
4.5.2	Simplified GPSSP Analyses — Modeling Options	93
4.5.3	Results	95
4.5.4	Modeling Multiple Anchors with GPSSP	96
4.6	USE OF GPSSP FOR LATERAL LOADS IN SOFT TO MED- IUM CLAYS	96
4.7	ILLUSTRATION OF SOME EFFECTS WITH GPSSP	100
4.7.1	Effect of Groundwater Table	100
4.7.2	Effect of the Shape of the Failure Surface	104
4.8	DISCUSSION	105
	REFERENCES	107

LIST OF FIGURES

<u>Figure</u>		<u>Page</u>
1	Permanent Ground Anchor Retaining Wall	2
2	Ground Anchor Components	3
3	Construction Steps for Ground Anchor Wall	4
4	Apparent Earth Pressure Diagrams	10
5	Base Stability for Excavation	12
6	Henkel's Method for Determining κ_A for Potential Base Failure	14
7	Failure Surface and Force Diagram for Overall Stability	16
8	Simple Rules for Determining Ground Anchor Lengths	16
9	Kranz's Method for Analysis of Anchored Bulkheads with Long Anchors	18
10	Kranz's Method for Analysis of Anchored Bulkheads with Short Anchors	20
11	Ranke and Ostermayer's Method for Analyzing Anchored Walls	21
12	Broms' 1968 Method for Analysis of Anchored Walls (Case 1)	24
13	Broms' 1968 Method for Analysis of Anchored Walls (Case 2)	24
14	Broms' 1988 Method for Analysis of Anchored Walls	25
15	Log-spiral Solution for Earth Pressure Coefficient Necessary for Stability in Sand Assuming a Corner Failure	28
16	Limiting Equilibrium Solution for Earth Pressure Coefficient in Clay Assuming a Corner Failure	30
17	Comparison of Measured and Predicted κ_A	31
18	Comparison of Predicted Earth Pressure Coefficient with Measured Earth Pressure Coefficient	32
19	Effect of Soil Friction Angle on Factor of Safety with Respect to Strength and Load for Terzaghi & Peck Sand Criteria	37
20	Effect of Soil Friction Angle on Factor of Safety with Respect to Strength and to Load Assuming κ_o Conditions	38

LIST OF FIGURES

(continued)

<u>Figure</u>		<u>Page</u>
21	Effect of $\gamma H / s_{u\text{avail}}$ on Factor of Safety (With Respect to Strength) Assuming Terzaghi & Peck Distribution for Stiff Clay Conditions	41
22	Effect of Friction Angle on Factor of Safety (With Respect to Strength) for Terzaghi & Peck Stiff Clay Criteria	42
23	Relationship Between Drained Friction Angle for Clays and Plasticity Index	43
24	Failure Surface Used in Limiting Equilibrium Analyses of Anchored Walls	44
25	Force Equilibrium Considerations for an Anchored Wall System	45
26	Force Equilibrium Considerations for an Anchored Wall System with the Failure Surface in Front of the Anchor Bond Length	47
27	Passive Earth Pressure Coefficients	49
28	Force Equilibrium Considerations for an Anchored Wall System with P_{reqd}	50
29	Effect of Soil Friction Angle on Factor of Safety for Surfaces that Pass Through the Bottom Corner and the Base Using Terzaghi & Peck Criteria for Sand	52
30	Effect of Sloping on Magnitude of $P_{reqd} / 0.5\gamma H^2$	55
31	Critical Failure Surfaces for Frictional Soils with Different Strengths and Different Slopes at Top of Wall	56
32	Comparison of Three Methods for Determining Minimum Unbonded Length of an Anchor, Horizontal Ground Surface	58
33	Comparison of Three Methods for Determining Minimum Unbonded Length of an Anchor, Sloped Ground Surface	59
34	Force Equilibrium Considerations for an Anchored Wall System with Failure Surface Passing Behind the Anchor	62
35	Definition of Non-dimensional Parameters χ , λ , and ξ	63
36	Effect of Mobilized Soil Strength on Position Required for Back of Anchor (base failure)	64

LIST OF FIGURES
(continued)

Figure		Page
37	Example for Determining Minimum Anchor Length for $\phi_{mob} = 33^\circ$ (base failure)	65
38	Effect of Mobilized Soil Strength on Position Required for Back of Anchor (corner failure)	66
39	Requirements for Anchor Load Along the Anchor Length (base failure)	68
40	Requirements for Anchor Load Along the Anchor Length (corner failure)	68
41	Equilibrium Considerations for Method of Slices	74
42	Considerations for Stability of Failure Surfaces Passing in Front of the Anchor Bond Length	75
43	Determining the Load Required for Stability of Soil in Front of the Anchor (potential failure surface passing in front of the anchor length and through the bottom corner of the excavation)	76
44	Determining the Load Required for Stability of Soil in Front of the Anchor (potential failure surface passing in front of the anchor length and between the bottom of the excavation and the soldier beam tip)	78
45	Determining the Load Required for Stability of Soil in Front of the Anchor (potential failure surface passing in front of the anchor length and below the soldier beam)	79
46	Effect of Method of Analysis and Friction Angle on the Magnitude of P_{reqd}	80
47	Relationship Between K_A and $\gamma H / s_u$ for Different Limiting Equilibrium Methods	81
48	Flow Through Resistance Provided by the Soldier Beams	83
49	Lateral Resistance Provided by the Soldier Beams	84
50	Determination of the Position Required for the Back of the Anchor to Satisfy External Stability	87
51	Position Required for the Back of the Anchor — Spencer's Method and Force Equilibrium Method	88

LIST OF FIGURES
(continued)

<u>Figure</u>	<u>Page</u>
	Position Required for Back of the Anchor
52	a. Comparison of Corps of Engineers' Method and Force Equilibrium Method 89 b. Comparison of Lowe and Karafiath Method and Force Equilibrium Method 89 c. Comparison of Janbu's Method and Force Equilibrium Method 90
53	Failure Surface Passing Through the Anchor Bond Zone 92
54	Means to Analyze Failure Surfaces Passing Through the Anchor Bond Zone 94
55	Variation of Factor of Safety for Failure Surfaces Passing Through a Long Anchor and a Short Anchor 95
56	Comparison of Computed Earth Pressure Coefficients from Limiting Equilibrium Analyses with Measured Coefficients for Soft to Medium Clays 98
57	Comparison of Completed Earth Pressure Coefficients from Limiting Equilibrium Analyses with Computed Earth Pressure Coefficients from the Apparent Earth Pressure Diagram for Soft to Medium Clays 99
	a. Positions Assumed for the GWT in Stability Analyses
	b. Effect of Mobilized Soil Strength ($FS = 1$) on the Position Required for the Back of an Anchor (base failure)—GWT at Excavation Level 102
58	c. Effect of Mobilized Soil Strength ($FS = 1$) on the Position for the Back of an Anchor (base failure)—Effect of Seepage Toward the Wall 102 d. Effect of Mobilized Soil Strength ($FS = 1$) on the Position Required for the Back of an Anchor — Comparison of Results for Failure Through the Bottom of the Excavation Versus Failure Through Base for Seepage Toward the Wall 103
59	Effect of Mobilized Soil Strength ($FS = 1$) on Position for the Back of the Anchor (base failure) — Comparison of Results for Non-circular and Circular Failure Surface 104

LIST OF TABLES

<u>Table</u>		<u>Page</u>
1	Henkel's Lateral Earth Pressure Coefficient, K_A	33
2	$FS_{strength}$ for an Apparent Earth Pressure Wall in Sand (corner failure) . .	36
3	$FS_{strength}$ and FS_{load} for K_o Conditions (corner failure)	38
4	Magnitudes of K_{reqd} for the Force Equilibrium Method (base failure) . . .	49
5	Comparison of Earth Pressure Coefficients K_{reqd} and K_{AR}	51
6	Comparison of P_{reqd} P_{reqd} for Different Wall Geometrics	54
7	Assumptions and Features of Some GPSSP Methods of Analysis	73

LIST OF ABBREVIATIONS AND SYMBOLS

AEP	=	Apparent earth pressure
B	=	Excavation width
b	=	Soldier beam width or diameter
B'	=	Width of soil block exerting pressure at the base of an excavation
c	=	Cohesion
c_{avail}	=	Cohesion available
c_{mob}	=	Cohesion mobilized
D	=	Distance from the bottom of the excavation to a hard stratum
d	=	Depth of the failure surface below the bottom of the excavation
FS	=	Factor of safety
FS_{load}	=	Factor of safety with respect to load
$FS_{strength}$	=	Factor of safety with respect to strength
F_x	=	Forces in the x-direction (horizontal)
F_y	=	Forces in the y-direction (vertical)
f	=	Factor used to determine the intensity of the earth pressure in the stiff clay apparent earth pressure diagram
$GPSSP$	=	General Purpose Slope Stability Programs
GWT	=	Groundwater table
H	=	Height of cut, height of wall
h	=	Height of a failure wedge
l	=	Anchor inclination
K_A	=	Coefficient of active earth pressure

LIST OF ABBREVIATIONS AND SYMBOLS (continued)

K_{AR}	=	Rankine coefficient of active earth pressure
K_{ARNT}	=	Rankine coefficient of active earth pressure excluding soil tension
K_o	=	Coefficient of earth pressure at rest
K_{meas}	=	Earth pressure coefficient computed from measured loads
K_P	=	Coefficient of passive earth pressure
K_{PR}	=	Rankine coefficient of passive earth pressure
K_{reqd}	=	Earth pressure coefficient required for stability
L	=	Length of the anchor behind the failure surface
$Load_{applied}$	=	Force applied by the ground anchor
$Load_{reqd}$	=	Force required for stability
L_{tot}	=	Anchor bond length
$L_{unbonded}$	=	Unbonded tendon length
M	=	Moment
N_c	=	Bearing capacity factor
N_s	=	Stability number
n_a	=	Vertical position of the resultant earth pressure load
P	=	Anchor force
P_{AEP}	=	Total load from an apparent earth pressure diagram
P_{AR}	=	Total load from a Rankine earth pressure diagram
P_a	=	Total load resulting from active earth pressure
P_{K_o}	=	Total load from at rest earth pressures
P_{LL}	=	Resistance to lateral movement of the wall

LIST OF ABBREVIATIONS AND SYMBOLS (continued)

P_P	=	Passive resistance provided at the toe
$P_{P\ avail}$	=	Passive resistance available from the toe
$P_{P\ reqd}$	=	Passive resistance required for stability
P_{reqd}	=	Anchor load, total horizontal force required for stability of a wall
P_{soil}	=	Load exerted on the wall by the soil
P_{TP}	=	Anchor force developed behind a limiting equilibrium failure surface
P_{tie}	=	Anchor load
P_v	=	Resistance to vertical movement of the wall
P_W	=	Wall force
p_{AEP}	=	Apparent earth pressure
p_{LL}	=	Unit resistance to lateral movement of a wall
$q_{applied}$	=	Vertical pressure at the base of an excavation
R	=	Load reduction factor to compute the anchor load for the portion of a ground anchor behind a limiting equilibrium failure surface
R	=	Soil resistance in a limiting equilibrium analysis
SP_h	=	Horizontal resistance provided by a wall
SP_v	=	Vertical resistance provided by a wall
s	=	Spacing between the anchors
s_u	=	Undrained shear strength
s_{ub}	=	Strength of the soil providing bearing resistance
$s_{u\ avail}$	=	Undrained shear strength available
$s_{u\ mob}$	=	Undrained shear strength mobilized

LIST OF ABBREVIATIONS AND SYMBOLS (continued)

T	=	Ground anchor capacity developed behind a limiting equilibrium failure surface, ground anchor load
T_K	=	Maximum deadman anchor force that can be developed
T_{mob}	=	Deadman anchor force required for stability, mobilized anchor capacity
T_{ult}	=	Ultimate pullout capacity of an anchor
V	=	Vertical reaction force at the toe of a wall
W	=	Weight
α	=	Angle of a limiting equilibrium failure plane with respect to the horizontal
β	=	Slope angle
ξ	=	Ratio that defines the depth of a limiting equilibrium failure surface below the bottom of the excavation with respect to height, H
ϕ	=	Friction angle for the soil, angle of internal friction
ϕ_{avail}	=	Angle of internal friction available
ϕ_{mob}	=	Angle of internal friction mobilized
ϕ_{reqd}	=	Angle of internal friction required
σ'_v	=	Vertical effective stress
δ	=	Angle of wall friction, interface friction angle between the embedded portion of the wall and the passive zone of the soil
γ	=	Total unit weight
χ	=	Ratio that defines the horizontal position of the back of a ground anchor with respect to height, H
λ	=	Ratio that defines the vertical position of the back of a ground anchor with respect to height, H

CHAPTER 1

INTRODUCTION

Permanent ground anchor wall systems, often called tiedback walls, use tensile elements anchored in the ground to support earth retaining structures or to stabilize landslides. These walls are built in excavated cuts from the top down. For most highway applications, ground anchor walls consist of anchored soldier beams with temporary wood lagging and a permanent cast-in-place concrete face. Figure 1 shows a typical anchored wall, and the major components of the wall. Soldier beams distribute the ground anchor load to the ground and support the earth at the face of the cut. The components of a ground anchor are shown in Figure 2.

The steps involved in constructing a permanently anchored soldier beam wall are shown in Figure 3. First the soldier beams are driven or drilled into the ground from the existing ground surface. After the soldier beams are installed, the excavation proceeds to the first ground anchor level. As the excavation is made, wood lagging or shotcrete is applied to support the ground between the soldier beams temporarily. Next, the ground anchors are installed. They are made by driving or drilling a hole into the ground behind the wall. After the hole has reached the desired depth, a prestressing steel tendon is grouted into the ground. The grouted anchor fixes the tendon to the ground at the far end. After the cement grout has cured, the ground anchor is load tested and locked-off to the soldier beam. Then the excavation and placement of lagging or shotcrete continues to the next anchor level or the bottom of the cut. If additional levels of ground anchors are required, the steps described above are repeated.

After the excavation is completed, prefabricated drains are attached to the lagging or shotcrete. An unreinforced concrete leveling pad is often cast at the bottom of the wall. The pad enables the wall forms to be easily set and it is not designed. A permanent, reinforced, cast-in-place concrete face is constructed from the bottom up. Headed studs are used to attach the concrete face to steel soldier beams. Grouted or epoxied dowels are used with drilled-in, reinforced concrete soldier beams.

Driven steel sheet piling, soldier piles in a deep soil-mixed trench, or structural diaphragm walls are occasionally used for the vertical elements of anchored walls. These walls are used when it is necessary to cut off groundwater from behind or under the wall. Sheet piling or deep soil mixed walls have been used when the ground between soldier beams will not support itself long enough to install lagging or shotcrete.

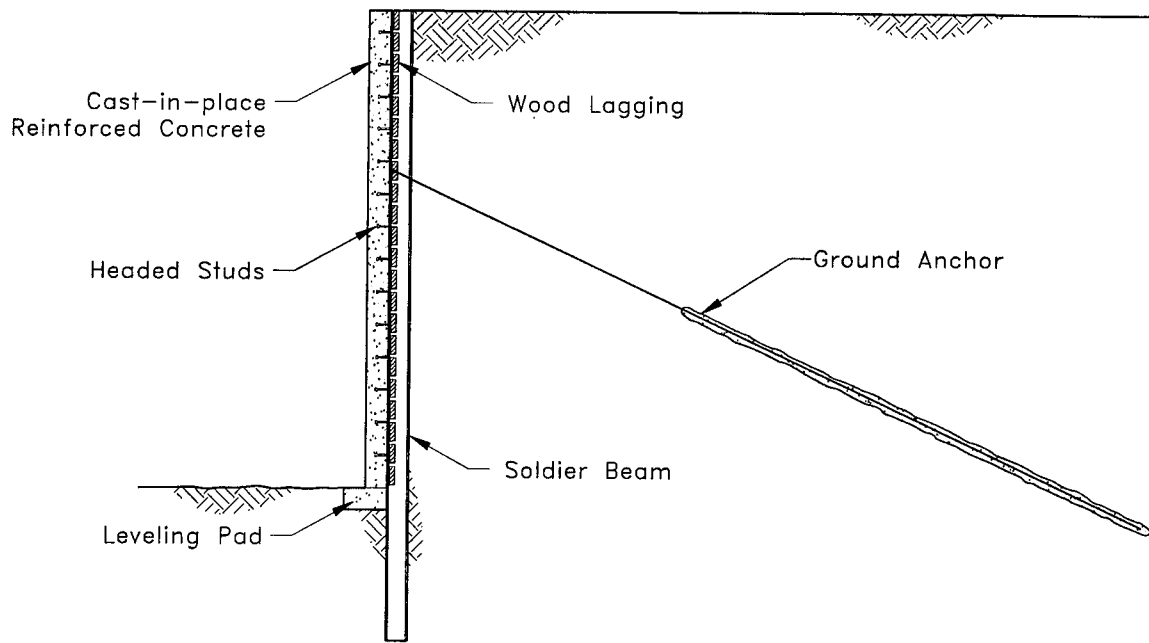


FIGURE 1
Permanent Ground Anchor Retaining Wall

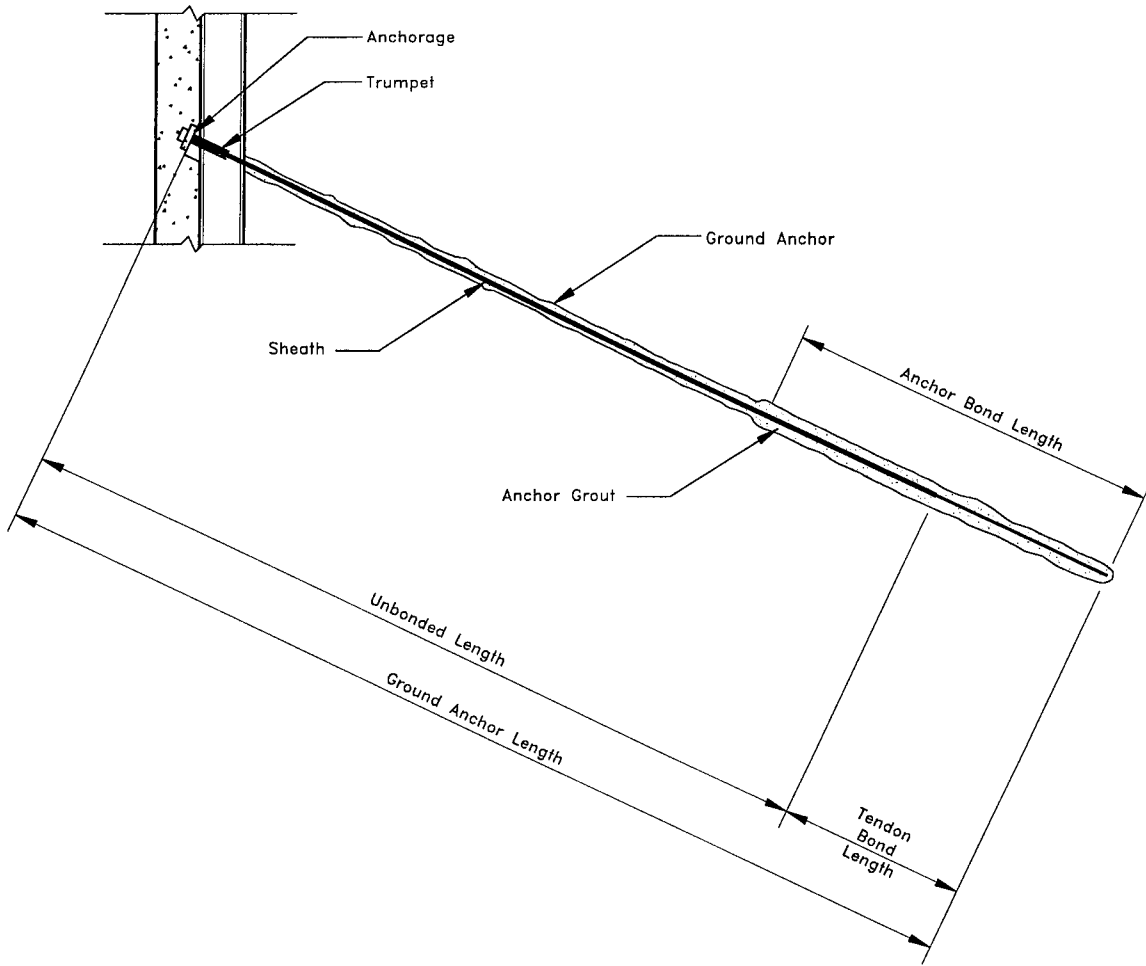
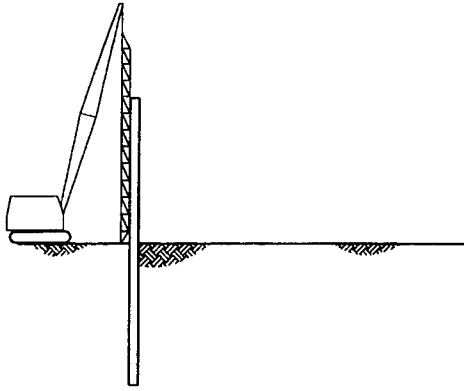
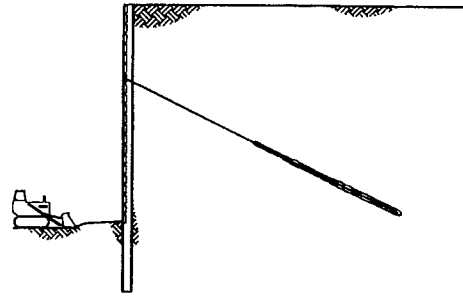


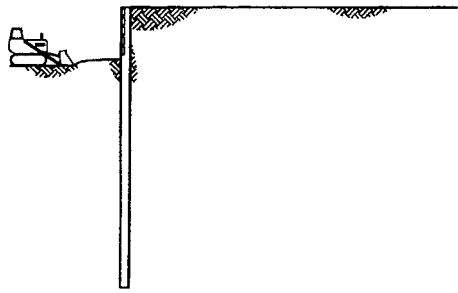
FIGURE 2
Ground Anchor Components



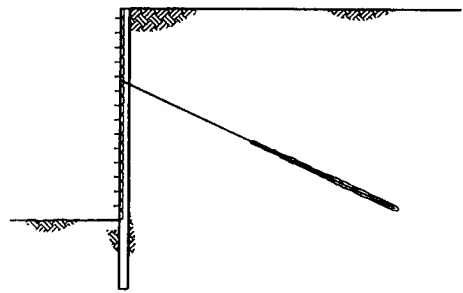
a) Install soldier beam



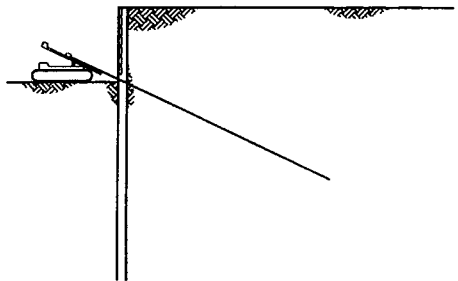
d) Complete excavation



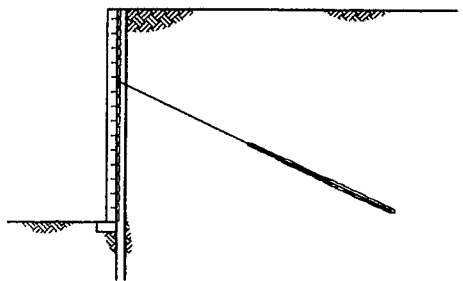
b) Excavate



e) Install headed studs and prefabricated drainage



c) Install ground anchor



f) Pour cast-in-place facing

FIGURE 3
Construction Steps for Ground Anchor Wall

Permanent ground anchor walls have been routinely built in the private sector since the late 1970's. A considerable base of empirical knowledge exists with respect to their design, construction, and performance. Public agencies have built many permanently anchored retained walls since the 1980's. Most walls in the public sector were designed using conservative guidelines adopted in the 1980's. In the late 1980's, the Federal Highway Administration (FHWA) recognized that the design guidelines could be improved. It funded a research program to improve the understanding of the behavior of permanent ground anchor walls and to develop a design manual for highway walls.

The research program was directed toward improving the understanding of permanent ground anchor walls constructed using tiedback soldier beams. For highway applications, these walls are generally less than 25 ft high, and they are supported by one or two rows of permanent ground anchors.

This volume is part of a four-volume report summarizing the research. It presents a summary of current practice, a review of limiting equilibrium analyses used for ground anchor wall design, and the results of limiting equilibrium studies. The chapters in Volume I include the following:

- Chapter 2 provides background information and a historical perspective on anchored walls. Apparent earth pressure methods for determining the lateral earth load are presented, and differences between anchored walls and braced cuts are discussed. Chapter 2 also reviews current force equilibrium methods (simple limiting equilibrium methods), and discusses the assumptions employed by each.
- Chapters 3 and 4 present methods for determining the overall force required for anchored wall stability. A force equilibrium method is developed in Chapter 3. It is used to illustrate the importance of anchor position, soil strength, and location of the failure surface (through the bottom corner of the excavation or through the base of the cut). Principles for determining the internal and external stability of anchored walls are presented. Chapter 4 addresses the use of general purpose slope stability (computer) programs for determining the force required for stability.

The other three volumes of the research report are entitled:

- Volume II Full-scale Wall Tests and a Soil-structure Interaction Model (Weatherby, et al., 1998)
- Volume III Model-scale Wall Tests and Ground Anchor Tests (Mueller, et al., 1998)
- Volume IV Conclusions and Recommendations (Weatherby, 1998)

The four volumes address the major elements of permanent ground anchor wall design and provide guidance and recommendations to be used in the development of a design procedure presented in a separate manual. Some research finds were incorporated in a computer code

developed for the design or analysis of permanent ground anchor walls. The manual is entitled *Design Manual for Permanent Ground Anchor Walls* (Weatherby, 1997), and the computer program is named *TB Wall - Anchored Wall Design and Analysis Program for Personal Computers* (Urzua and Weatherby, 1998).

Recommendations presented in this report are intended to apply to permanent ground anchor walls for typical highway applications. They were not developed for temporary earth support systems, but many principles presented apply to both permanent and temporary construction.

CHAPTER 2

BACKGROUND AND CURRENT PRACTICE

2.1 INTRODUCTION

Design methods for anchored walls have much in common with design methods for braced cuts. However, additional considerations for anchored walls are necessary because anchored walls are internally supported.

2.2 APPARENT EARTH PRESSURE

The distribution and magnitude of earth pressures on excavation support systems are derived principally from experiences with internally strutted excavations in which the increase in a strut load is measured as excavation proceeds. Struts are commonly prestressed to levels less than 50 percent of their design load because they are axially stiff. Relatively little displacement is required for the struts to build up load as the excavation proceeds. Strut load measurements have served as the basis for the development of design criteria such as apparent earth pressure (AEP) envelopes (Terzaghi, et al., 1996). These apparent earth pressure envelopes are used to design strutted excavation support walls and anchored walls.

Anchors are less stiff than struts and, accordingly, must be tensioned to loads close to their full design load to minimize lateral wall movements during excavation. Because they are relatively extensible, ground anchor load does not change significantly during excavation. Thus, the measured load reflects the pre-load (lock-off load) in the system rather than the load imposed by the ground during the excavation process (as observed with strutted excavations).

Experience with support of braced walls in the last 100 years has shown that, while the total magnitude of lateral force measured on braced walls is close to the value calculated from active earth pressure theory, the distribution of earth pressure on the wall does not fit the classical theories of Coulomb and Rankine. Instead of earth pressure increasing linearly with depth (e.g., a triangular distribution), it has long been observed that high pressures develop in the upper part of the wall, as bracing is placed. The restraint provided by the bracing results in higher pressures in the upper portions of the wall than would result if the wall were free to rotate outward at the top sufficiently to reduce the pressures to the active earth pressure case (triangular distribution).

Field measurements of strut loads on internally braced excavations in sands (principally in Berlin, Munich, New York City) and in clays (principally in Chicago) led to the development of a design procedure for bracing using apparent earth pressure envelopes (Peck, 1969). Apparent earth pressures were calculated by dividing measured strut loads by the area of the wall supported by each strut.

Apparent earth pressure distribution will vary depending on the details of construction. For example, higher loads may develop in some struts because they are more highly pre-loaded, or because they are installed with less delay than other struts.

The apparent earth pressure envelope used for design encompasses the highest apparent earth pressures determined from the measured strut loads, and thus, will predict greater pressures than measured in most struts. Accordingly, the design capacity of a wall, based on the apparent earth pressure, will be greater than measured earth pressures. The shape of most apparent earth pressure envelopes used in design is rectangular (magnitude constant with depth) or trapezoidal (magnitude constant with depth over central 50 to 60 percent of wall height, but with reduced pressures at top and/or bottom). Typical apparent earth pressure envelopes are presented in Figure 4.

The apparent earth pressure envelope for sand (Figure 4a) is a rectangle with an apparent earth pressure (p_{AEP}) equal to

$$p_{AEP} = 0.65K_A \gamma H \quad \dots [2.1]$$

where K_A is the Rankine coefficient for active earth pressure ($K_A = \tan^2 \{45 - \phi/2\}$), γ is the total unit weight of the soil, and H is the height of the cut. Applying the apparent earth pressure along the full height of the cut produces a total lateral force that is 1.3 times the value that would be predicted from Rankine active earth pressure theory.

The maximum apparent earth pressure for soft to medium clays is expressed as

$$p_{AEP} = K_A \gamma H \quad \dots [2.2]$$

where $K_A = 1 - 4s_u/\gamma H$, γ is the total unit weight of the soil, H is the height of the cut, and s_u is the undrained shear strength of the soil. Soft to medium clays are defined as having a ratio of $\gamma H/s_u$ greater than about six. The distribution of apparent earth pressure varies from zero to full pressure at a depth of $0.25H$ (Figure 4b). The pressure remains constant for all depths greater than $0.25H$. Applying the apparent earth pressure along the full height of the cut produces a total lateral force that is 1.75 times the value that would be predicted from Rankine active earth pressure theory.

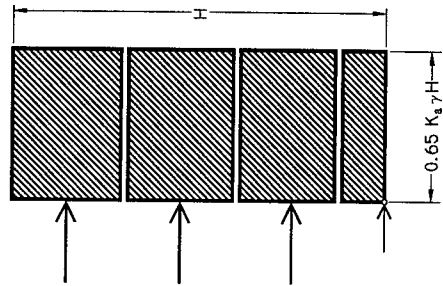
The distribution for the apparent earth pressure for stiff clays is shown in Figure 4c. The maximum apparent earth pressure for stiff clays is

$$p_{AEP} = 0.2\gamma H \text{ to } 0.4\gamma H \quad \dots [2.3]$$

Stiff clays are identified as those with ratios of $\gamma H/s_u$ less than four. For comparison, the apparent earth pressure diagram using $0.2\gamma H$ will yield the same total force as determined for a granular soil with a friction angle of 32.6° (assuming Rankine conditions). Similarly, the apparent earth pressure diagram using $0.4\gamma H$ corresponds to a soil with a friction angle equal to 14.5° (assuming Rankine conditions).

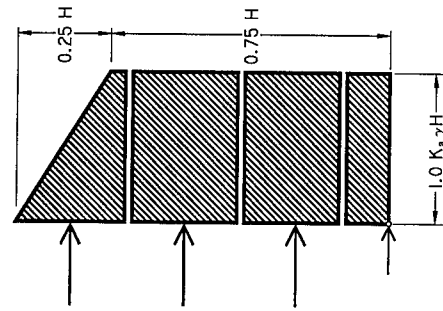
Apparent earth pressures for cuts in cohesive soils having values of $\gamma H/s_u$ between four and six are evaluated using both the soft to medium clay diagram (Figure 4b and Equation 2.2) and the stiff clay (Figure 4c and Equation 2.3) diagram. The diagram giving the highest total lateral load is used.

The above apparent earth pressure diagrams assume that the wall is either in a granular or a fine-grained soil. Frequently, excavation support systems and anchored walls are built in mixed grounds. In mixed grounds, selecting the appropriate apparent earth pressure diagram and determining the intensity of the earth pressure can be difficult. To avoid these uncertainties, Schnabel (1982) recommended using a trapezoidal apparent earth pressure diagram having an intensity of pressure equal to $25H$ (Figure 4d). Thousands of temporary and permanent anchored walls built in sands, clays, and mixed soil profiles have been designed using this diagram. The total load estimated using Schnabel's diagram is approximately equal to the load from Terzaghi and Peck's diagram for a sand with an angle of friction of 35° , or their diagram for a stiff clay with the pressure equal to $0.2\gamma H$. Most measured strut loads in sands and clays fit within the $25H$ envelope. Walls built to support low-strength cohesive soils do not fit this diagram.



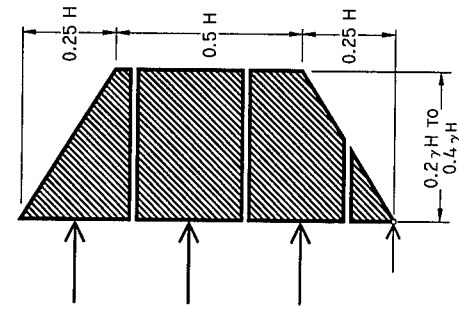
$$K_a = \tan^2 (45 - \phi/2)$$

a) Sands

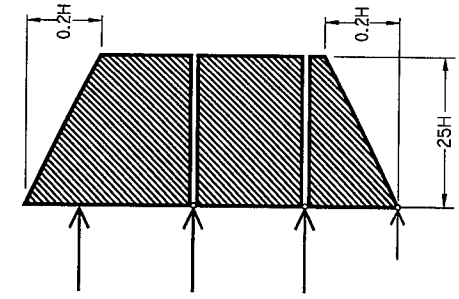


$$K_a = 1 - \frac{4s_u}{\gamma H}$$

b) Soft to medium clay



c) Stiff-fissured clays



d) 25H trapezoid

FIGURE 4
Apparent Earth Pressure Diagrams

2.3 EFFECT OF BEARING CAPACITY

The apparent earth pressures discussed above and illustrated in Figure 4 are for conditions where the soil below the cut provides good support. However, excavations in deep deposits of soft to medium clay may fail or displace excessively because the weight of the retained soil exceeds the bearing capacity of the soil beneath the cut. Accordingly, special attention is given to assessing the base stability of a cut in soft to medium clay and the effect of base stability on apparent earth pressures.

2.3.1 Assessing Base Stability

Soil retained by and next to the wall exerts pressures on the soil under the excavation. Significant basal heave and a significant increase in apparent earth pressures can result if the pressure exceeds or approaches the bearing capacity at the base of the excavation. Shown in Figure 5a is an illustration of a cut in soft clay H deep and B wide. The block of soil $abcd$ exerts a vertical pressure q_{applied} on strip cd equal to its weight minus the shear resistance of the soil along plane bd ($q_{\text{applied}} = \{HB'\gamma - s_u H\}/B'$). The bearing capacity of a cohesive soil is equal to $N_c s_u$ where N_c is the bearing capacity factor and equal to 5.14. The factor of safety can be estimated as the ratio of the bearing capacity to the bearing pressure as

$$FS = \frac{5.14 s_u}{H(B'\gamma - s_u)/B'} \quad \dots [2.4]$$

Based on Equation 2.4, the factor of safety will decrease for increasing width B' ; however, based on the geometry of the failure surface, B' cannot exceed $B/\sqrt{2}$. Thus, the minimum FS for Equation 2.4 is

$$FS = \frac{5.14 s_u}{H(\gamma - \frac{s_u \sqrt{2}}{B})} \quad \dots [2.5]$$

The width, B' , may be affected if a hard stratum is located near the bottom of the cut (Figure 5b). The failure surface is restricted to pass above the hard stratum. For this case, B' is equal to depth D . Substituting D for B' in Equation 2.4, the expression for FS becomes

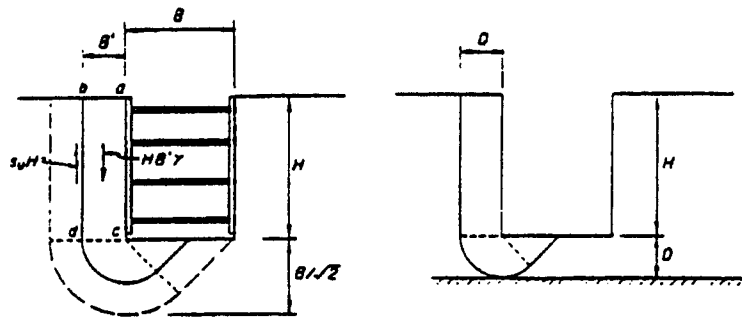
$$FS = \frac{5.14 s_u}{H(D\gamma - s_u)/D} \quad \dots [2.6]$$

For the simplified and limiting case of a very wide cut in a homogenous soft to medium clay of constant strength, the factor of safety in Equation 2.4 can be expressed as

$$FS = \frac{5.14}{\gamma H/s_u} = \frac{5.14}{N_s} \quad \dots [2.7]$$

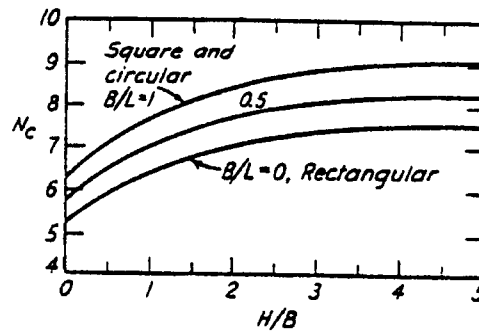
where N_s is a stability number. The magnitude of the stability number can be an indicator of potential for movement and basal heave. Small values of N_s (with respect to 5.14) indicate adequate basal stability and small ground movements.

A refinement for estimating stability of the base is to consider the plan dimensions of the cut. The bearing capacity factor for the cut is taken to be identical to a footing with similar plan dimensions. Accordingly, the bearing capacity factor (N_c) is affected by the depth of embedment (H/B), and the plan dimensions of the cut (width/length). Values of the bearing capacity factor, N_c , proposed by Janbu, et al. (1956) are shown in Figure 5c. Janbu's bearing capacity factor can be substituted in Equation 2.7 to give an estimate of base stability that takes into account dimensions of the cut. Peck, et al. (1974) confirm Janbu's chart and indicate that, when N_s exceeds eight, collapse was likely.



a)

b)



c)

- a) plane of failure through soil
- b) plane of failure affected by stiff underlying layer
- c) bearing capacity factor, N_c , as a function of relative depth (H/B) and plan dimension (width/length) from Terzaghi, et al. (1996)

FIGURE 5
Base Stability for Excavation

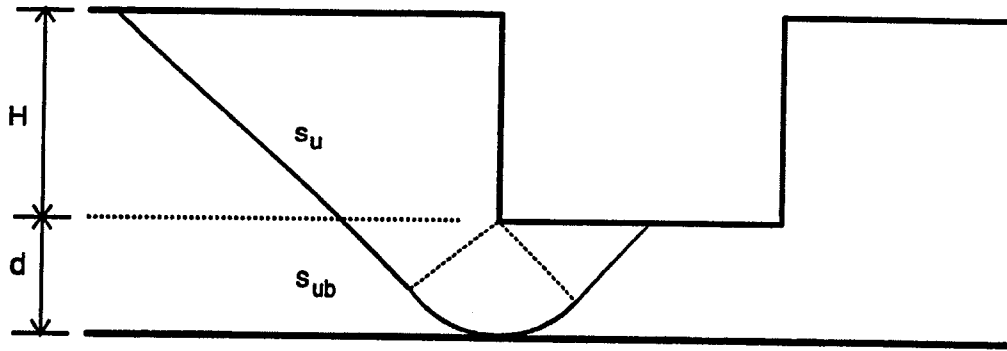
2.3.2 Assessing Apparent Earth Pressure

Terzaghi, et al. (1996) observed that Equation 2.2 (with $\kappa_A = 1 - 4s_u/\gamma H$) underestimated lateral pressures exerted on walls supporting cuts in deep deposits of soft to medium clay where base stability was poor. Henkel (1971) developed an equation for estimating the active earth pressure coefficient that includes the effect of failure through the base of a cut. The equation for the earth pressure coefficient is

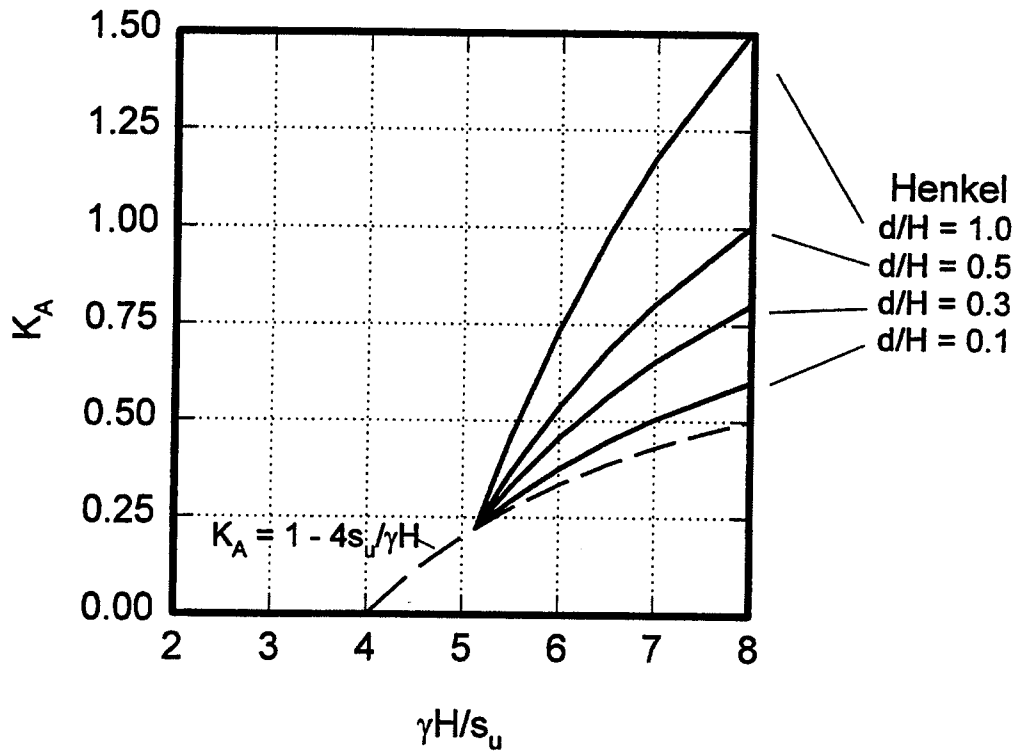
$$\kappa_A = 1 - \frac{4s_u}{\gamma H} + 2\sqrt{2} \frac{d}{H} \left(1 - (2 + \pi) \frac{s_{ub}}{\gamma H} \right) \quad \dots [2.8]$$

where d is the depth of the failure surface below the cut, s_u is the undrained shear strength of the soil through which the excavation extends, and s_{ub} is the strength of the soil providing bearing resistance (Figure 6a). Henkel's estimate for κ_A , Equation 2.8, should be used in Equation 2.2 when estimating apparent earth pressures for deep cuts in soft to medium clay where base stability is poor.

Relationships between κ_A and $\gamma H/s_u$ are shown in Figure 6b for Henkel's method. For purposes of illustration, the soil in which the excavation occurs is taken as uniform in strength, but with different ratios of d/H (depth of soil below excavation/height of cut). Shown in solid lines are the relationships predicted with Henkel's method. The earth pressure coefficient (κ_A) increases with the ratio $\gamma H/s_u$ and with d/H . The Rankine active earth pressure ($\kappa_A = 1 - 4s_u/\gamma H$) provides a lower bound relationship for κ_A . Agreement between values of earth pressure observed and those predicted with Henkel's method are good.



a) Failure pattern assumed for Henkel's method



b) Effect of $\gamma H / s_u$ on d/H on active earth pressure

FIGURE 6
Henkel's Method for Determining K_A for Potential Base Failure

2.4 LATERAL EARTH PRESSURE

Apparent earth pressure diagrams are used directly to calculate strut loads or anchor loads. Bending moments in the soldier beam above the first support also may be based on the apparent earth pressure diagram. However, for portions of the soldier beam below the first support, the actual distribution of pressure will be different from that given by the apparent earth pressure diagram. Lateral deflection of the beam results in redistribution of soil pressures (arching) so that lateral pressures are reduced along the deflected portion of the beam and redistributed through the soil to the stiffer portions of the wall (at the supports). Accordingly, some design approaches allow a reduction in bending moments calculated from apparent earth pressure diagrams. Therefore, earth pressures used to determine bending moments (for portions of the soldier beam below the first support) are assumed to be two-thirds of the apparent pressures (Peck, et al., 1974). It is also recognized that should the soldier beams yield in bending, they will not be subject to progressive failure that could lead to collapse (as will struts that become overloaded).

Lagging thickness and span are typically selected on the basis of experience and soil type. Soldier beams typically are spaced 6 to 10 ft center to center.

2.5 ANCHORED WALL GEOMETRY

The geometry required for an anchored wall is governed by construction requirements and by design. The final design must exhibit stability for all potential failure surfaces passing through and behind the anchors. Design procedures typically use simple guidelines to identify preliminary requirements for anchor length and toe depth. The preliminary design is then modified, as necessary, to meet the specific site requirements for safety and economy.

Total anchor length must be sufficient to maintain overall stability of the soil mass in which the anchor is located. The total length required for overall stability requires evaluation of a soil wedge (Figure 7), which includes the entire anchor as an internal force within the soil wedge. The failure plane is assumed to pass through back of the anchor (or through some predetermined portion of the anchor). Several methods proposed for assessing the overall stability of anchored walls are discussed later in this section. Further recommendations for evaluating overall stability are described in Chapter 3, Limit Equilibrium.

Simple guidelines for establishing the initial geometry for an anchored wall supporting a cut of height, H , are illustrated in Figure 8. The unbonded length of the anchor should extend behind the active wedge and be a minimum of 15 ft for strand tendons and 10 ft for bar tendons. The minimum unbonded lengths are used to minimize reductions in transfer loads as the anchors are locked-off to the supported structure. Some codes use an additional distance behind the active wedge of $H/5$ or 5 ft (this was originally recommended to ensure under-reamed anchors developed their load-carrying capacity behind the active wedge). Anchor bond length will depend on the capacity that can be developed in a given soil with a given installation pro-

cedure. Anchor length, hole diameter, and grouting pressure are three significant parameters influencing capacity. Ground anchor capacity should be verified using performance tests and proof tests (Weatherby, 1982 and AASHTO-AGC-ARTBA Task Force 27 Report *Specification for Permanent Ground Anchors*, 1990). Each anchor is tested to verify its load-carrying capacity.

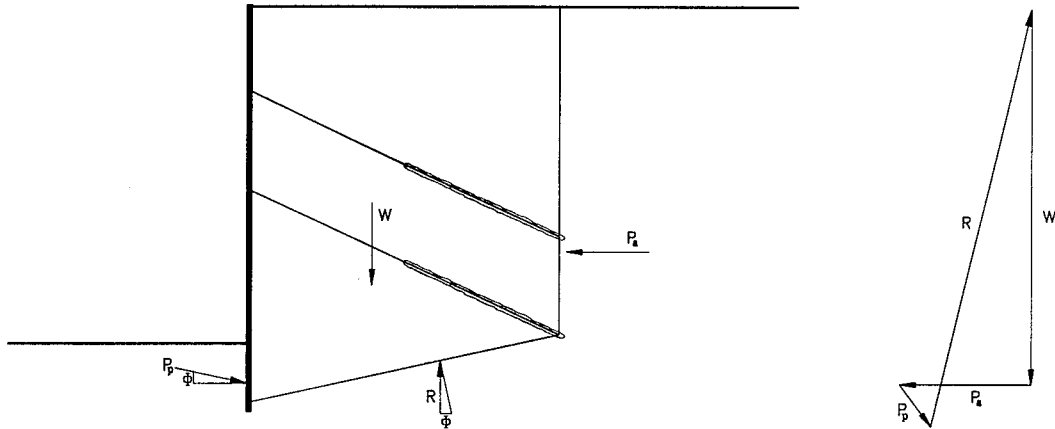


FIGURE 7
Failure Surface and Force Diagram for Overall Stability

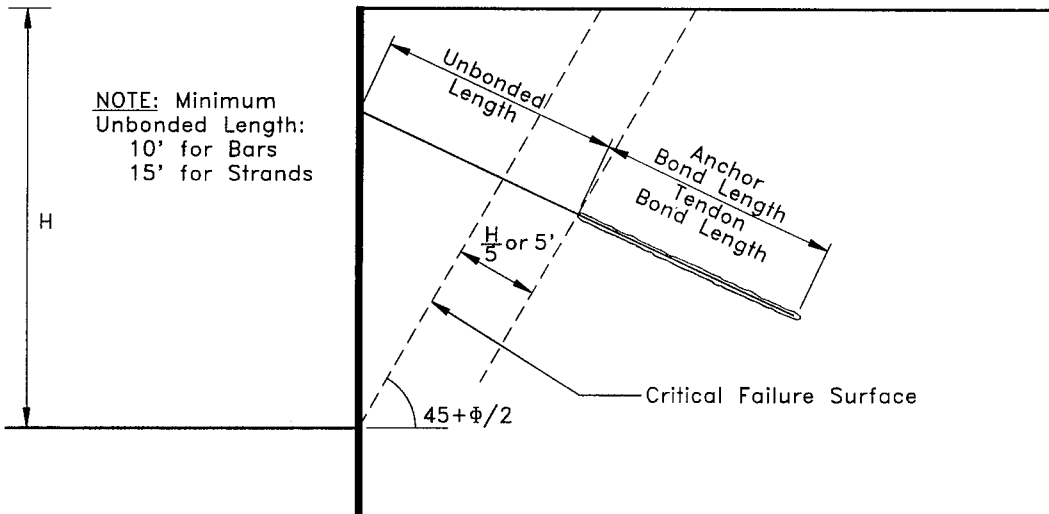


FIGURE 8
Simple Rules for Determining Ground Anchor Lengths

2.6 ANCHORED WALL STABILITY

Methods commonly used for studying the stability of an anchored wall are presented herein. These methods assume the soil is at a limit equilibrium state, and use force equilibrium ($\Sigma F_x = 0$, and $\Sigma F_y = 0$) to solve for specific unknowns. Several analysis methods employ different definitions for the factor of safety that makes comparison between methods difficult. Consequently, each method will yield a different factor of safety for an identical wall. Details and assumptions for each method are discussed in this section.

2.6.1 Kranz's Method

Kranz (1953) proposed a method to design anchored bulkheads with short and long deadman anchors with particular emphasis directed toward stability analysis for bulkheads with short anchors. Kranz used force equilibrium to determine the stability of the anchored wall and defined the factor of safety with respect to anchor load. Kranz's paper was published in German and has been referenced widely in American ground anchor design guidelines. Unfortunately, many (English language) references have misinterpreted important details for determining wall stability using the Kranz method. The discussion below is based on a review of the original version.

2.6.1.1 Long Anchors

Kranz analyzed the soil mass behind the anchored wall as a free body. He distinguished between long and short anchors by comparing the active zone behind the wall with the passive zone in front of a deadman anchor (Figure 9). An anchor was identified as long if the active zone behind the wall did not intersect the passive zone in front of the deadman. Thus, the capacity of a long anchor is unaffected by the presence of the wall.

The shape of the active wedge and an accompanying free body diagram is shown in Figure 9. The bottom surface of the active wedge extends at $45 + \phi/2$ from the tip of the wall to the ground surface. Force equilibrium is used to determine the load necessary for the anchor to ensure stability (Figure 9). Kranz defined factor of safety as

$$FS = \frac{T_{ult}}{T_{mob}} \quad \dots [2.9]$$

where T_{ult} is the ultimate pullout capacity of the anchor and T_{mob} is the mobilized capacity of the anchor.

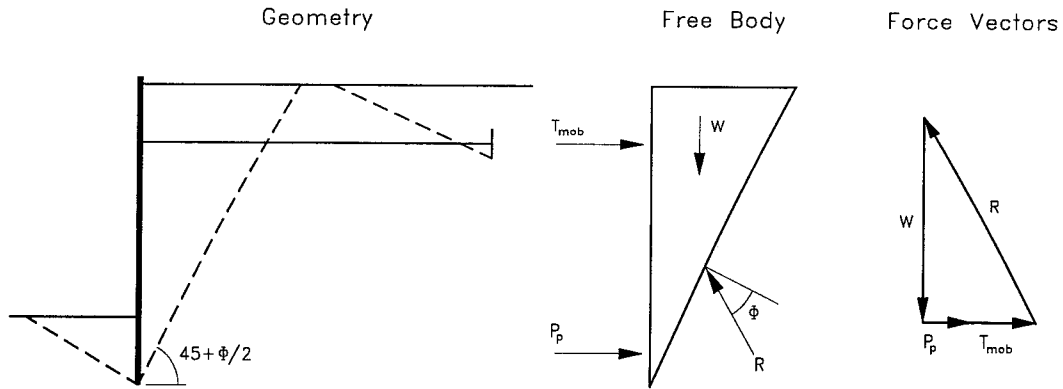


FIGURE 9
Kranz's Method for Analysis of Anchored Bulkheads with Long Anchors

2.6.1.2 Short Anchors

Kranz also developed analyses to determine the factor of safety for anchored bulkheads with short deadman anchors. Anchors were identified as short when the active zone behind the wall intersected the passive zone in front of the anchor. Thus, the capacity of the anchor was affected by the presence of the wall.

The analysis divides the failure wedge (ACEF) into two sub-wedges (Figure 10a and 10b). A free body for the upper wedge is used to determine the anchor force required for stability (T_{mob}), and a free body for the lower wedge is used to determine the maximum deadman anchor force that can be developed (T_K).

The upper wedge is the active wedge (ABF) assumed to form at the top of the soil mass. A free body diagram for wedge ABF is used to determine the magnitude of the anchor load (T_{mob}) required for stability. As illustrated in Figure 10a, the magnitude of T_{mob} is determined by summing vector forces contributed from the self weight of the upper wedge (W), the passive resistance provided at the toe (P_p), and the reaction force along the bottom plane of the wedge (R_a).

Equilibrium considerations for the lower wedge (BCEF) are used to determine T_K . Kranz identified T_K as the maximum deadman anchor force. The upper wedge (FAB) imposes a load R_a on the free body (BCEF) as shown in Figure 10b. Soil resistance, R , is provided along the bottom surface (EF) and active earth pressure, P_a , is provided along the vertical surface CE. The weight of the free body is w . The force vector diagram is constructed to solve for the force, T_K , required to bring all the forces on the free body into equilibrium ($\Sigma F_x = 0$, $\Sigma F_y =$

0). Kranz defined the factor of safety as the ratio between the mobilized anchor load, T_{mob} , and T_K as shown in Equation 2.10 below.

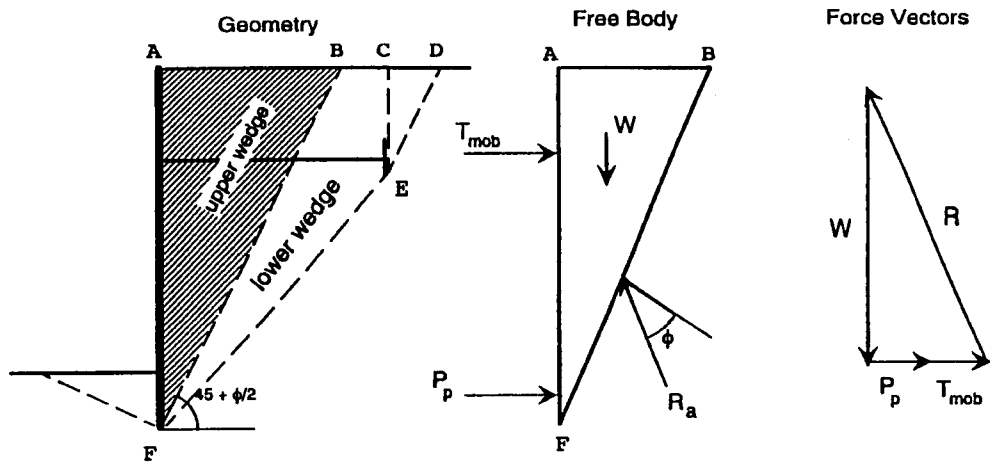
$$FS = \frac{T_K}{T_{mob}} \quad \dots [2.10]$$

Kranz suggests that several trial failure surfaces be used to identify the minimum value for T_K . Trial failure surfaces are created by allowing the lower surface of the lower wedge (line EF in Figure 10b) to intersect line segment BF anywhere between point B and F. However, Kranz argues that the lower wedge passing through the back of the anchor and the bottom of the wall usually results in the minimum factor of safety.

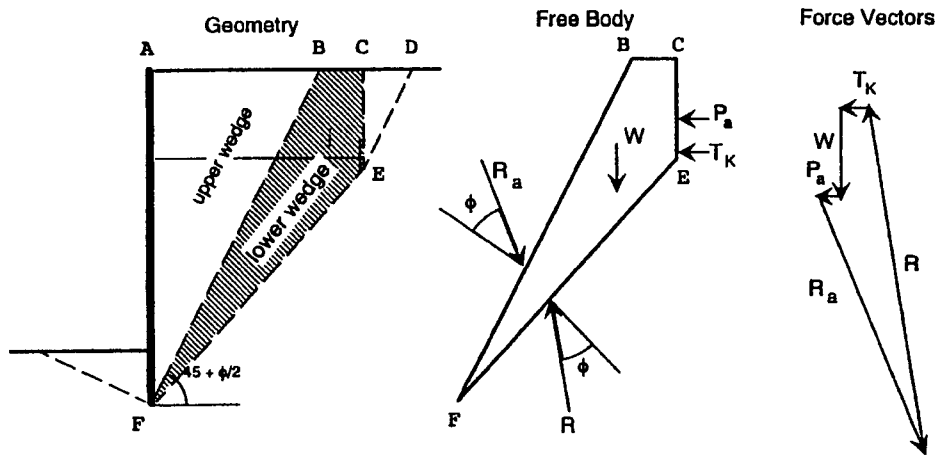
2.6.1.3 Discussion

The Kranz method has been proposed as an analysis method for anchored walls and has served as a foundation for several newer methods. However, the free body diagrams, force equilibrium analysis, and definition for factor of safety are inappropriate for anchored walls. Important details and limitations of Kranz's method are:

- The Kranz method was developed for sheet piles with deadman anchors. A deadman anchor develops its resistance from a passive wedge in front of it, while ground anchors develop most of their resistance along the anchor bond length. Thus, assumptions made by Kranz may not be appropriate for assessing the interference between the anchor and the wall.
- The kinematics of the free body diagram are inappropriate for anchored walls. The free body diagrams implicitly assume that the active wedge (ABF in Figure 10a) displaces downward with respect to the free body selected (BCEF). However, for the lower wedge BCEF to fail, the lower wedge must move down with respect to the active wedge (ABF), or move with the active wedge. Neither condition can occur. Therefore, the kinematics assumed are inappropriate for failure of the lower wedge.
- The failure surface is assumed to pass through the bottom of the wall. However, the failure surface for an anchored soldier beam and lagging system, or for an anchored sheet pile wall may pass through the toe above the bottom of the soldier beam or sheet pile.
- Kranz defined the factor of safety for a wall as a ratio of anchor capacity to mobilized anchor load (T_K/T_{mob} for short anchors and T_{ult}/T_{mob} for long anchors). This definition can yield a very different FS than other more conventional definitions used for anchored walls (such as $FS = \text{available strength}/\text{mobilized strength}$, or $FS = \text{applied tie force}/\text{tie force required for stability}$). Consequently, the definition for factor of safety used by Kranz is not recommended as a reliable measure for wall stability.



a) Upper wedge



b) Lower wedge

FIGURE 10
Kranz's Method for Analysis of Anchored Bulkheads with Short Anchors

2.6.2 Ranke and Ostermayer's Method

Ranke and Ostermayer (1968) presented an analysis for anchored walls for single and multiple rows of anchors. The Ranke and Ostermayer method extends the Kranz method to include ground anchors, and to include multiple levels of anchors. Like the Kranz analyses, Ranke and Ostermayer define the factor of safety in terms of anchor force (T_{mob}), and the maximum

anchor force (τ_K). Also like the Kranz method, the Ranke and Ostermayer paper is written in German, and has been misinterpreted in some English language references. The discussion below is based on a review of the original version.

The wall geometry analyzed by Ranke and Ostermayer is illustrated in Figure 11 along with forces on the free body and the resulting force vector diagram. Wall force, P_w , acting on the free body is determined as the result of earth pressures acting on the wall. The failure surface passes through the middle of the anchor. Like the Kranz method, force equilibrium is used to determine the force τ_K . This force is used as the numerator in defining the factor of safety (Equation 2.10). The denominator in Equation 2.10 is taken as the existing force in the anchor.

Ranke and Ostermayer extended the method to include analyses of multiple rows of anchors. Several different potential failure surfaces are selected that pass through some anchors, while passing behind other anchors. Factors of safety are determined using Equation 2.10.

Since Ranke and Ostermayer use a similar definition for factor of safety as Kranz, the same criticisms (discussed earlier) for Kranz's method also apply to this method. The definition for factor of safety is misleading for anchored walls. For example, if the denominator in Equation 2.10 is taken as the anchor lock-off load, then higher lock-off loads will result in a lower factor of safety. Consequently, the definition for factor of safety used by Kranz, and by Ranke and Ostermayer, is neither a meaningful measure of wall stability nor a factor that is easily compared with other definitions for factor of safety.

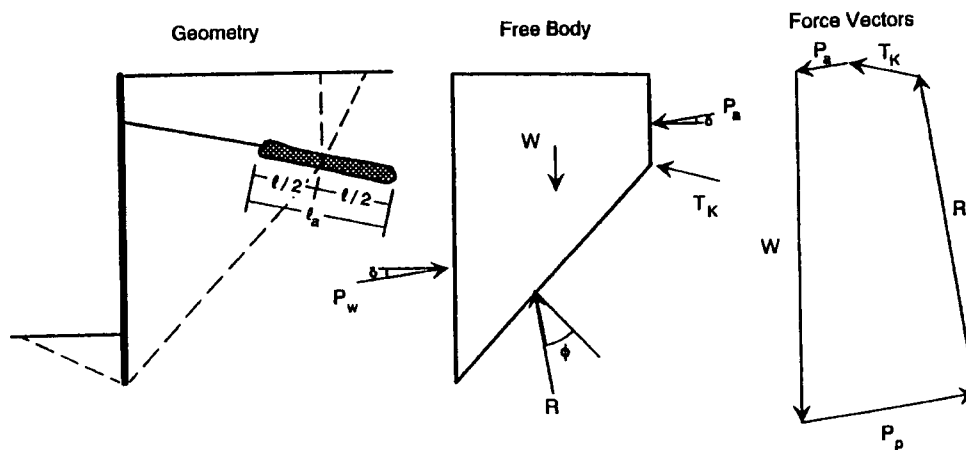


FIGURE 11
Ranke and Ostermayer's Method for Analyzing Anchored Walls

2.6.3 Broms' 1968 Method

Broms and Bennemark (1968) proposed a force equilibrium procedure for evaluating the overall stability of a sheet pile wall anchored with a single row of anchors. The method uses several trial failure surfaces to determine the minimum factor of safety. The factor of safety is defined with respect to the maximum and mobilized passive soil resistance at the toe of the wall. Additional requirements for the stability of the soil mass also are suggested by Broms.

The potential failure surface for an anchored sheet pile wall is shown in Figure 12 as line EDC. The failure plane passes through the toe at point E (which is identified as the minimum penetration required for $FS = 1$). The failure plane extends to point D, which is located 2 m from the back of the anchor. A distance of 2 m was suggested by Broms to account for variations in the failure plane between anchors and to account for inconsistencies in the as-constructed lengths of ground anchors. Active earth pressure is assumed to act on the vertical failure plane BD.

The driving forces acting on the free body (ABDE in Figure 12) are the weight of the free body, W , and the resultant active earth pressure acting on plane BD, P_a . The forces resisting movement are the resultant passive earth pressure at the toe, P_p , and the soil resistance along the failure plane ED, R , and the capacity from the portion of the anchor outside the free body, T . The vertical reaction force at the toe of the sheet pile wall, V , is also treated as a force acting on the free body. All forces are combined in a force polygon to determine the magnitude of $P_{p\ reqd}$, as shown in Figure 12.

The ground anchor is assumed to be positioned far from the wall where the anchor load has no influence on the wall pressure (and vice versa). Broms suggests that the anchor be located behind a line drawn from the tip of the wall (point C) at $45 + \phi/2$ from the horizontal, and that the anchor be at least 5 m below the ground surface.

Broms suggested that the factor of safety for the wall be determined by selecting a specific geometry for the anchor wall and ground anchor, and solving for the passive resistance required for force equilibrium ($FS = 1$). The passive soil resistance for this case is identified as $P_{p\ reqd}$. Broms identifies the factor of safety as the ratio between the Rankine passive resistance available for the as-built toe, $P_{p\ avail}$, and the passive pressure required for stability, $P_{p\ reqd}$, as shown below:

$$FS = \frac{P_{p\ avail}}{P_{p\ reqd}} \quad \dots [2.11]$$

Broms recommends constructing several trial failure surfaces passing through different positions along the anchor length, and selecting the critical failure surface as the one that yields the lowest factor of safety. Broms recommends that the FS be greater than 1.5 to ensure adequate stability at the toe of the wall.

Broms also recommends evaluating the stability along the failure surface ED. The soil strength along ED is reduced by 1.3 (so that $\tan(\phi_{reqd}) = \tan(\phi_{avail})/1.3$). The magnitude for $P_{p reqd}$ determined for this case should be less than $P_{p avail}$ to ensure adequate stability.

Finally, Broms also emphasized the importance of adequate vertical capacity at the toe, suggesting that vertical displacements are responsible for some wall failures and undesirable displacements. Broms recommends embedding the toe in soil that provides adequate bearing capacity and/or reducing the vertical component of the anchor load by decreasing the anchor inclination.

The method suggested by Broms has the following disadvantages:

- The procedure does not adequately emphasize the importance of the ground anchor length. It would be possible to compensate for a short anchor length with increased toe penetration, which could lead to failure of the wall by overturning.
- The definition for factor of safety is based on the passive resistance at the toe of the wall. Resistance to failure of the soil mass can be provided by the portion of the anchor outside the failure surface (T), the soil resistance (R), and the passive soil resistance, P_p . A factor of safety based on only one of these components is unrepresentative of the overall FS .
- Broms includes the vertical component of the anchor force by assuming that all the vertical force is transferred to the toe (which is a reasonable assumption for most vertical walls). Thus, the vertical force is transmitted outside the free body and analyzed as a vertical force, v . Implicitly, this assumes the soil at the base of the wedge does not develop any additional normal component (which is not true). In fact, an increase in normal pressure at the base along the failure plane would result in greater resistance and result in a higher factor of safety. The assumption to include the vertical force, v , essentially reduces the gravity force at the base of the soil wedge to $w-v$, and results in lower (more conservative) estimates of factor of safety for Case 1 (Figure 12), in which the soil reaction, R , is angled away from the wall. However, the same assumption results in a higher (less conservative) factor of safety for Case 2 (Figure 13), where the soil reaction is angled toward the wall.

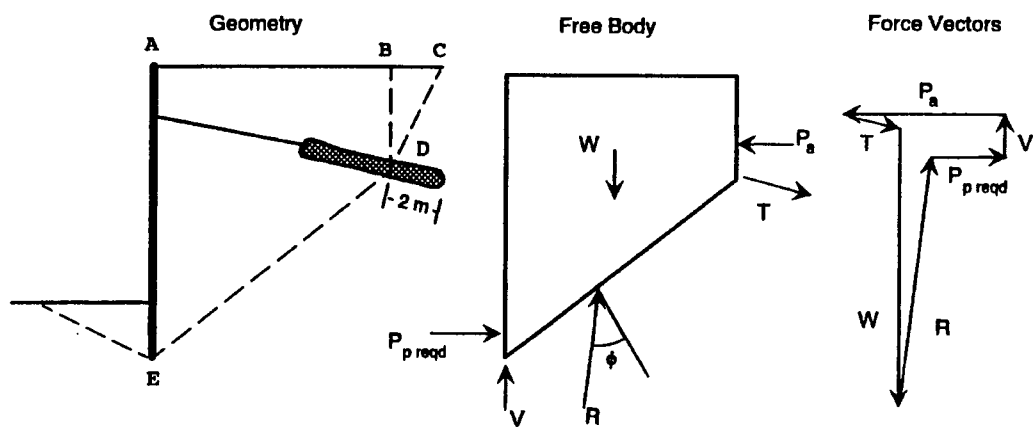


FIGURE 12
Broms' 1968 Method for Analysis of Anchored Walls (Case 1)

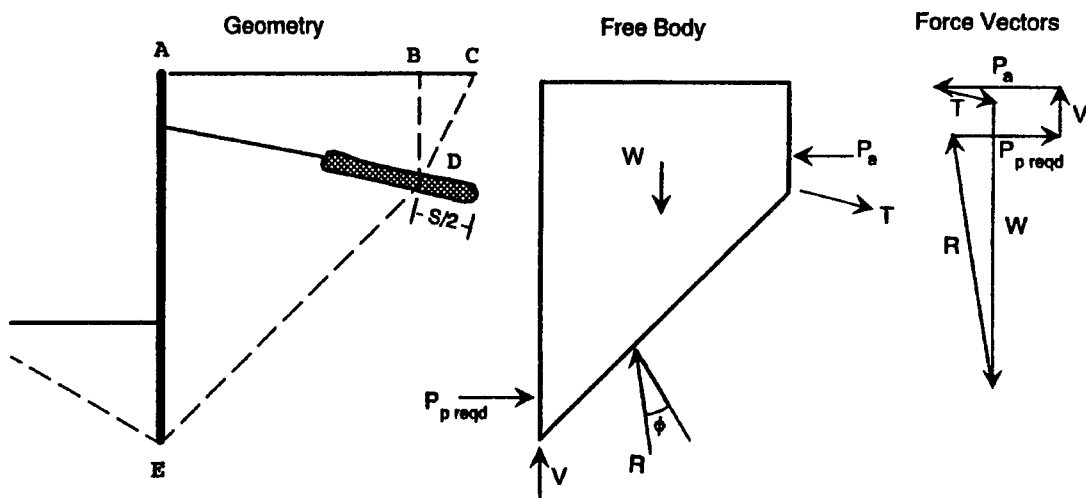


FIGURE 13
Broms' 1968 Method for Analysis of Anchored Walls (Case 2)

2.6.4 Broms' 1988 Method

Broms (1988) modified his earlier method (Broms, 1968) by excluding the vertical component of force v from the free body diagram (Figure 14). Furthermore, he recommended that the failure surface pass through a point located a distance of $s/2$ from the back of the anchor where s is the spacing between anchors. Other aspects of the Broms' analyses are similar to his previous method.

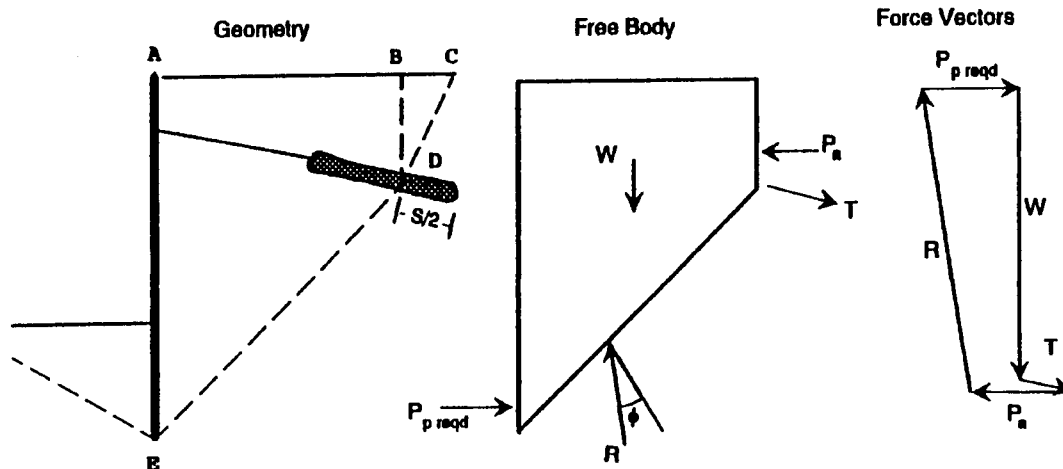


FIGURE 14
Broms' 1988 Method for Analysis of Anchored Walls

2.7 SUMMARY

A variety of design methods are available for determining the requirements for an anchored wall. Many of these methods originate from experience with braced cuts and anchored bulkheads. One important way in which anchored walls differ from braced cuts is that the load in the anchors is controlled, while earth pressures applied to braced cuts are a result of the ground transferring load to the struts as the excavation continues below the strut level. One important way in which anchored walls differ from anchored bulkheads is that an anchored bulkhead requires ground and wall movements to mobilize anchor load; however, a ground anchor is prestressed and therefore does not require wall and ground movement to mobilize anchor load.

Apparent earth pressure diagrams based on experience with braced cuts provide reasonable guidelines for anchored walls. Support for this conclusion is developed further in Chapter 3 and in the *Summary Report of Research on Permanent Ground Anchor Walls, Volume III Model-scale Wall Tests and Ground Anchor Tests* (Mueller, et al., 1998).

CHAPTER 3

LIMITING EQUILIBRIUM

3.1 INTRODUCTION

Limiting equilibrium methods provide a means for quantitatively assessing the stability of an anchored wall system and can be used in combination with empirical methods for the design of anchored walls. The use of equilibrium methods to determine the stability of an anchored wall system and the required anchor loads are discussed in this chapter.

First, the role of limiting equilibrium in developing current earth pressure diagrams is discussed. Factors of safety are defined and then evaluated for the apparent earth pressure diagrams for sand, soft clay, and stiff clay. Next a simplified equilibrium method is introduced and developed. The equilibrium method is used to assess the stability of an anchored wall system, and to determine the requirements for ground anchor geometry and capacity. Failure surfaces passing through the bottom of the cut (corner failures), and failure surfaces passing below the bottom corner of the cut (base failures) are considered. The limiting equilibrium approach considers minimum requirements for stability of the wall and the ground anchor/wall system. Additional comments are provided to address effects of multiple anchor levels, seepage, toe resistance, and layered soils on anchored wall stability.

3.2 PRECEDENCE FOR USING LIMITING EQUILIBRIUM PROCEDURES TO DETERMINE THE OVERALL FORCE REQUIRED FOR STABILITY

Apparent earth pressure distributions for braced cuts are based on measurements made on full-scale excavations. The total load exerted on braced cuts is based on limiting equilibrium methods. Terzaghi, et al. (1996) outline the basis on which the total load can be predicted for sands, soft to medium clays, and stiff clays. Their results were introduced in Chapter 2 and discussed herein.

3.2.1 Sands

The stability of a braced cut was investigated by determining the stabilizing force required for a failure surface passing through the bottom of the cut (Figure 15). For convenience of analysis, the failure surface was assumed to be in the shape of a log spiral. Because of the boundary conditions imposed by the bracing, the failure surface is oriented vertically at the intersection with the top ground surface. The vertical position for the stabilizing force (n_a) was varied between $0.30H$ and $0.5H$ in agreement with field measurements. Several stability analyses were conducted, varying the vertical position of the load (n_a) and the magnitude of wall friction (δ), and results of the log spiral stability analyses were compared with the magnitude of force that would be predicted using a simple relationship, such as Rankine theory. In all cases, the log

spiral was terminated at the bottom of the excavation, and the failure surface was oriented vertically as the failure surface intersected the ground surface.

Differences between loads predicted using the log spiral method and the Rankine method were generally small (Figure 15). Thus, Terzaghi and Peck identify the Rankine method as a simple means to establish requirements for earth support, and the total load predicted from Rankine active earth pressure is factored by 1.3 and distributed rectangularly to create the apparent earth pressure diagram (Figure 4). Rankine active earth pressure coefficient, K_{AR} , for a frictional material is

$$K_{AR} = \frac{1 - \sin \phi}{1 + \sin \phi} = \tan^2(45 - \phi/2) \quad \dots [3.1]$$

where ϕ is the friction angle for the soil.

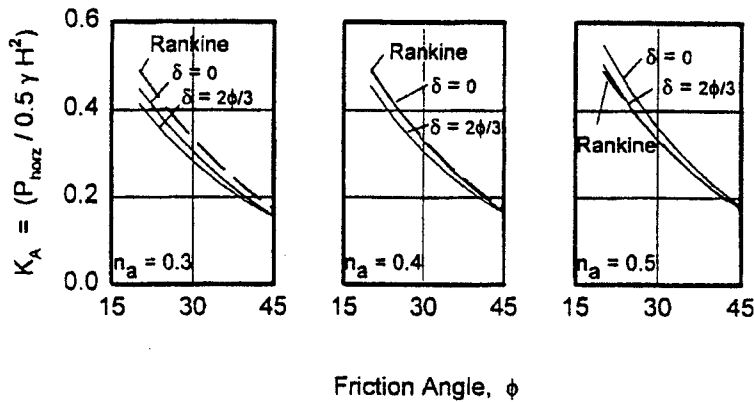
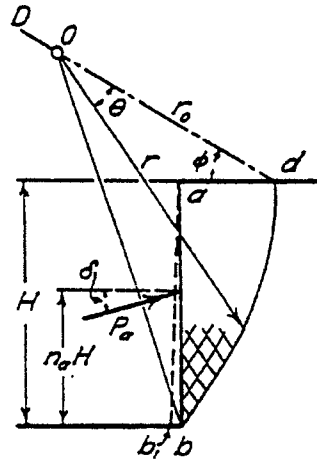


FIGURE 15
Log-spiral Solution for Earth Pressure Coefficient Necessary
for Stability in Sand Assuming a Corner Failure
(Terzaghi, et al., 1996)

3.2.2 Soft to Medium Clays

The method used by Terzaghi and Peck to establish the total load required to support a braced cut in soft to medium clay proceeds in a manner similar to that for sand. The initial estimates of load (required to keep a cut stable) are determined on the basis of stability computations. A circular failure surface is assumed to pass from the top of the ground surface through the bottom of the cut (Figure 16). Furthermore, due to deformation constraints, the failure surface is assumed to be vertical when it intersects the top of the ground surface. Stability calculations are based on summing moments. The position of the required load is assumed between $0.3H$ and $0.5H$ (from measurements) up from the bottom of the cut. The analyses are based on the undrained strength of the soil.

Estimates of the force required using the limit method compare favorably with load estimates using Rankine active earth pressures (Figure 16); thus, Terzaghi and Peck developed empirical rules for the apparent earth pressure diagram for soft to medium clays based on the Rankine active earth pressure. The active Rankine earth pressure coefficient, K_{AR} , for a cohesive material can be expressed as

$$K_{AR} = 1 - \frac{4s_u}{\gamma H} \quad \dots [3.2]$$

where s_u is the undrained strength, γ is the total unit weight of the soil, and H is the height of the cut.

Flaate (1966) compared measured earth pressures against braced cuts in soft to medium clays with earth pressures predicted using Equation 3.2 (Figure 17). The results of his study are represented by the small solid circles. Good agreement was found for cuts in soils with $\gamma H/s_u$ greater than 5.5, and with stiff soils below the base of the cut. Cuts excavated down to stiff soil force the most probable failure surface through the corner and thus satisfy assumptions made in the original limiting equilibrium analyses reported by Terzaghi, et al. (1996) (Figure 16). The agreement is remarkable considering the simplicity of the Rankine equation and the complexity of the excavation and bracing procedures.

Equation 3.2 is derived by summing horizontal forces and includes tensile stresses developed in the upper portions of the cut. However, the resistance of a soil to tensile stress is unreliable. Accordingly, the coefficient of active earth pressure was rederived excluding tension and is expressed as

$$K_{ARNT} = 1 - \frac{4s_u}{\gamma H} + \frac{4s_u^2}{\gamma^2 H^2} \quad \dots [3.3]$$

The “no-tension” formula for active Rankine earth pressure (K_{ARNT}) is similar to Equation 3.2 with an additional term. K_{ARNT} will always be greater than K_{AR} .

Comparisons of measured earth pressures with earth pressures predicted excluding tension and including tension are shown in Figure 18. Data included measurements reported by Flaate (1966) and data from Knapp and Peck (1941). The measurements reported by Knapp and Peck include cuts with $\gamma H/s_u$ values between 3.8 and 5.5. It can be seen that the active Rankine earth pressure including tension (Equation 3.2) can under-predict pressures significantly for $\gamma H/s_u$ values between 3.8 and 5.5. Excluding tensile stresses results in better estimates for earth pressure, particularly in the $\gamma H/s_u = 3.8$ to 5.5 range. In practice, the stiff clay apparent earth pressure diagram is used to estimate the earth pressures in the $\gamma H/s_u = 3.8$ to 5.5 range.

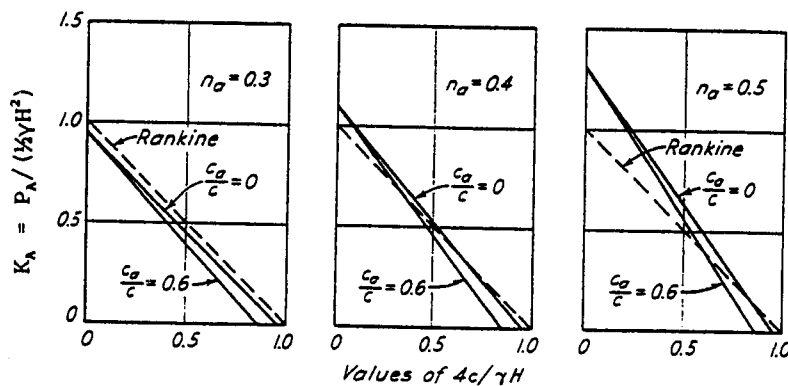
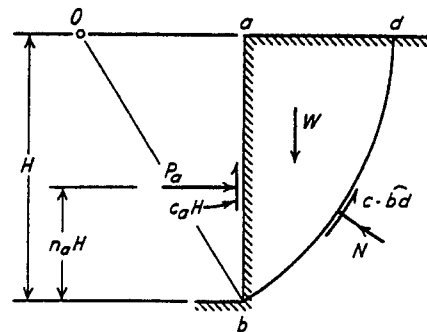
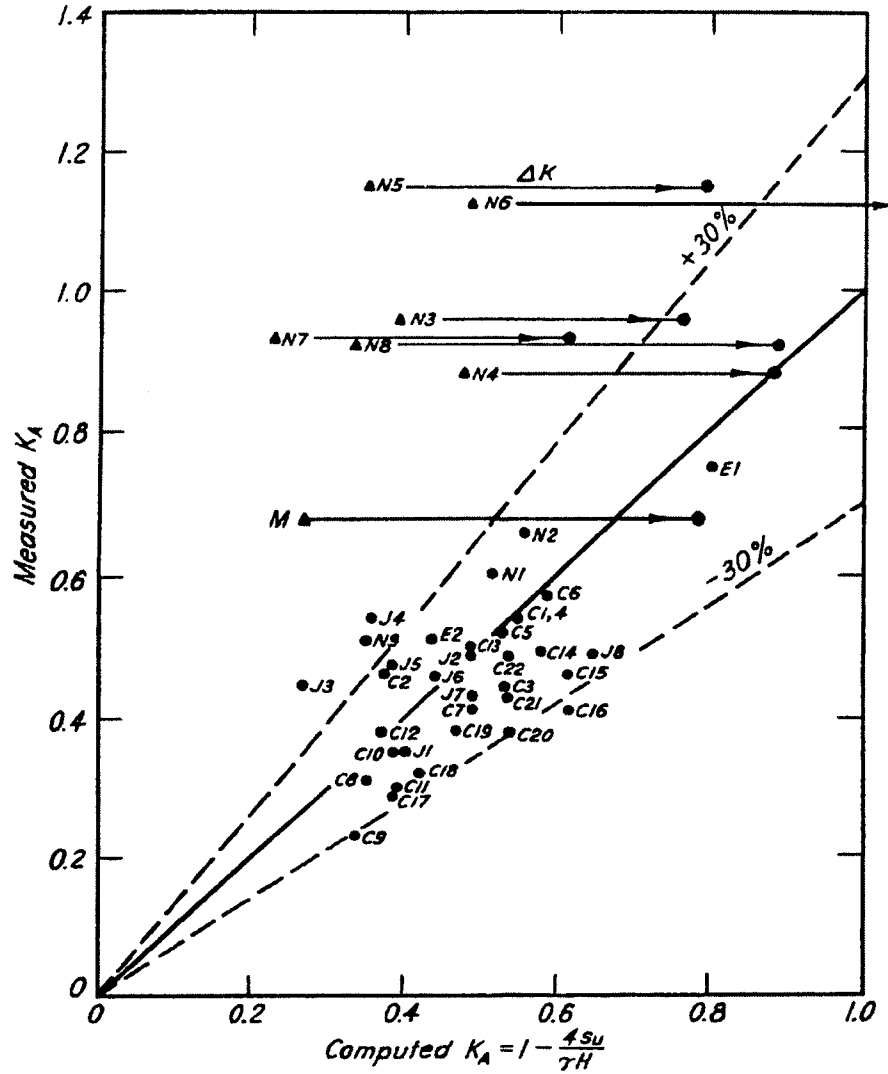


FIGURE 16
Limiting Equilibrium Solution for Earth Pressure
Coefficient in Clay Assuming a Corner Failure
(Terzaghi, et al., 1996)



Mexico:
M Mexico City

Japan:
J1 Tokyo T-Bldg (Endo 1963)
J2 Tokyo Subway (Ishihara and Yuasa 1963)
J3-7 Tokyo M-Bldg (Endo 1963)
J8 Osaka H-Bldg (Endo 1963)

Chicago:
C1-4, Subway S1A (Peck 1943)
C5,6 Subway S3 "
C7 Subway S4B "
C8 Subway S8A "
C9 Subway S9C "
C10,11 Subway D6E "
C12-16 Subway D8 (Wu and Berman 1953)
C17,18 Inland Steel Bldg (Lacroix 1956)
C19-22 Harris Trust (White 1958)

Oslo:
N1,2 Grønland 2 (NGI 1965)
N3,4 Vaterland 1 (NGI 1962)
N5,6 Vaterland 2 (NGI 1962)
N7,8 Vaterland 3 (NGI 1962)
N9 Enerhaugen (NGI 1962)

England:
E1 Poole Power Sta. (Megaw 1951)
E2 Shellhaven (Skempton and Ward 1952)

FIGURE 17
Comparison of Measured and Predicted K_A
(Terzaghi, et al., 1996)

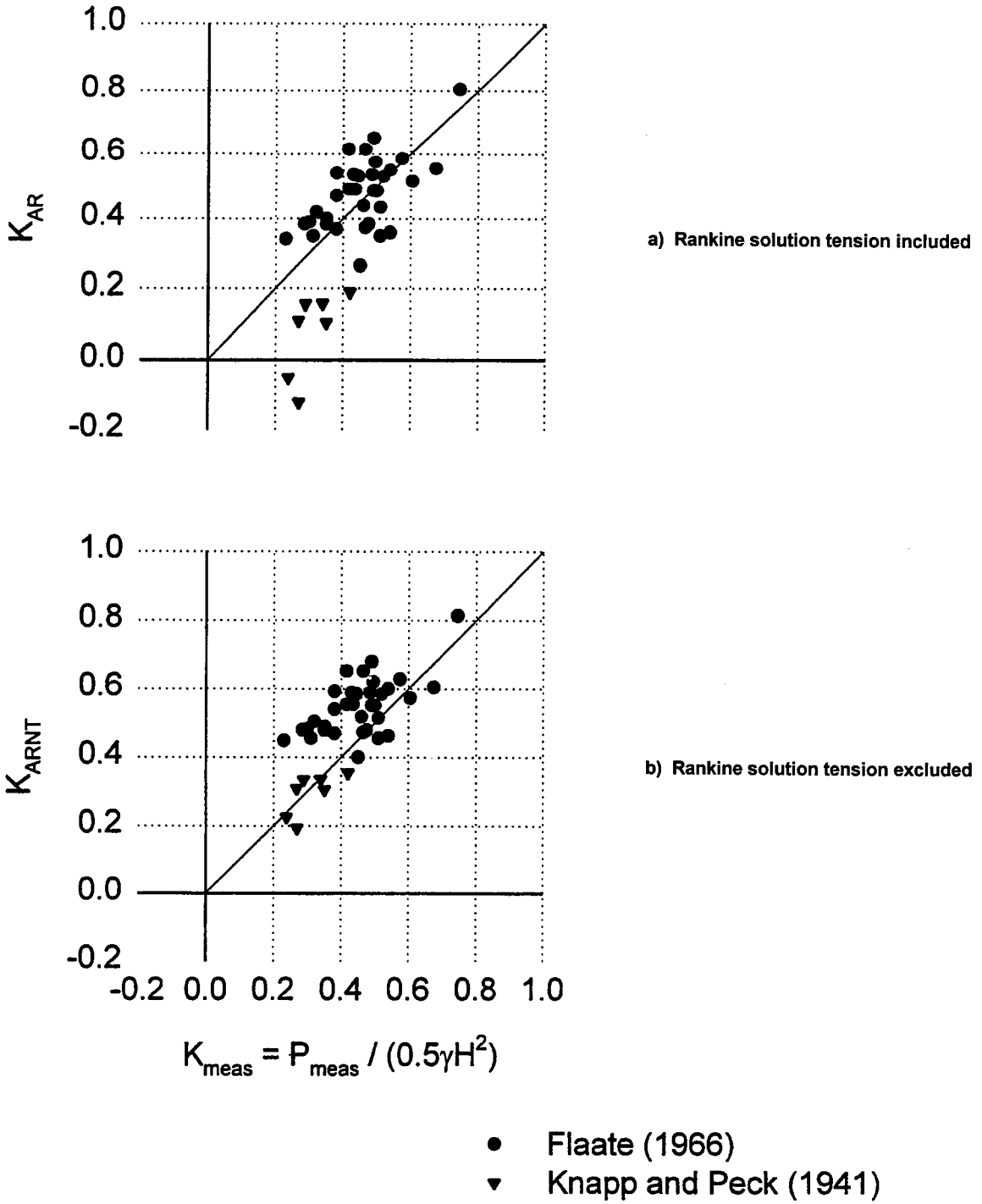


FIGURE 18
Comparison of Predicted Earth Pressure Coefficient with Measured Earth Pressure Coefficient
(Flaate, 1966, and Knapp and Peck, 1941)

The failure surface is assumed to pass through the bottom of the excavation (corner failure) for all these analyses. This assumption is justified in that most excavations are conducted down to firm strata, thus forcing the most probable failure surface through the bottom of the cut.

For sites in which the potential failure surface passes beneath the bottom of the cut (base failure), a larger force will be required for stability. Henkel's (1971) method, described in Chapter 2 provides a means to determine the additional earth pressure when the potential for failure through the base of the excavation is great. The equation for the earth pressure coefficient, K_A , is:

$$K_A = 1 - \frac{4s_u}{\gamma H} + 2\sqrt{2} \frac{d}{H} \left(1 - (2+\pi) \frac{s_{ub}}{\gamma H} \right) \quad \dots [3.4]$$

where d is the depth of the failure surface below the cut, s_u is the undrained shear strength of the soil through which the excavation extends, and s_{ub} is the strength of the soil providing bearing resistance (Figure 6). Use of Equation 3.4 may yield values of earth pressure too small when the soil at the base is stiff enough to force failure through the bottom of the cut. Accordingly, the estimate of K_A should be the greater of Equations 3.2 and 3.4. Henkel (1971) reported the method provided reasonable estimates for earth pressures in excavations in deep deposits of soft to medium clay soils (Table 1).

TABLE 1
Henkel's Lateral Earth Pressure Coefficient, K_A
(Christian, 1989)

SITE	OBSERVED K_A	HENKEL'S SOLUTION
Vaterland 1	0.88	0.89
Vaterland 1	1.12	1.06
Vaterland 1	0.92	0.90
Mexico City	0.66 to 0.80	0.79

3.2.3 Stiff Clays

Stability computations using undrained strengths are misleading for stiff clays ($\gamma H/s_u < 4$) because the clay appears to be self-supporting. However, strut measurements indicate that stiff clays must be supported. The apparent earth pressure distribution recommended by Terzaghi, et al. (1996) result in a total force proportional to $0.75f\gamma H^2$. Based on full-scale measurements, values of f vary between 0.2 and 0.4 (Figure 4c). No undrained stability analyses support the magnitude of load observed from these measurements.

3.2.4 Discussion

Estimates of total load from apparent earth pressure diagrams are based on reasonable agreement between earth pressures predicted using Rankine active earth pressure theory and pressures measured in the field during excavation of braced cuts. Total loads predicted on the basis of limiting equilibrium analyses matched the loads measured in the field.

The determination of the ground anchor force required to support a cut using limiting equilibrium analysis, or slope stability computations, is consistent with an extension of the original work of Terzaghi and Peck (1967). The use of limiting equilibrium procedures has several advantages in that it is a more general formulation of the boundary condition problem, and therefore can accommodate changes in the wall geometry, strength properties, and groundwater conditions in a more fundamental way. However, the use of limiting equilibrium or slope stability computations requires that a consistent definition for a factor of safety be used. The next two sections will define the factor of safety, and quantify the factor of safety inherent with the use of apparent earth pressure diagrams.

3.3 DEFINITION OF FACTOR OF SAFETY AND COMMON VALUES

Ground anchor loads determined using apparent earth pressure diagrams include a factor of safety. When apparent earth pressure diagrams are not used to determine the ground anchor load, there are two means to impose a factor of safety on the anchored wall system. Either the support load required for stability is increased by a factor, FS_{load} , or the anchor load required for stability is determined for a soil with strength reduced by a factor $FS_{strength}$. Both definitions for factor of safety have been used in engineering practice for wall systems. However, the two definitions often result in the different design loads.

3.3.1 Factor of Safety with Respect to Strength — $FS_{strength}$

One method to quantify a factor of safety is to determine the ratio of soil strength available ($\tan \phi_{avail}$) to the soil strength required for stability or mobilized strength ($\tan \phi_{mob}$). The factor of safety for soil exhibiting friction can be defined as

$$FS_{strength} = \frac{\tan \phi_{avail}}{\tan \phi_{mob}} \quad \dots [3.5]$$

For soils exhibiting cohesion, c , the $FS_{strength}$ is defined as

$$FS_{strength} = \frac{c_{avail}}{c_{mob}} \quad \dots [3.6]$$

Factors of safety to quantify the stability of failure surfaces passing below the structural wall components and behind the ground anchors are well suited to use Equations 3.5 and 3.6.

Equations 3.5 and 3.6 can also be applied to failure surfaces intersecting structural or anchor components. The mobilized strength is the strength necessary for stability with the design loads applied. Design loads can be selected to obtain the factor of safety wanted.

Common factors of safety used in practice for the design of anchored walls or slopes range between 1.1 and 1.5. Values adopted for a factor of safety vary with the importance of the wall or slope, the consequences of failure, and economics.

3.3.2 Factor of Safety with Respect to Load — FS_{load}

Another means to quantify the factor of safety for an anchored wall system is the ratio of the applied load to the load required for stability. The factor of safety with respect to load (FS_{load}) is defined as

$$FS_{load} = \frac{Load_{applied}}{Load_{reqd}} \quad \dots [3.7]$$

This definition of factor of safety is applied to failure surfaces passing in front of the anchor, where anchor loads affect the stability of supported soil. Typical values for FS_{load} vary from 1.2 to 2.0.

3.3.3 Factors of Safety for an Example Wall

A simple example is provided to illustrate the difference between a $FS_{strength}$ and the FS_{load} based on a design using the apparent earth pressure envelope for sand (Figure 4a). A vertical cut is assumed to be supported by an anchored wall system. The sand exhibits a friction angle, $\phi = 40^\circ$. The horizontal pressure selected for wall stability and control of displacement is based on the apparent earth pressure concept (Terzaghi, et al., 1996). Apparent earth pressure is assumed to be uniform and horizontal along the full depth of excavation with a magnitude of $0.65K_{AR}\gamma H$, where K_{AR} is the active Rankine earth pressure coefficient and is equal to $\tan^2(45 - \phi/2)$. The uniform pressure corresponds to a total load from apparent earth pressure of $P_{AEP} = 0.65K_{AR}\gamma H^2$, while the minimum load required for stability is $P_{AR} = 0.5K_{AR}\gamma H^2$ (assuming Rankine conditions). The FS_{load} equals 1.3 ($FS = 0.65K_{AR}\gamma H^2 / 0.5K_{AR}\gamma H^2$).

To calculate $FS_{strength}$ ($\tan\phi_{avail}/\tan\phi_{mob}$), ϕ_{mob} must be back calculated. The mobilized friction angle, ϕ_{mob} , is the friction angle required for P_{AR} to equal P_{AEP} calculated using ϕ_{avail} .

$$0.5 \tan^2\left(45 - \frac{\phi_{mob}}{2}\right) \gamma H^2 = 0.65 \tan^2\left(45 - \frac{\phi_{avail}}{2}\right) \gamma H^2 \quad \dots [3.8]$$

For a ϕ_{avail} of 40° , ϕ_{mob} equaled 34° . Therefore, $FS_{strength}$ equals 1.244. Thus, factors of safety based on load may be different from factors of safety based on strength and they cannot be considered equivalent.

3.3.4 Back-calculated Values for Factor of Safety

Before limiting equilibrium analyses can be used to determine the loads required to support anchored walls, estimates of the factor of safety that result from using apparent earth pressure envelopes need to be determined. Apparent earth pressures recommended by Terzaghi, et al. (1996) are used herein to back-calculate factors of safety with respect to load and factors of safety with respect to strength. Their estimates for apparent earth pressures assume that the potential failure surface passes through the bottom corner of the excavation. The effect of failure surfaces passing below the bottom of the excavation will be discussed later.

3.3.4.1 Sand — Apparent Earth Pressures

The apparent earth pressure for sands is a uniform pressure of $0.65K_{AR}\gamma H$ along the height of the wall. Total load from apparent earth pressure is $P_{AEP} = 0.65K_{AR}\gamma H^2$. Assuming Rankine conditions, which is consistent with assuming failure through the corner of the excavation, the total load required for stability is $P_{AR} = 0.5K_{AR}\gamma H^2$. The FS_{load} is the ratio of the two forces (P_{AEP}/P_{AR}), which is equal to 1.3. This ratio is independent of soil strength and wall height.

The $FS_{strength}$ is determined as the ratio of the available strength $\tan(\phi_{avail})$ to the mobilized strength $\tan(\phi_{mob})$. The mobilized strength is determined as the strength required for stability with the apparent earth pressure applied and can be expressed as

$$\phi_{mob} = 2 \left[45^\circ - \text{atan} \left[\sqrt{1.3} \cdot \tan \left(45^\circ - \frac{\phi_{avail}}{2} \right) \right] \right] \quad \dots [3.9]$$

Using Equation 3.9 for defining ϕ_{mob} and Equation 3.5 for defining $FS_{strength}$, the FS varies for different values of soil strength, as shown in Figure 19 and Table 2.

TABLE 2
 $FS_{strength}$ for an Apparent Earth Pressure Wall in Sand (corner failure)

SOIL STRENGTH ϕ_{avail} (deg)	MOBILIZED STRENGTH ϕ_{mob} (deg)	FACTOR OF SAFETY ($\tan\phi_{avail}/\tan\phi_{mob}$)
30	23.29	1.341
35	28.61	1.283
40	34.00	1.244
45	39.43	1.216

The apparent earth pressure diagram for sand was developed for soils with friction angles between 35° and 40° . In this range the $FS_{strength}$ varies between 1.244 and 1.283.

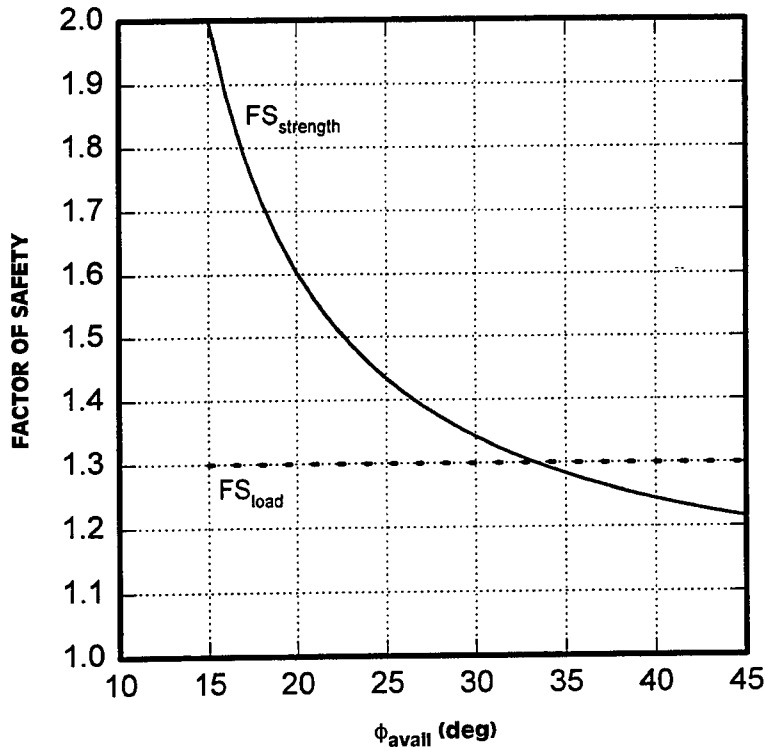


FIGURE 19
Effect of Soil Friction Angle on Factor of Safety with
Respect to Strength and Load for Terzaghi & Peck Sand Criteria
(failure surface passes through bottom corner of the excavation)

3.3.4.2 Sand — K_o Conditions

Factors of safety also can be determined for “at-rest” (K_o) conditions, and may provide a means to identify an upper bound FS for wall design. Although K_o conditions may provide an upper-bound for estimates of earth pressure, requirements imposing loads and deformations consistent with K_o conditions may be uneconomical to achieve in the field.

The FS_{load} can be determined by comparing the total horizontal force required to maintain K_o conditions with the force required to maintain active conditions (K_{AR}). Assuming K_o equals $0.95(1 - \sin\phi_{avail})$, and the total at-rest horizontal force $P_{K_o} = 0.5K_o\gamma H^2$, the FS_{load} can be determined as $FS_{load} = P_{K_o}/P_{AR}$. Similarly, the $FS_{strength}$ for K_o conditions can be determined as $FS_{strength} = \tan\phi_{avail}/\tan\phi_{mob}$. Table 3 shows both values of FS for different strength soils. The relationship is also shown in Figure 20.

For sands, the $FS_{strength}$ can be determined as $\tan(\phi_{avail})/\tan(\phi_{mob})$, where ϕ_{mob} is

$$\phi_{mob} = 2 \left[45^\circ - \text{atan} \sqrt{0.95(1 - \sin\phi_{avail})} \right] \quad \dots [3.10]$$

And the FS_{load} can be expressed as

$$FS_{load} = 0.95 [1 + \sin(\phi_{avall})]$$

... [3.11]

TABLE 3
 $FS_{strength}$ and FS_{load} for K_o Conditions (corner failure)

SOIL STRENGTH, ϕ_{avall} (deg)	$FS_{strength}$	FS_{load}
30	1.52	1.42
35	1.50	1.49
40	1.48	1.56
45	1.46	1.62

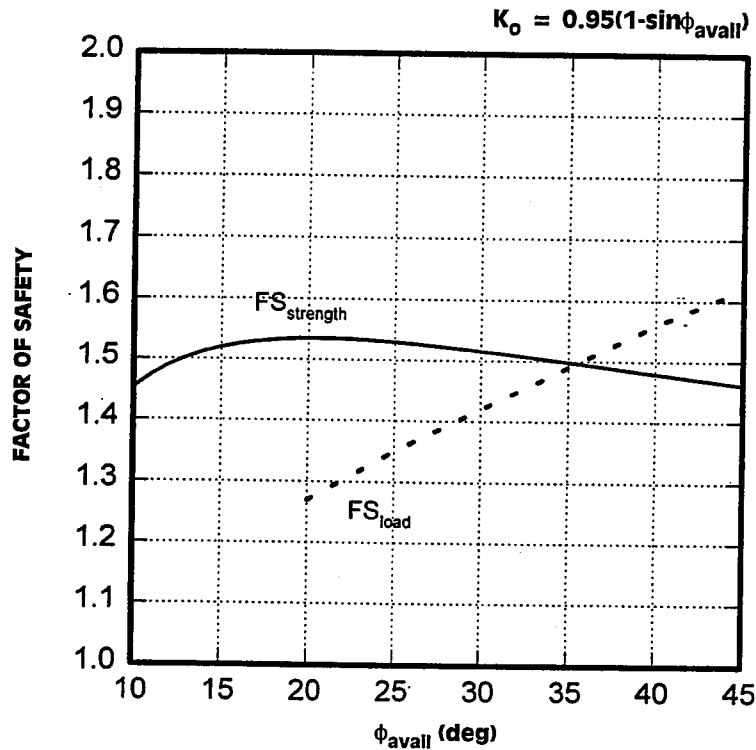


FIGURE 20
Effect of Soil Friction Angle on Factor of Safety with
Respect to Strength and Load Assuming K_o Conditions
(failure surface passes through the corner of the excavation)

The comparison illustrates how the two definitions can indicate different trends in the FS . The $FS_{strength}$ remains almost constant for the range of ϕ illustrated, while the FS_{load} increases considerably with increasing soil strength. The $FS_{strength}$ provides a convenient and more stable reference value for an upper bound FS of approximately 1.5.

3.3.4.3 Sand — Discussion

Based on the back-calculated values of FS using apparent earth pressure and K_o conditions, the total force on the wall, P_{reqd} , should result in a $FS_{strength}$ between 1.2 and 1.5 to be consistent with current design procedures. Walls with FS between 1.0 and 1.2 may be stable, but may also experience undesirable displacements near the wall. Walls constructed with a $FS_{strength}$ near 1.3 result in design loads similar to walls designed to support apparent earth pressures. Walls built with FS between 1.3 and 1.5 may result in smaller displacements (if stiff wall components are also used). Anchored walls built with $FS_{strength}$ of 1.5 may replace the at-rest horizontal pressures for normally loaded sands if at-rest deformation conditions can be maintained. Attempts to control the deformations and satisfy K_o conditions may result in significant horizontal loads that are uneconomical to implement.

3.3.4.4 Soft to Medium Clay ($\gamma H/s_u > 4$)

Anchored walls can provide support for cuts in soft clay. The soft clay criterion is evaluated in terms of FS_{load} and $FS_{strength}$. The apparent earth pressure diagram for soft clays is shown in Figure 4b. In the diagram, the pressure increases linearly to a value of $K_A \gamma H$ at a depth of $0.25H$. The apparent earth pressure remains constant below a depth of $0.25H$. The value of K_A is $1-4s_u/\gamma H$ and the apparent pressures are cited for conditions where the potential failure is through the bottom corner of the cut rather than a base failure. Bottom corner failures occur for conditions where the excavation ends at, or near high strength ground.

Based on the shape of the apparent earth pressure envelope for soft clay (Figure 4b), the total force applied is $0.875\gamma H^2(1-4s_{uavail}/\gamma H)$. Assuming a triangular pressure distribution, the total force is $0.5\gamma H^2(1-4s_{uavail}/\gamma H)$. Using Equation 3.7, the FS_{load} for the soft clay criteria is 1.75 (determined as $0.875/0.5$), which is independent of soil strength and height of the wall.

The same apparent earth pressure results in a $FS_{strength}$ that varies significantly with the term $\gamma H/s_u$. By setting the total force from the apparent earth pressure diagram, $0.875\gamma H^2(1-4s_{uavail}/\gamma H)$, equal to the total force lateral load, $0.5\gamma H^2(1-4s_{umob}/\gamma H)$, s_{umob} can be calculated. Then the $FS_{strength}$ can be calculated using Equation 3.6. For example, the $FS_{strength}$ equals 1.0 at $\gamma H/s_u = 4$, and 4.0 at $\gamma H/s_u = 8$. Accordingly, the apparent earth pressure for soft clay provides little guidance for an appropriate value for $FS_{strength}$. Guidelines for $FS_{strength}$ for soft to medium clays can be developed from the original data reported by Flaate (1966) and Knapp and Peck (1941).

Measured active earth pressure coefficients reported by Flaate (1966) and Knapp and Peck (1941) are summarized in Figure 18a and were used to determine a $FS_{strength}$. Values of K_{AR}

(Equation 3.2) were re-calculated using factored strengths ($s_{u\text{ mob}} = s_u / FS_{\text{strength}}$) and compared with K_{meas} . The FS was increased until K_{AR} for each case history was calculated to be greater than K_{meas} . All values for FS_{strength} were less than or equal to 1.4. Accordingly, a FS_{strength} equal to 1.4 provides conservative estimates of K_{AR} for computing total lateral force ($0.5 \gamma H^2 K_{AR}$) for the cited case studies. However, the calculation for K_{AR} (Equation 3.2) allows tension to be developed in the soil, and effects of soil tension become significant for cuts with $\gamma H / s_u < 5.5$.

Earth pressures were calculated for the same case studies described above, except the soil could not develop tension (Equation 3.3 and Figure 18b). All values of K_{ARNT} were calculated to be greater than K_{meas} for each case study when a $FS_{\text{strength}} = 1.25$. Accordingly, estimates of earth pressure that do not allow tension in the soil require only a $FS_{\text{strength}} = 1.25$.

3.3.4.5 Stiff Clays ($\gamma H / s_u < 4$)

The apparent earth pressure diagram recommended by Terzaghi, et al. (1996) for stiff clay is trapezoidal in shape with maximum pressure, $p = f \gamma H$ (Figure 4c). Values of f between 0.2 and 0.4 are recommended. The pressure increases linearly from the ground surface to a depth of $0.25H$, remains constant from $0.25H$ to $0.75H$, and then decreases linearly to zero at $1.0H$. The resulting total force is $0.75f \gamma H^2$.

An FS_{load} for temporary walls in stiff clay cannot be defined because the strength of the stiff clay ($\gamma H / s_{u\text{ avail}} < 4$) is theoretically enough to require no additional horizontal force for support of the cut. Therefore, FS_{load} cannot be defined. However, the FS_{strength} can be determined for the stiff clay by comparing the available strength of the clay to the minimum strength of the clay required for supporting the cut. The results are

$$FS_{\text{strength}} = \frac{4}{\frac{\gamma H}{s_{u\text{ avail}}} (1 - 1.5f)} \quad \dots [3.12]$$

where f is between 0.2 and 0.4. The variation of FS_{strength} with the non-dimensional term $\gamma H / s_u$ is shown in Figure 21 for values of f equal to 0.2, 0.3, and 0.4. The results show that the FS_{strength} becomes very large for small values of $\gamma H / s_u$ and illustrates that *undrained strength stability analyses for anchored walls in stiff clays should not be done*.

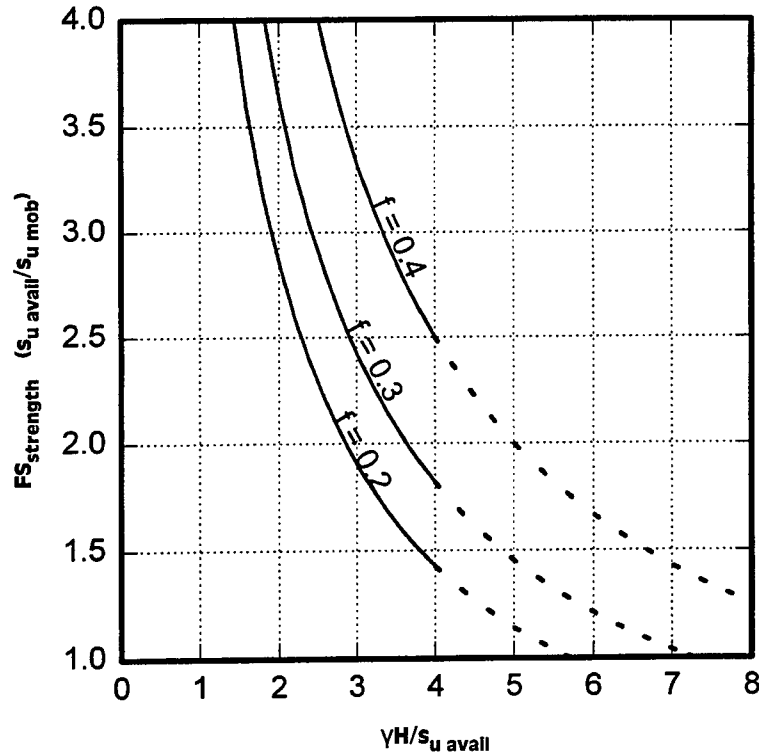


FIGURE 21
Effect of $\gamma H / s_{u \text{ avail}}$ on Factor of Safety (With Respect to Strength)
Assuming Terzaghi & Peck Distribution for Stiff Clay Conditions
(failure surface passes through the bottom corner of the excavation)

3.3.4.6 Interpretation of the Stiff Clay Criteria as a Frictional Soil

The relationship between apparent earth pressure for stiff clay and the drained strength that would be required for stability is established in this section. The equivalent strength, ϕ_{mob} , for a frictional soil is back-calculated using P_{AEP} from the stiff clay criteria and $P_{AR} = 0.5\gamma H_2 K_{AR}$, where $K_{AR} = \tan^2(45 - \phi_{mob}/2)$. The resulting equation is

$$\phi_{mob} = 2 \left(45^\circ - \text{atan} \sqrt{1.5f} \right) \quad \dots [3.13]$$

Using Equation 3.13, values of $f = 0.2, 0.3$ and 0.4 result in ϕ_{mob} of $32.5^\circ, 22.2^\circ$, and 14.5° , respectively. Therefore, a soil with a friction angle of 32.5° would require an apparent earth pressure envelope with $f = 0.2$ to support a vertical cut (with $FS_{\text{strength}} = 1.0$). Relationships between FS_{strength} and ϕ_{avail} based on Equation 3.13 are shown in Figure 22 for three values of f (0.2, 0.3, and 0.4).

Figure 22 may be used by assigning the stiff clay a friction angle corresponding to its drained strength (ϕ_{avail}). Friction angles for the clay may be determined from information available to

identify the soil, such as results of strength tests, classification tests, or geologic origin. Friction angles plotted as a function of plasticity indexes are shown for some clays in Figure 23; however, it can be seen that, while there is a trend for decreasing strength with greater plasticity, the scatter prevents a unique relationship from being drawn. Furthermore, drained strengths of a soil will depend on the soil's stress history, degree of fissuring, and degree of pre-shearing. At certain stress levels, the drained strength of overconsolidated clays may be represented by an effective stress friction angle and cohesion.

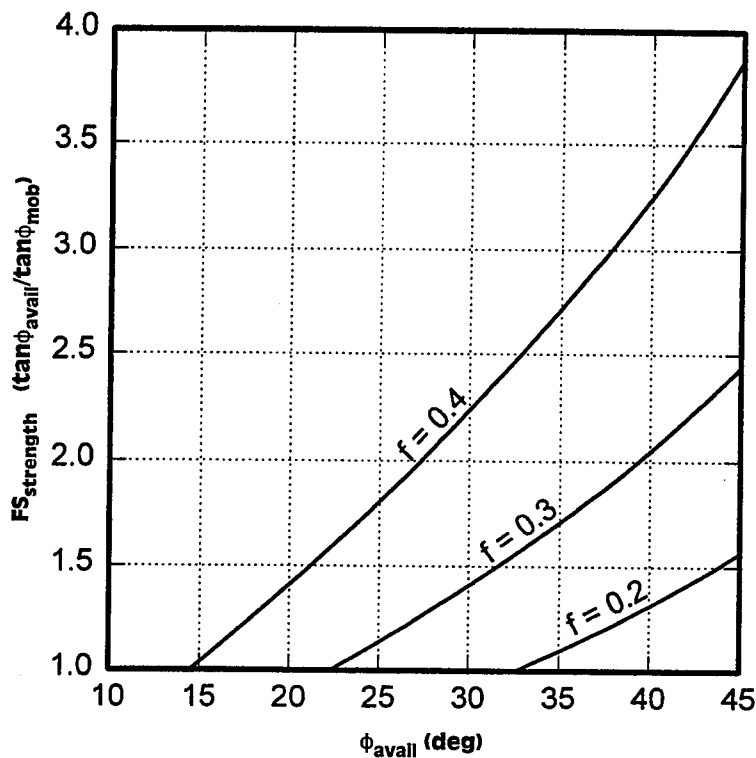


FIGURE 22
Effect of Friction Angle on Factor of Safety (With
Respect to Strength) for Terzaghi & Peck Stiff Clay Criteria
(failure surface passes through the bottom corner of the excavation)

To illustrate this reinterpretation, a soil with drained strength ϕ_{avall} equal to 25° would correspond to an $f = 0.28$ for a $FS = 1$. A factor of about 0.36 would be required for a $FS_{strength} = 1.5$.

Since this reinterpretation does not include a cohesion intercept, this method may predict pressures greater than necessary for support. Including cohesion may give a more realistic representation of the soil strength.

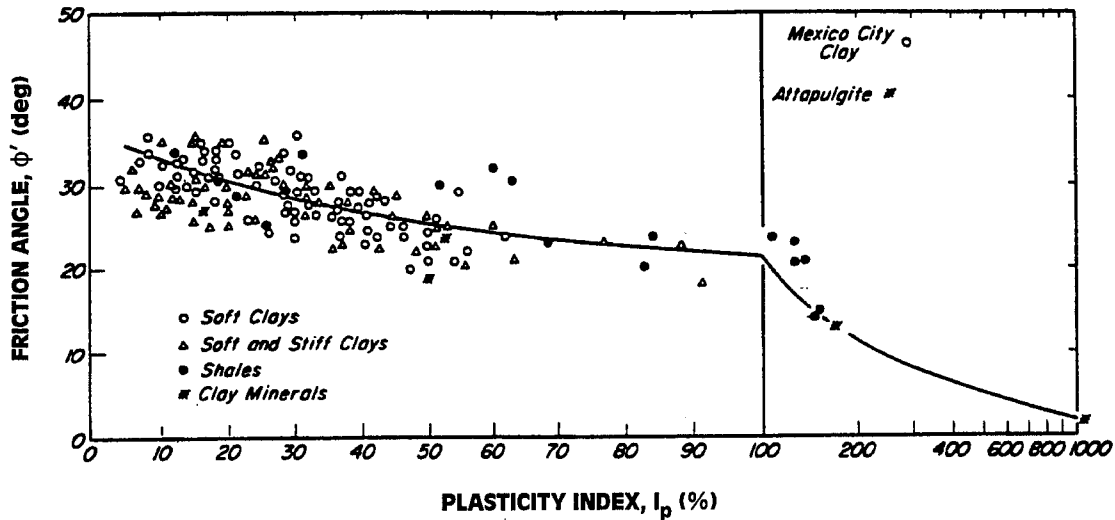


FIGURE 23
Relationship Between Drained Friction Angle for Clays and Plasticity Index
(from Terzaghi, et al., 1996)

3.3.4.7 Discussion

Terzaghi, et al. (1996) ensured that the total force from the apparent earth pressure was adequate for wall safety by comparing more fundamental methods, such as limiting equilibrium, with simple estimates, such as those obtained by Rankine analyses. Therefore, limiting equilibrium methods provide a fundamental and valid approach to determining the total force necessary to support a cut. The limiting equilibrium approach is consistent with the current approach for apparent earth pressures, and therefore, can be used for determining the overall load required for the stability of a vertical cut. General trends for designs built with apparent earth pressures are that the $FS_{strength}$ for frictional ground varies between 1.25 and 1.3.

Limiting equilibrium analyses for anchored walls in soft clays should exhibit $FS_{strength}$ between 1.25 and 1.4. In addition, the total anchor force determined from the limiting equilibrium analysis should be checked using apparent earth pressure diagrams for soft to medium clay.

Limiting equilibrium should not be used for the design of anchored walls constructed in stiff clay soils ($\gamma H/s_u < 4$). Anchored walls in stiff clays should be designed to support apparent earth pressures. If drained shear strength parameters are known, they can be used in a limiting equilibrium analysis or the appropriate apparent earth pressure diagram to determine the total ground anchor load. Permanent ground anchor walls in stiff clays should be designed to support the largest earth pressure determined from either the stiff clay apparent earth pressure or using drained shear strength parameters.

3.4 SIMPLIFIED LIMITING EQUILIBRIUM APPROACH

A force equilibrium method is used herein to illustrate the effects of wall components on the stability of an anchored wall system. Results of the equilibrium formulation are compared with some traditional formulations for quantifying earth pressures.

A simple and rational approach to determine the requirements for stability of a soil mass is to determine the additional force required to satisfy both horizontal and vertical equilibrium. Coulomb (1776) first used this approach for analysis of gravity retaining walls. Force equilibrium also provides a basis for several existing design and analysis methods for determining the stability of anchored wall systems (Kranz, 1953; Ostermayer, 1977; Broms and Benne-mark, 1968; Broms, 1988).

Limiting equilibrium can be used to determine total anchor force. The anchor loads will equal the force required to support the active wedge of soil. Limiting equilibrium also is used to determine the overall stability of the soil/anchor system acting as a mass. The assessment of total anchor load, and overall stability are the objectives of a stability analyses where failure surfaces are drawn at any point between the end of the anchor and the active wedge (Figure 24).

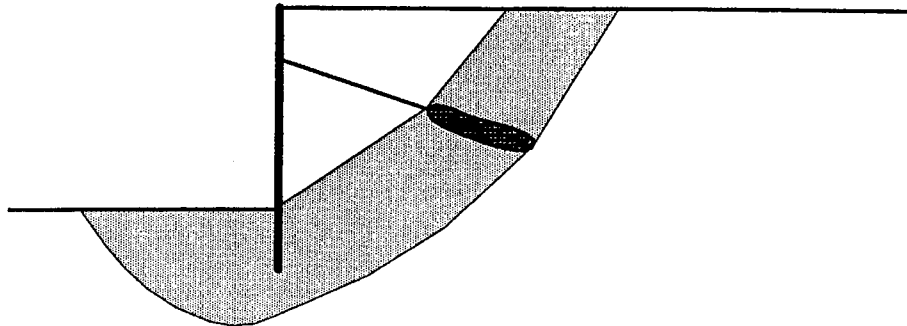
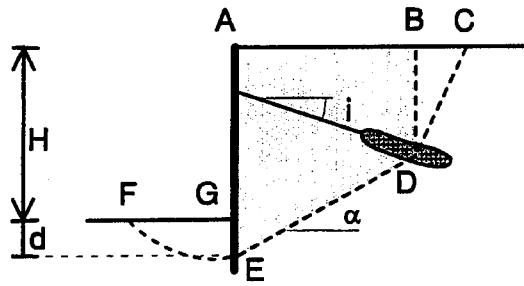
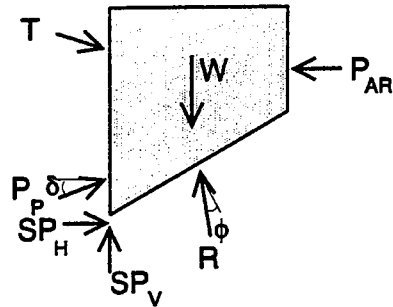


FIGURE 24
Failure Surface Used in Limiting Equilibrium Analyses of Anchored Walls

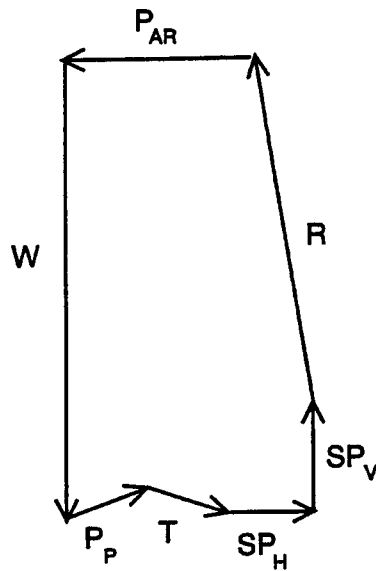
An anchored wall is shown in Figure 25a to illustrate the components of the wall system. The shaded area (ABDEG) represents the portion of soil for which stability will be determined. The potential failure surface is illustrated as a dashed line (FEDB and FEDC). The potential failure surface is assumed to pass through part of the ground anchor (point D), beneath the bottom of the cut through the soldier pile (point E), and then surfaces at some distance from the wall at point F.



a) Example of tiedback wall system



b) Free-body diagram



c) Force vectors acting on area ABDEG

FIGURE 25
Force Equilibrium Considerations for an Anchored Wall System

The soil mass ABDEG is represented as a free body in Figure 25b along with the forces exerted by the components of the anchored wall system. Gravity forces exerted by the shaded

portion of the soil mass are represented as a force vector W . Active soil pressure acts on the right vertical face (BD) and is represented as a force with a total magnitude of P_{AR} . The force applied by the anchor to the free body is represented by T . The magnitude of T depends on the location that the potential failure surface intersects with the anchor bond length (point D). For a failure surface passing between the wall and the anchor zone, full anchor force is available for support of the shaded soil mass. However, no anchor force is available for a potential failure surface that passes outside the anchor zone, because the anchor provides no external forces to the shaded area. If the failure surface (point D) passes through the anchor, the anchor force must be assigned a load that can be developed along the length of the anchor outside the area ABDEG.

Resistance due to the soil strength along the bottom surface is represented as force vector R , and the passive soil resistance provided by the soil on the left side of line EG is represented by P_p . Resistance provided to the free body by the components of the wall (soldier pile) that extend beyond the boundaries of the free body (ABDEG) are horizontal resistance, SP_h , and vertical resistance, SP_v .

The composite action of all the force vectors is illustrated in Figure 25c. Summing the forces in the x-direction (horizontal) gives

$$\Sigma F_x = P_p \cos(\delta) + T \cos(i) + SP_h - R \sin(\alpha - \phi) - P_{AR} \quad \dots [3.14]$$

and summing forces in the y-direction (vertical) results in

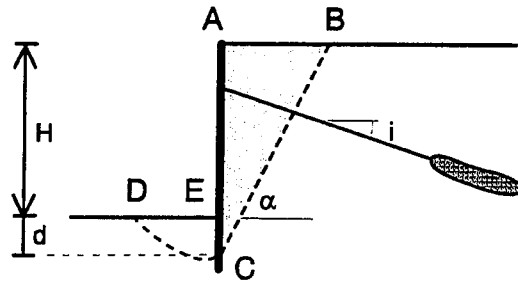
$$\Sigma F_y = W - P_p \sin(\delta) + T \sin(i) - SP_v - R \cos(\alpha - \phi) \quad \dots [3.15]$$

The term δ is the interface friction angle between the embedded portion of the wall and the passive zone of the soil. Equations 3.14 and 3.15 are the basic equilibrium equations used to determine the safety of an anchored wall system. The equations can be arranged to determine:

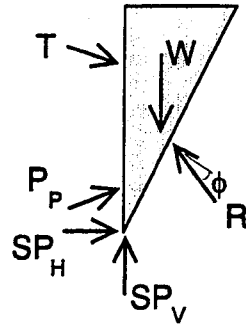
- Minimum soil strength required to provide stability for a given anchor load.
- Toe resistance required by the soldier piles.
- Anchor force necessary to provide stability.

3.4.1 Results for a Simple Failure Surface

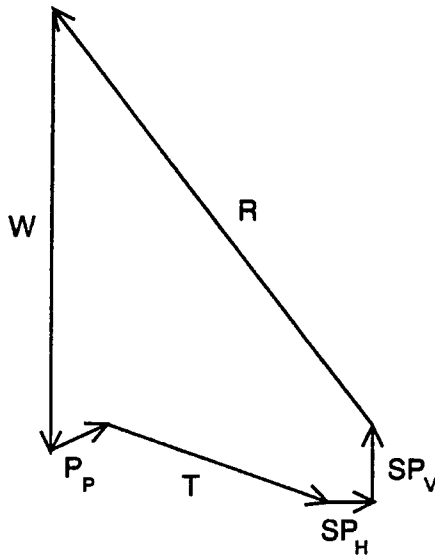
The force equilibrium method is used to determine the total force required to support the cut. An example of an anchored wall system is adopted to illustrate the force equilibrium method (Figure 26a). The anchored wall system retains a vertical cut in a sand with frictional strength, ϕ , unit weight, γ , and height, H . The unbonded length of the anchor extends far behind the wall to ensure that the most critical failure surface passes above the anchor zone and the full anchor load contributes to wall stability. The potential failure plane passes through the toe at depth, d , and mobilizes a passive resistance from the soil, P_p , and a horizontal and vertical resistance from the soldier pile (SP_h , SP_v , respectively).



a) Example of tiedback wall system



b) Free-body diagram



c) Force vectors acting on area ABCE

FIGURE 26
Force Equilibrium Considerations for an Anchored Wall System
with the Failure Surface in Front of the Anchor Bond Length

For simplicity, the shape of the planar failure surface is assumed to be a straight line (BC), as shown in Figure 26a. Although a number of shapes could have been used for the failure sur-

face, a straight line approximation for the active portion of retained soil has been found to be adequate (Taylor, 1948; Terzaghi, et al., 1996). Beneath the bottom of the cut, the failure surface is assumed to be shaped as a log spiral on the passive portion of the soil. For soldier pile and lagging walls, significant soil to soil contact exists, thus interface resistance along the vertical face CE is assumed to be equal to the strength of the soil.

Passive toe resistance is $P_p = 0.5\gamma d^2 K_p$. The passive earth pressure represents the passive resistance provided by the soil above the failure surface at the toe. Passive earth pressure coefficients were determined assuming a log spiral failure surface in the passive zone (Terzaghi, et al., 1996). Passive earth pressure coefficients are shown in Figure 27.

The contribution of forces from the anchor and soldier pile are shown as force vectors T , SP_h , and SP_v . For simplicity and for ease of comparison with other solutions, the three forces are treated as a horizontal force with magnitude P_{reqd} . Thus, P_{reqd} represents the horizontal force required to provide stability to the vertical cut. Taking P_{reqd} as horizontal implicitly assumes that the vertical force in the soldier pile (SP_v) is equal in magnitude (and opposite in direction) to the vertical component of the anchor load ($T \cdot \sin(i)$). This allows consideration of the forces that act on the *soil* (not the soil/wall system). The forces on the soil are shown in Figure 28.

The solution for the external force required for stability (P_{reqd}) continues by summing the forces in the x-direction to get

$$\Sigma F_x = P_p \cos(\delta) + P_{reqd} - R \sin(\alpha - \phi) \quad \dots [3.16]$$

and summing forces in the y-direction (vertical) to get

$$\Sigma F_y = W - P_p \sin(\delta) - R \cos(\alpha - \phi) \quad \dots [3.17]$$

Combining the two equations and solving for P_{reqd} results in the following expression:

$$P_{reqd} = \frac{1}{2} \gamma H^2 \left[\frac{(1+\xi)^2}{\tan(\alpha)} - K_p \xi^2 \left(\sin(\delta) + \frac{\cos(\delta)}{\tan(\alpha - \phi)} \right) \right] \tan(\alpha - \phi) \quad \dots [3.18]$$

where ξ is the ratio of d/H , α is the angle of the failure plane with respect to the horizontal, and all other parameters have been defined previously. The solution proceeds by varying values of ξ and α until a maximum for P_{reqd} is determined. Solutions were determined for soil friction angles of 20°, 30°, and 40°, and are presented in Table 4 in non-dimensional form as $K_{reqd} = P_{reqd} / (0.5\gamma H^2)$.

TABLE 4
Magnitudes of K_{reqd} for the Force Equilibrium Method (base failure)

ϕ (deg)	K_{reqd}	ξ	α
20	0.570	0.162	54
30	0.349	0.047	60
40	0.220	0.012	65

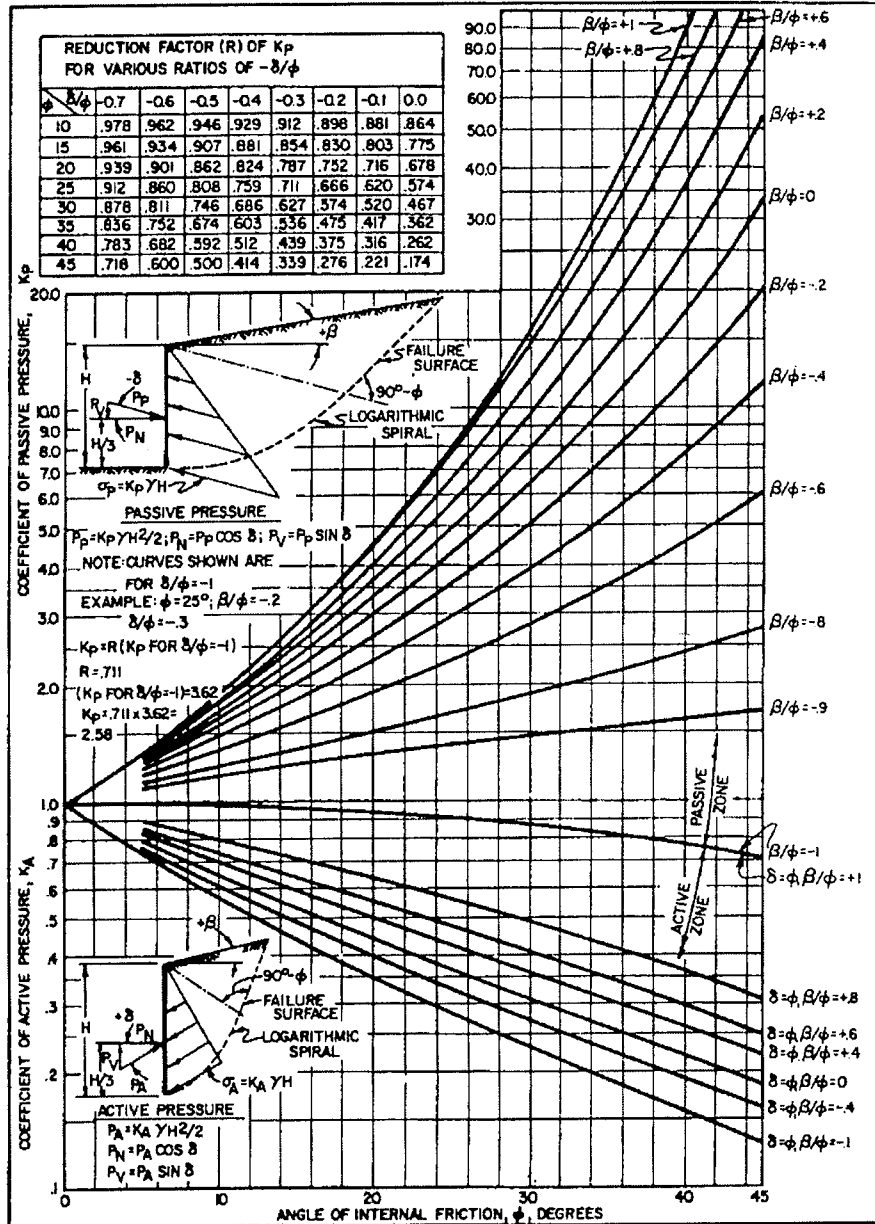
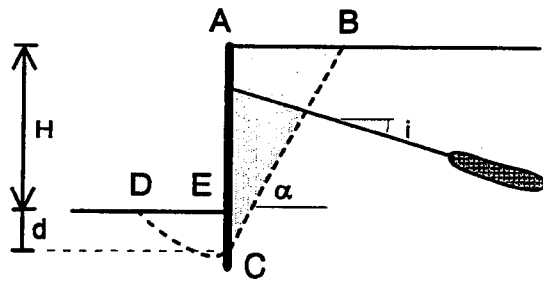
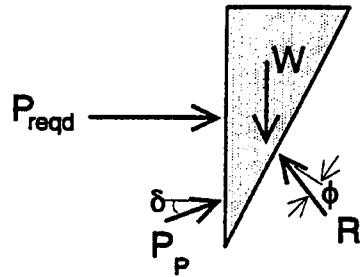


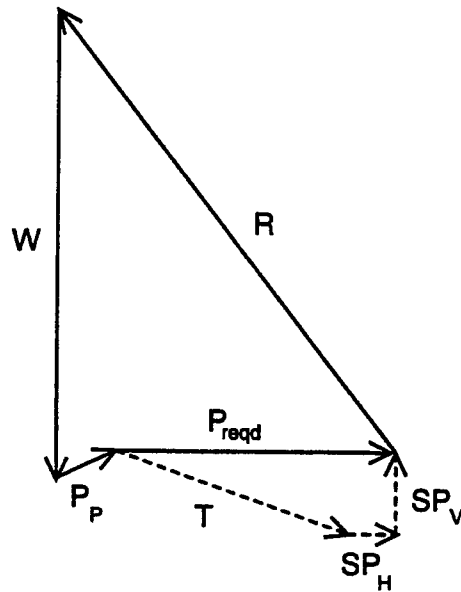
FIGURE 27
Passive Earth Pressure Coefficients (NAVFAC DM7.2, 1982)



a) Example of tiedback wall system



b) Free-body diagram



c) Force vectors acting on area ABCE

FIGURE 28
Force Equilibrium Considerations for an Anchored Wall System with P_{reqd}

Thus, the magnitude of load required to support a vertical cut of height, H , would be $P_{reqd} = 0.5\gamma H^2 K_{reqd}$.

Equation 3.18 requires failure surfaces that pass below the bottom of the cut. For soil strength below 30° , failure surfaces passing below the bottom of the cut require more anchor load for stability than failure surfaces passing through the bottom corner of the cut. However, most conventional methods for determining the required load for support assume the failure surface passes through the bottom of the cut. Accordingly, the magnitude of P_{reqd} for low-strength soils is expected to be greater than the total force estimated from apparent earth pressure methods that assume failure surfaces through the bottom of the cut.

3.4.2 Comparison with Rankine Analysis

A Rankine analysis is an approach frequently used to estimate the active earth pressures against a wall, and provides a good measure with which to compare the simplified force equilibrium analysis. The estimate of load required to support a wall is determined as $P_{AR} = 0.5\gamma H^2 K_{AR}$ where K_{AR} is the active earth pressure coefficient determined as $K_{AR} = \tan^2(45 + \phi/2)$. The use of Rankine earth pressure and H implicitly assume the maximum force required to support the cut coincides with a failure surface that passes through the bottom corner of the cut (corner failure). However, failure may also occur below the bottom of the cut (this is identified as a base failure and is illustrated in Figure 28). A comparison of the magnitude of K_{AR} and K_{reqd} is shown below in Table 5 for three soil strengths.

TABLE 5
Comparison of Earth Pressure Coefficients K_{reqd} and K_{AR}

ϕ (deg)	K_{reqd} (base failure)	K_{AR} (corner failure)
20	0.570	0.490
30	0.349	0.333
40	0.220	0.217

Reasonable agreement between the two failure modes exists for friction angles equal to or greater than 30° . However, the K_{reqd} is 16 percent greater than K_{AR} for a soil with a friction angle of 20° . The failure surface for a soil with a friction angle of 20° extends below the bottom of the cut far enough to cause this difference in earth pressure coefficients.

Factors of safety were determined for the case of a vertical cut supported by the apparent earth pressure for sand. Factors of safety were determined for base and corner failures to illustrate the effect of the mode of failure. The factor of safety with respect to load and strength is shown in Figure 29. The difference between a corner failure and base failure is minor for friction angles equal to or greater than 30° , but the difference is significant for friction angles less than 30° . Since most granular soils exhibit friction angles greater than 30° , the differences between base and corner failures will be small for most cuts.

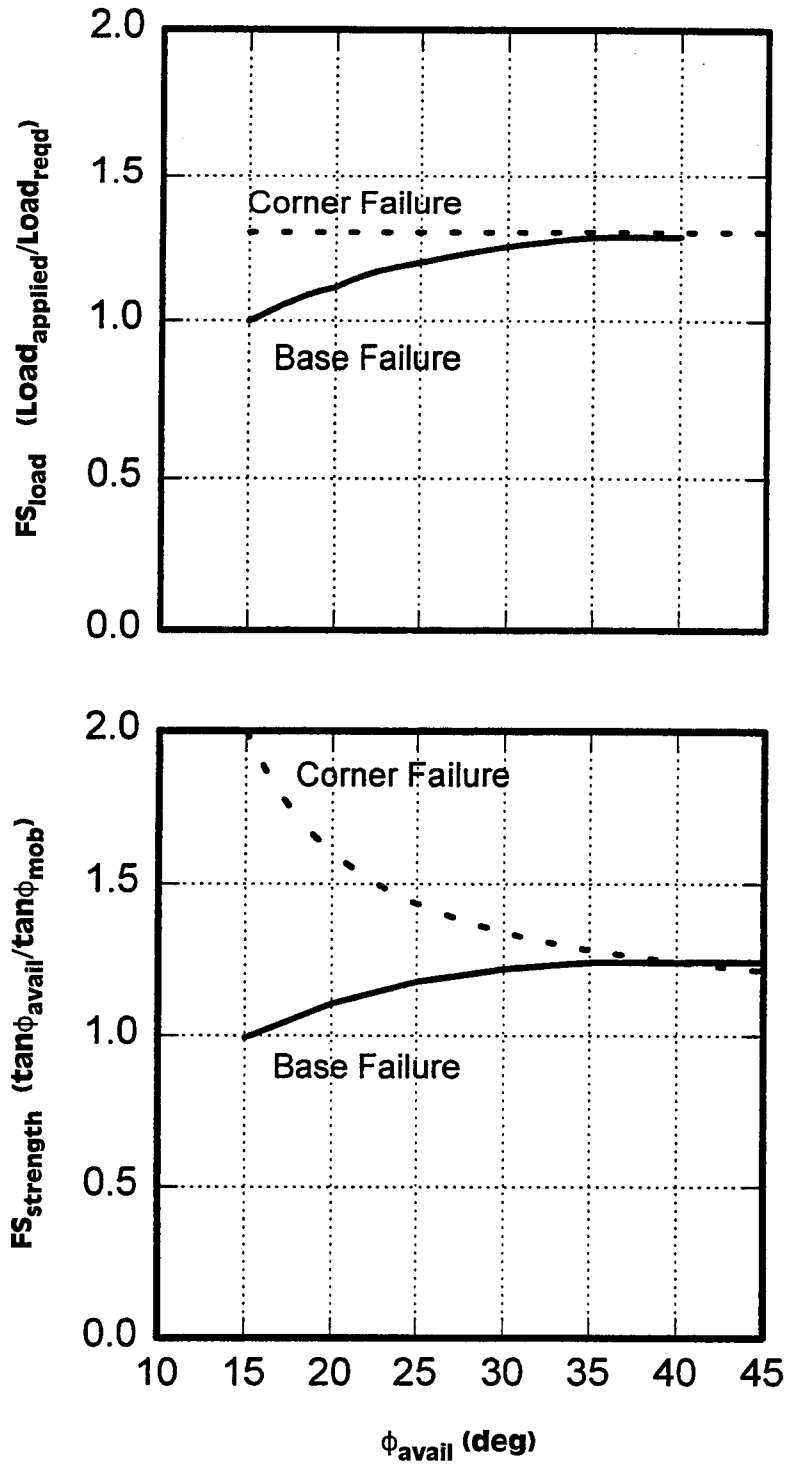


FIGURE 29
Effect of Soil Friction Angle on Factor of Safety
for Surfaces that Pass Through the Bottom Corner of
the Base Using Terzaghi & Peck Criteria for Sand

3.4.2.1 Discussion of Force Equilibrium

The example problem shows the use of force equilibrium for determining the stability of an anchored wall. The potential failure surface that provides the least resistance to sliding will in general be nonlinear; however, studies by Taylor (1948), Terzaghi, et al. (1996), and others have shown that only small errors are associated with approximating the potential failure surface as linear. Furthermore, the method presented herein considers only force equilibrium. Many of the analyses presented have been compared with more rigorous methods that consider force and moment equilibrium. Agreement was found to be excellent between the methods presented and the more rigorous methods. Additional discussion of advantages and disadvantages of requiring moment equilibrium can be found in Duncan (1992), Fredlund and Krahn (1977), and Wright, et al. (1973).

3.5 USING LIMITING EQUILIBRIUM AS AN APPROACH FOR DESIGN

A procedure that uses the force equilibrium method for design of anchored walls is described in three parts: (1) requirements for the wall to provide stability for potential failure surfaces passing completely within the unbonded portion of the anchor (*internal stability*); (2) requirements for potential failure surfaces passing beyond the anchored portion of the anchor (*global stability*); and (3) requirements for failure surfaces that may pass through the anchor zone (*intermediate stability*).

3.5.1 Simplified Approach — Internal Stability

The internal stability for an anchored wall system determines the total force required to keep that wall system stable, and also can be used to determine the unbonded length ($L_{unbonded}$) of the ground anchor system. The procedure to determine P_{reqd} and $L_{unbonded}$ is described in this section. Equations developed herein use force equilibrium procedures similar to those described above.

3.5.1.1 Development of Equations for Determining Internal Stability

The internal stability of an anchored wall system is ensured by providing an external force, P_{reqd} , that satisfies all requirements for equilibrium. An example failure surface is illustrated in Figure 26. The equation relating P_{reqd} to wall geometry and soil properties is given in Equation 3.18 assuming a horizontal soil surface at the top of the wall. If the soil at the top of the wall slopes at angle β , Equation 3.18 is modified to:

$$P_{reqd} = \frac{1}{2} \gamma H^2 \left[\frac{(1+\xi)^2}{\tan(\alpha) - \tan(\beta)} - K_p \xi^2 \left(\sin(\delta) + \frac{\cos(\delta)}{\tan(\alpha - \phi)} \right) \right] \tan(\alpha - \phi) \quad \dots [3.19]$$

where all parameters α , β , γ , δ , ξ , ϕ , and H have been defined previously. The effect of the slope, β , on P_{reqd} is given in Table 6. The maximum P_{reqd} is determined by varying the non-

dimensional depth factor ξ and the slope of the potential failure surface α . The magnitude of P_{reqd} for soil strengths between 20° and 40° and slope angles between 0° and 20° is shown in Figure 30. The combination of depth and angle that correspond to the maximum P_{reqd} identifies the location of the potential failure surface. Failure surfaces for slope angle β between 0° and 20° , and soil strength ϕ between 20° and 40° are shown in Figure 31.

TABLE 6
Comparison of P_{reqd} for Different Wall Geometries

ϕ (deg)	β (deg)	P_{reqd} BASE FAILURE (kN/m)	P_{reqd} BOTTOM FAILURE (kN/m)
20	0	570	490
25		442	406
30		349	333
35		275	271
40		220	217
20	5	618	524
25		472	431
30		369	352
35		288	284
40		230	227
25	10	511	462
30		394	374
35		305	300
40		241	238
30	15	426	402
35		324	319
40		254	251
35	20	350	344
40		271	267

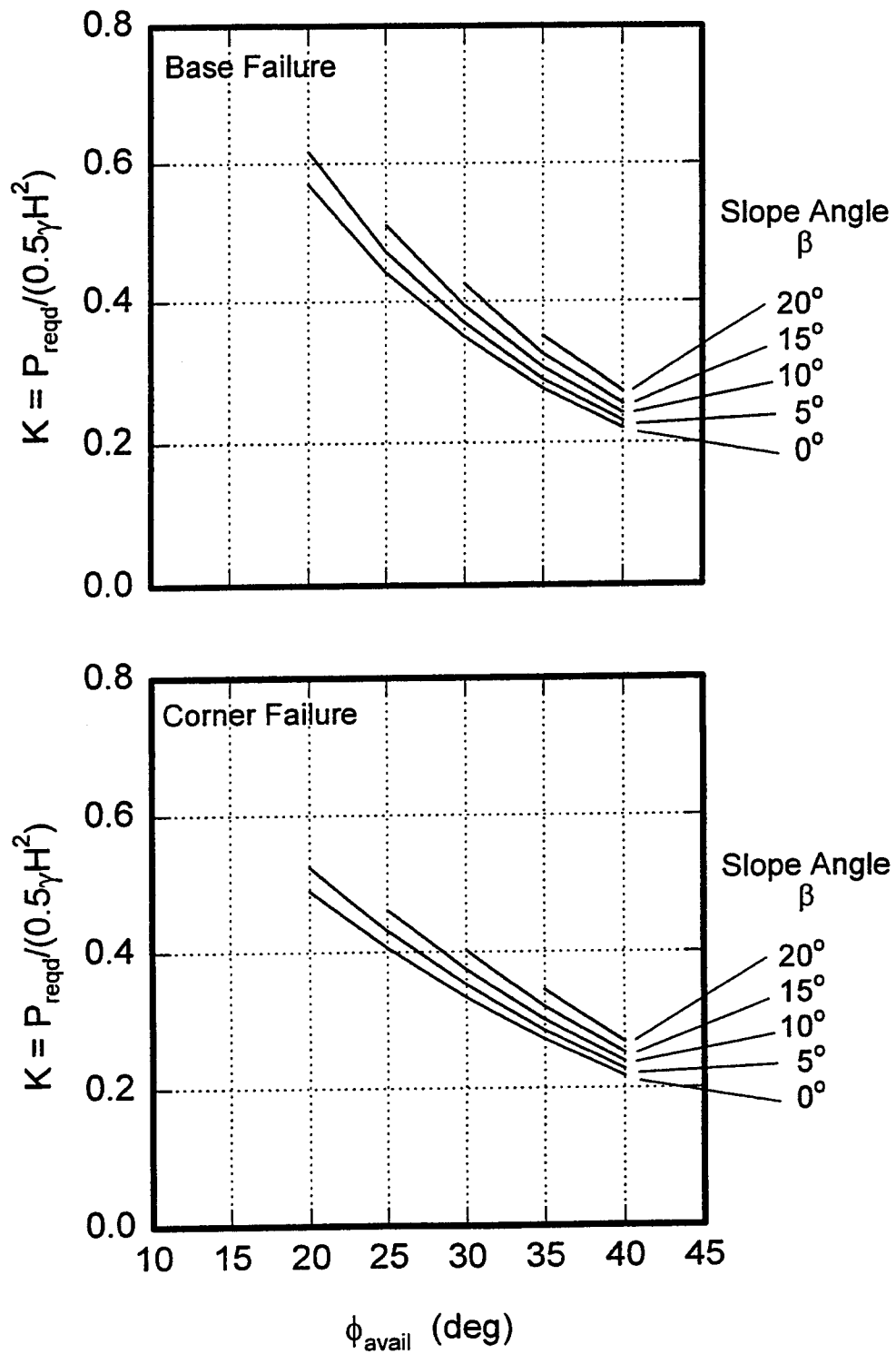


FIGURE 30
Effect of Sloping on Magnitude of $P_{reqd}/(0.5\gamma H^2)$

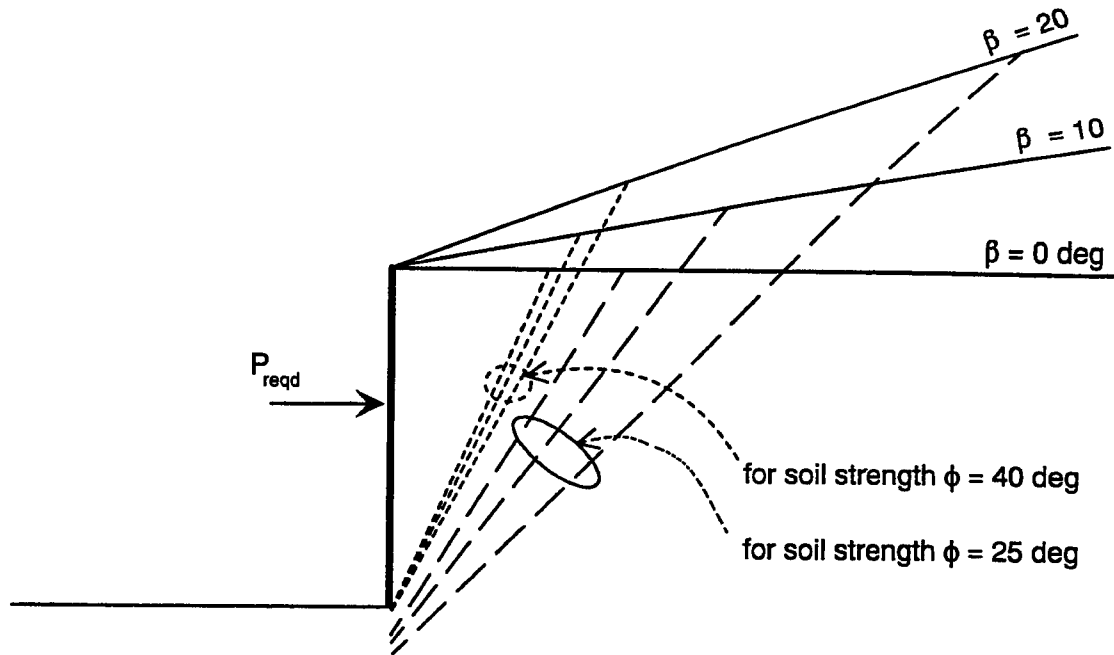


FIGURE 31
Critical Failure Surfaces for Frictional Soils with Different
Strengths and Different Slopes at Top of Wall

3.5.1.2 Evaluation of Minimum Unbonded Length

The anchor bond length, the portion of a ground anchor that contributes to the stability of a retained soil, should be behind the critical failure surface. Any portion of an anchor within the zone of sliding cannot contribute to the support of the cut. Thus, it is important to identify the location of the potential failure surface to determine the minimum unbonded length of the anchor and where to locate the anchor bond length.

Three methods for determining the minimum unbonded anchor length will be presented and compared. They are: a method based on Rankine analysis, a method proposed by Peck, et al. (1974), and a method based on the force equilibrium method (Equations 3.18 and 3.19).

The Rankine method identifies the potential plane of sliding as a plane of failure passing through the bottom of the wall and angled up at $\alpha = 45 + \phi/2$ with respect to a horizontal plane. The anchor bond length must be behind this failure plane.

The second method, proposed by Peck, et al. (1974), modified the Rankine method by requiring the unbonded length of an anchor to extend beyond the Rankine failure plane by a length equal to one-fifth of the total height of the wall.

The third method employs the force equilibrium method (Equations 3.18 and 3.19). The potential failure surface can be identified by determining the angle of the failure plane (α) and a depth ratio (ξ) of the potential failure plane that result in the largest magnitude of P_{reqd} . Magnitudes of α and ξ for soils with different strengths are presented in Table 4. Illustrations of the failure plane for some combinations of soil strength, ϕ , and soil slope, β , are shown in Figure 31. Ground anchors should develop their load-carrying capacity in the soil beyond the failure plane, therefore, the position of the failure plane identifies the minimum unbonded length.

A comparison of the minimum unbonded length predicted using the three methods is shown in Figure 32 for soil strengths of 20° and 40° . For soils having an angle of internal friction equal to 20° , the Rankine failure surface is closest to the wall, and thus, results in the shortest unbonded lengths. The method suggested by Peck, et al. (1974) gives the greatest lengths, while the force equilibrium method yields intermediate lengths. For $\phi = 40^\circ$, the force equilibrium and the Rankine failure surfaces pass through the bottom of the cut and make an angle with the horizontal equal to $45 + \phi/2$.

A comparison of the predicted failure surfaces for walls with back slopes is shown in Figure 33. It can be seen that the minimum unbonded lengths required by Peck, et al. (1974) agree reasonably with the force equilibrium method (base failure) for low-strength soil ($\phi = 20^\circ$). However, for the stronger soil ($\phi = 40^\circ$), the method by Peck, et al. (1974) predicts greater unbonded lengths.

The force equilibrium method considers the strength of the soil and geometry and provides a good estimate of the location of the critical failure surface. When using the force equilibrium method to determine the unbonded length, the unbonded length must extend behind the failure surface to ensure that the ground anchor develops its load-carrying capacity behind the critical failure surface. Current Federal Highway Administration (FHWA) practice is to extend the unbonded length behind the critical failure surface 5 ft or a distance equal to 20 percent of the height of the wall.

The force equilibrium method provides a better estimate for the location of the potential failure plane, and therefore, a better estimate for the required unbonded length. The Rankine failure surface identifies unbonded lengths that are either in agreement or shorter than those required by the force equilibrium method. The method suggested by Peck, et. al. (1974) appears to predict unbonded lengths greater than the force equilibrium method when the ground behind the wall is level, and unbonded lengths greater than or approximately equal to lengths predicted with the force equilibrium method when the ground behind the wall slopes upward.

Agreement between methods may not always be predictable because of the influence of soil non-homogeneity, surcharges behind the wall, and presence of groundwater and seepage. Consideration of these elements would require a more general analysis of stability (discussed in Chapter 4).

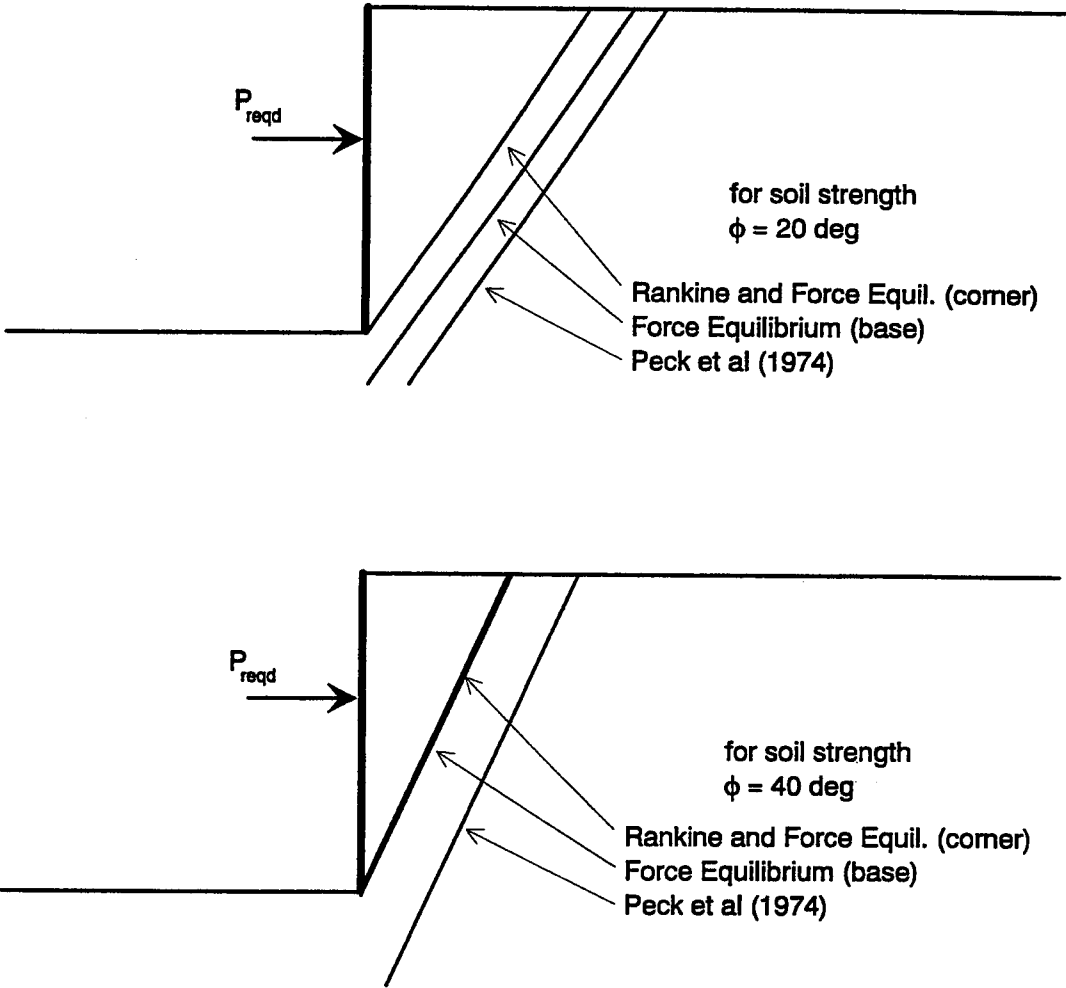


FIGURE 32
Comparison of Three Methods for Determining Minimum Unbonded Length of an Anchor, Horizontal Ground Surface

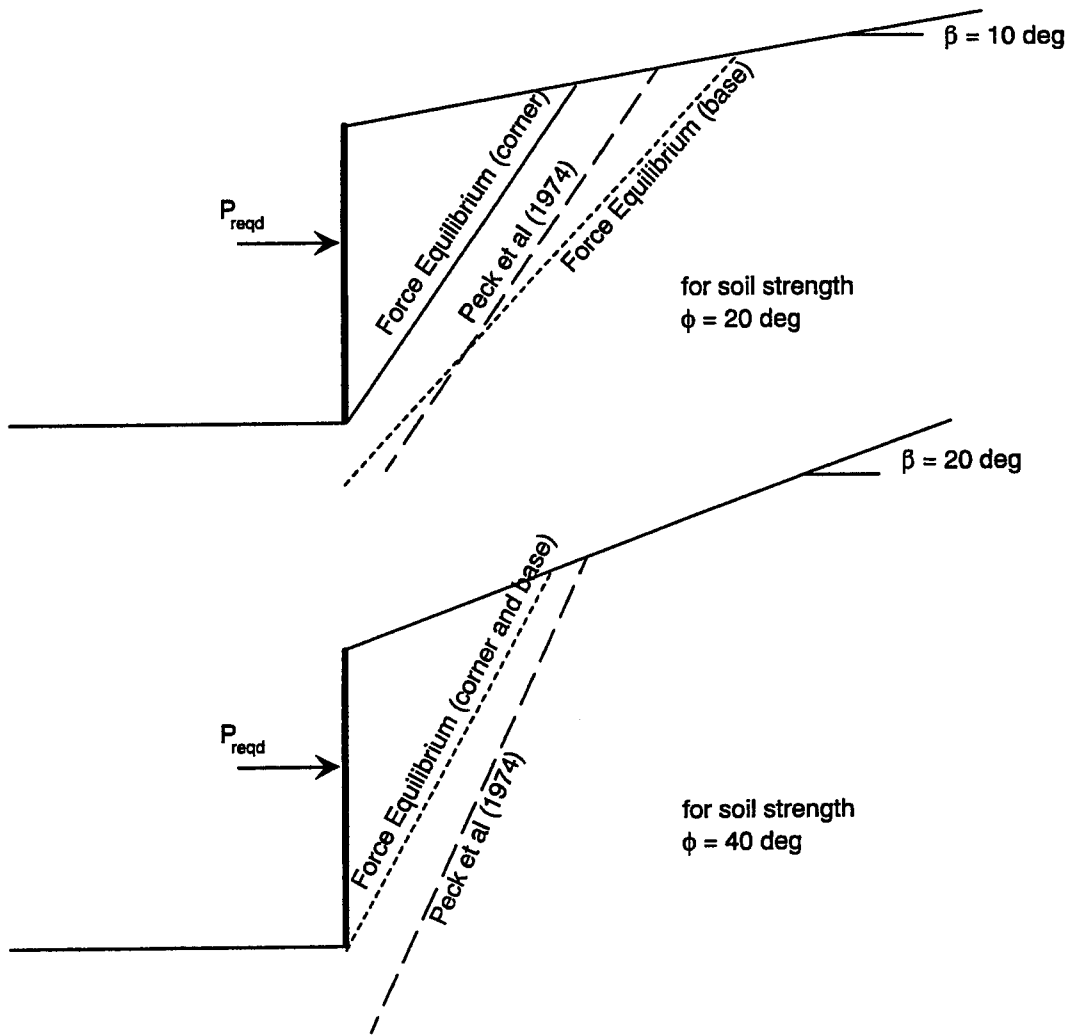


FIGURE 33
Comparison of Three Methods for Determining Minimum Unbonded Length of an Anchor, Sloped Ground Surface

3.5.2 Simplified Approach — External Stability

The external stability of an anchored wall is the stability of the wall and soil mass with respect to failure surfaces that pass behind the ground anchor(s). The total length of an anchor should be designed to achieve the required factor of safety. Global stability and external stability are terms used to identify this type of potential failure.

3.5.2.1 Analysis for External Stability

Stability analyses can be conducted for the soil mass and anchor system using limiting equilibrium procedures that employ the method of slices (see Chapter 4). Force equilibrium procedures also can be used, and represent a common approach for determining the external stability of anchored wall systems. Discussed herein is the development of, and results from, a force equilibrium analysis on an anchored wall system. Results from the simple force equilibrium approach are used to illustrate important aspects of anchored wall design, specifically, the length required for a ground anchor, and the depth required for the anchored wall.

The external stability of an anchored wall system is determined by assuming that the potential plane of sliding passes “behind” the anchor (Figure 34) and below the soldier pile. Since anchors are spaced at a horizontal distance, s , the potential failure surface may assume a three-dimensional shape rather than the two-dimensional shape assumed in these analyses. The failure surface near an anchor may pass behind the anchor, but the failure surface may become steeper and move in closer to the wall for portions of the soil between anchors. To use a two-dimensional failure surface to approximate the three-dimensional failure surface, assume that the failure surface intersects the ground anchor at a distance of one-third the horizontal anchor spacing ($s/3$) from the back of the anchor (Figure 34). Broms (1988) has also suggested the use of $s/3$.

The distance $s/3$ is about 3 ft for a typical permanent ground anchor wall. Since the distance is small, current practice is to assume that the two-dimensional analysis realistically represents the three-dimensional shape of the failure surface. However, if the ground anchor spacing becomes much greater than 10 ft, then the distance $s/3$ may become significant, and increasing the total anchor length by the distance $s/3$ may be warranted.

The stability for the soil mass is determined by requiring horizontal and vertical force equilibrium. The soil mass under consideration is the soil prism ABDEG. The left vertical boundary is defined by the anchored wall while the bottom is defined by a failure plane that passes below the bottom of the cut to a position near the back of the anchor. The vertical boundary on the right side of the soil mass extends from the back of the anchor (minus $s/3$) and is oriented vertically (Figure 34).

Forces exerted and resisted by the mass of soil are illustrated in Figure 34b and 34c. The soil mass acts downward with a magnitude equal to its weight. On the left face, passive soil resistance acts at an angle δ . Active soil pressure is assumed on the right vertical face. On the bottom, soil resistance acts at an angle ϕ from the perpendicular to the failure plane. The forces will sum to zero in the horizontal and vertical directions for an $FS = 1$ and a friction angle equal ϕ_{mob} . The actual $FS_{strength}$ will be $\tan\phi_{avall}/\tan\phi_{mob}$. A $FS_{strength}$ of 1.3 is used in practice.

The passive force is provided by the soil in front of the wall. The passive resistance is influenced by the mobilized friction angle (ϕ_{mob}) and by the wall friction angle (δ) and expressed as

$P_p = 0.5\gamma d^2 K_p$, where d is the depth below grade of the passive failure and K_p is a passive earth pressure coefficient. Passive earth pressure coefficients for different mobilized friction angles (ϕ_{mob}) and wall friction angles (δ) are given in Figure 27 assuming a log spiral failure. For an anchored wall system consisting of soldier beams and lagging, the strength along the interface (along the vertical line) should be near the soil strength. Thus, for the analyses, passive earth pressure coefficients were selected by taking $\delta = \phi_{mob}$.

The right vertical face (line BD in Figure 34) is acted upon by active pressures. The earth pressure along BD is determined assuming Rankine active conditions, and the total force (P_{AR}) is calculated as $P_{AR} = 0.5\gamma h^2 K_{AR}$, where h is the length of line BD.

The failure plane is defined to pass through the back portion of the anchor. The coordinates for the back of the anchor are presented in non-dimensional form with the horizontal position as χ (horizontal distance from wall/wall height), and the vertical position as λ (difference between the elevation of the top of the wall and the back portion of the anchor/wall height) as shown in Figure 35. The depth of the failure plane beneath the bottom of the cut is identified in non-dimensional terms as $\xi = d/H$. Summing forces in the x-direction (horizontal) results in

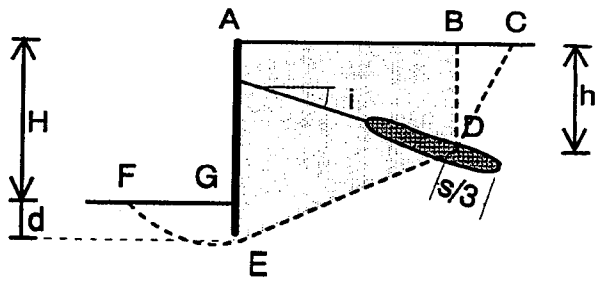
$$\Sigma F_x = P_{AR} - P_p \cos(\delta) - R \sin(\phi - \alpha) = 0 \quad \dots [3.20]$$

Summing forces in the y-direction (vertical) results in

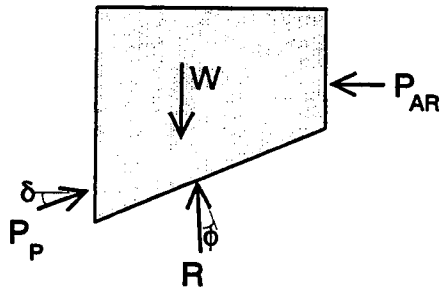
$$\Sigma F_y = W - P_p \sin(\delta) - R \cos(\phi - \alpha) = 0 \quad \dots [3.21]$$

The two equations can be combined to obtain the following requirement for equilibrium:

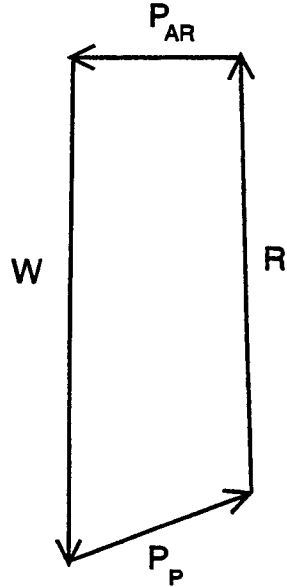
$$(1 + \xi + \lambda)\chi - K_p \xi^2 \sin \delta + \frac{K_p \xi^2 \cos \delta - K_A \lambda^2}{\tan(\phi - \alpha)} = 0 \quad \dots [3.22]$$



a) Example of tiedback wall system



b) Free-body diagram



c) Force vectors acting on area ABDEG

FIGURE 34
Force Equilibrium Considerations for an Anchored Wall System with Failure Surface Passing Behind the Anchor

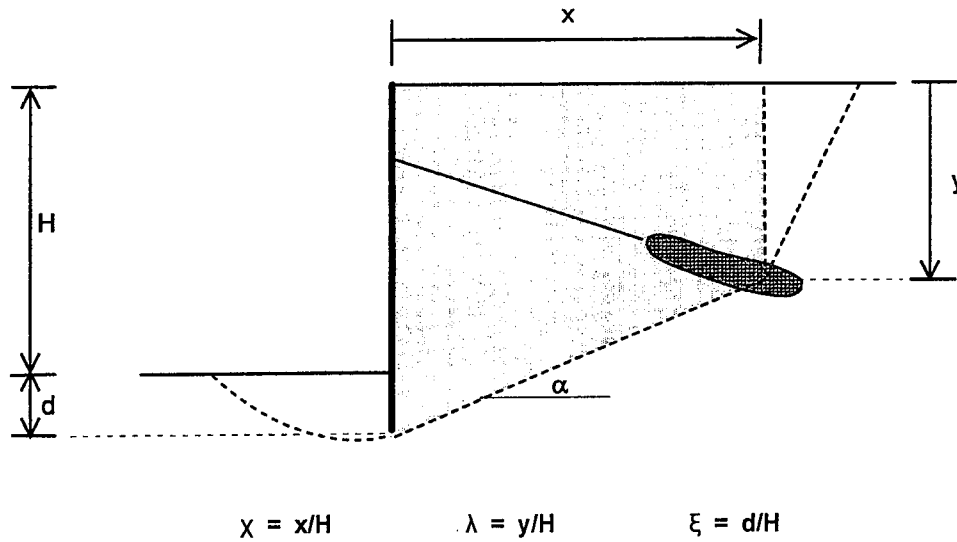


FIGURE 35
Definition of Non-dimensional Parameters χ , λ , and ξ

3.5.2.2 Base Failures (Below the Bottom of the Cut)

Equation 3.22 specifies equilibrium requirements for the overall stability for an anchored wall system. To evaluate global stability, specify the position for the back of the anchor (χ , λ), vary the depth (ξ), and solve for the maximum soil strength (ϕ_{mob}) required to satisfy Equation 3.22. The angle of the failure plane (α) varies, but is defined by the anchor position (χ , λ) and the depth (ξ).

Contours for soil strength required for stability are given in Figure 36 for failure surfaces passing beneath the bottom of the cut. The contours provide a relationship between the geometry (the position of the back of the anchor) and minimum soil strength required for stability. Contours of the position required for the back of the anchor are given for soil strengths, ϕ , of 20° , 30° , and 40° for $FS = 1$. Note that, as the mobilized soil strength decreases, the length required for the anchor increases and the failure surface passes deeper below the bottom of the cut.

Figure 36 allows the determination of the total anchor length to achieve any required factor of safety. For example, an anchored wall is being constructed in a soil with a friction angle of 40° , and an FS of 1.3 is required for external stability. A factor of safety of 1.3 is equivalent to a mobilized friction angle of about 33° . A dashed line is drawn in Figure 37 as an interpolation between the lines $\phi_{mob} = 40^\circ$ and $\phi_{mob} = 30^\circ$.

The depth of the failure surface below the bottom of the cut also is a consideration. As the soil strength decreases, the failure plane passes below the bottom of the cut. In poor ground, the failure surface may extend deeper than toes commonly used for anchored walls.

When the excavation extends through poor ground into rock or firm bearing, a base failure cannot occur. For these conditions, conduct the external stability analyses for failure surfaces through the bottom of the cut.

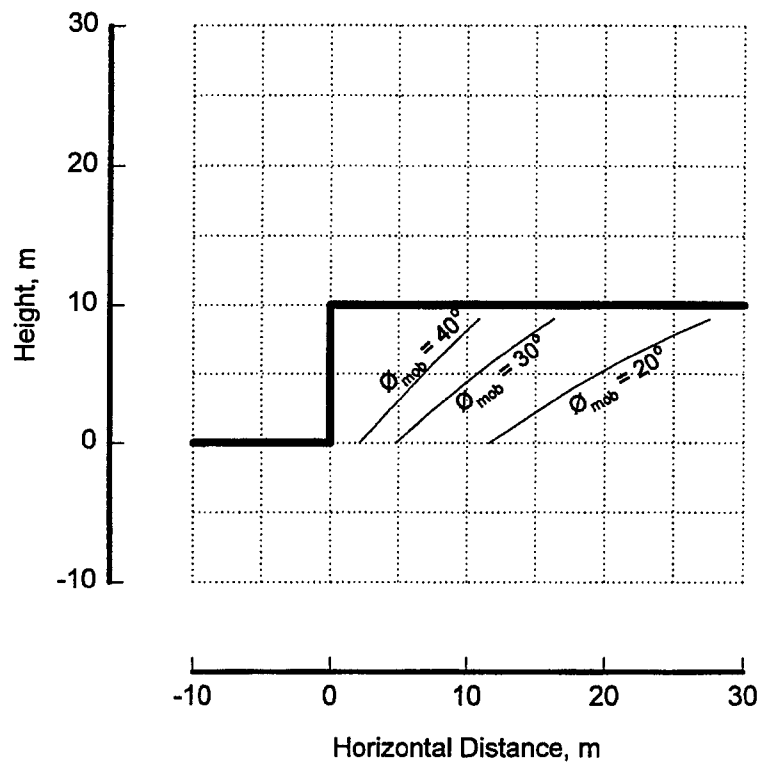


FIGURE 36
Effect of Mobilized Soil Strength on Position Required for Back of Anchor
(base failure)

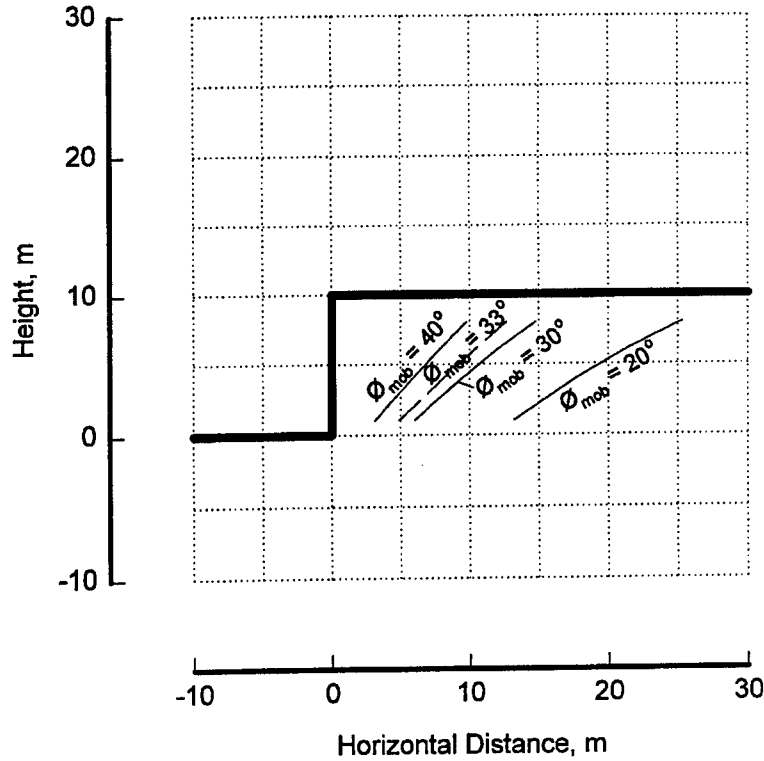


FIGURE 37
Example for Determining Minimum Anchor Length for $\phi_{mob} = 33^\circ$
(base failure)

3.5.2.3 Failures Through the Bottom of the Cut

The failure surface will pass through the bottom corner of the cut when the excavation goes to rock or firm bearing. Equations 3.20 to 3.22 are applicable, but without the passive resistance provided at the toe. The resulting equations for equilibrium simplify to

$$\chi(1 + \lambda) - \frac{K_A \lambda^2}{\tan(\phi - \alpha)} = 0 \quad \dots [3.23]$$

where $\alpha = \text{atan}((1-\lambda)/\chi)$. Equation 3.23 can be used to determine the minimum ground anchor length for the 10-m-high wall when the failure surface passes through the bottom corner of the cut. The shear resistance and the lateral capacity of the soldier beams is ignored. Minimum total anchor lengths are shown in Figure 38 as contours for soils with different mobilized friction angles.

The minimum total anchor lengths in Figure 38 are less than the lengths in Figure 37. When low-strength ground is located below the bottom of the excavation, the ground anchors will have to be longer to satisfy external stability.

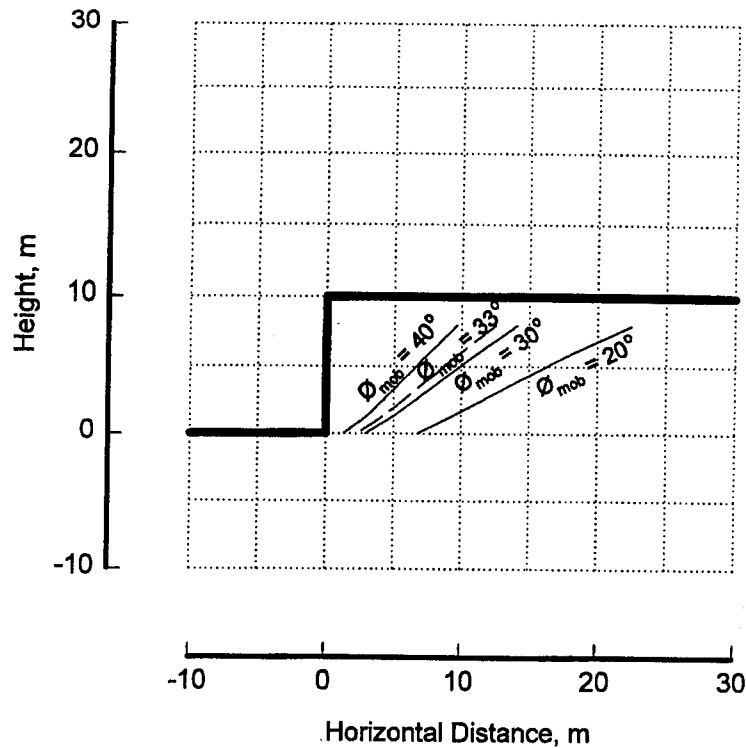


FIGURE 38
Effect of Mobilized Soil Strength on Position Required for Back of Anchor
(corner failure)

3.5.3 Wall Stability — Failure Surface Passing Through Anchor

The third case to be investigated is the case where a potential failure surface passes through the anchor bond length. Failures of this type have not been reported. However, it is possible that the factor of safety for a failure plane passing through the anchor bond length may be less than the factor of safety passing in front of or behind the anchor.

Force equilibrium again is used to illustrate the influence of a failure plane passing through the anchor bond length. The equations are similar to the equations developed for bottom failure and base failure, except that a partial anchor force is added to the wall. The partial anchor force represents the anchor force that can be included for a failure surface passing through the anchor bond length. For example, if the failure surface passes completely in front of the an-

chor zone, then the full anchor force should be applied to the left vertical face. On the other hand, if the failure plane passes halfway through the anchor bond length, then only part of the total anchor force would be available and applied to the left vertical face. The exact proportion of the total anchor load depends upon the load transfer characteristics along the length of the anchor and the factor of safety used in the design of the ground anchor. Force vectors and an illustration are shown in Figure 25. The resulting equation that includes the partial anchor force, P_{TP} , is

$$\frac{P_{TP}}{\frac{1}{2}\gamma H^2} - K_A \lambda^2 + K_P \xi^2 \cos \delta - (K_P \xi^2 \sin \delta - (1 + \xi + \lambda) \chi) \tan(\phi - \alpha) = 0 \quad \dots [3.24]$$

The solution to Equation 3.24 for a 10-m-high wall is shown graphically in Figure 39 for a soil with a friction angle of 33° and an anchor force P . Equation 3.24 was solved by assuming the applied anchor force was a certain portion of the total anchor force (P). Contours identifying the back of the failure surface were determined by selecting a vertical elevation for the back of the failure surface (λ , Figure 35) and then finding the greatest horizontal distance (χ) that could still satisfy Equation 3.24. For each trial distance, depth (ξ) was also varied to satisfy Equation 3.24. The parameter α is defined by the geometry (χ , λ and ξ). The horizontal distance (χ) was increased until no depth (ξ) could satisfy Equation 3.24.

Contours identifying the position required for specific proportions of the total anchor load are shown in Figure 39. The contours for $1.0P$ and for $0P$ agree with the two previous analyses: failure surface for local stability, and failure surfaces for external stability. Portions of the anchor force less than P and greater than zero are also shown in Figure 39, and illustrate that the required anchor length for $0.5P$ is greater than halfway between the length required for P and $0P$.

The effect of a firm stratum at the base of the excavation is shown in Figure 40. A firm stratum at the base forces the potential failure surface to pass through the bottom corner of the excavation. The effect is to cause a shallower failure surface that results in shorter anchor lengths.

Thus, Figures 39 and 40 illustrate the importance of developing most of the total anchor capacity beyond the minimum unbonded anchor length, and the desirability of using long bond lengths rather than short ones. These analyses also suggest that the stability of walls with anchors extending through ground where the upper soils are stronger than the lower soils should be carefully evaluated.

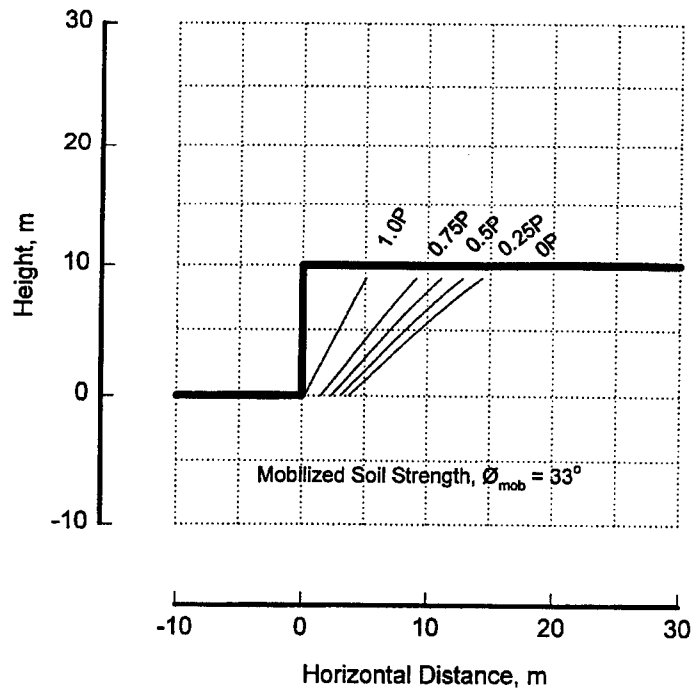


FIGURE 39
Requirements for Anchor Load Along the Anchor Length (base failure)

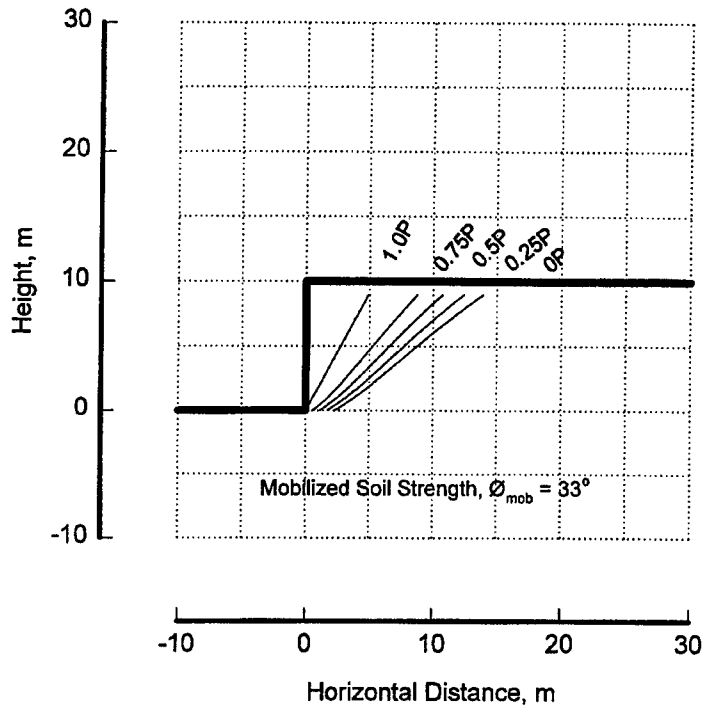


FIGURE 40
Requirements for Anchor Load Along the Anchor Length (corner failure)

3.6 USE OF LIMITING EQUILIBRIUM EQUATIONS AND GENERAL PURPOSE SLOPE STABILITY COMPUTER PROGRAMS

The equations presented in this chapter solve force equilibrium equations for an anchored wall with simple geometry and simple soil properties. However, soil layering, slope geometry, seepage conditions, surface loadings, and other site conditions require a more general solution and methodology. Several computer programs are available that can account for general conditions of surface loading, layered soil profiles, seepage conditions, and overall wall geometry. The use of these programs is described in Chapter 4.

CHAPTER 4

USE OF GENERAL PURPOSE SLOPE STABILITY PROGRAMS

4.1 INTRODUCTION

General Purpose Slope Stability (computer) Programs (GPSSP) offer a means to determine requirements for the equilibrium of anchored wall systems. GPSSP solve for the minimum resistance along potential failure surfaces passing through the soil. These potential failure surfaces may be circular or non-circular. Many GPSSP include capabilities to consider variable slope geometry, layered soil profiles, groundwater table and seepage effects, internal loads, and surface loads. However, reliable use of these programs may be compromised by an incomplete understanding of the limitations of the GPSSP or by undocumented errors in programming.

Use of GPSSP is discussed herein. Approaches that use GPSSP to determine the anchor loads necessary for stability are discussed, and approaches to determine the position of the anchor necessary for overall stability are presented. Methods to investigate the stability for failure surfaces passing through the anchor bond zone are also discussed. Examples are provided to illustrate these approaches. Results using GPSSP are compared with results using a force equilibrium method developed in Chapter 3. Finally, some additional examples are provided to illustrate the effect of using non-circular versus circular failure surfaces, and the seepage effects on requirements for anchored walls.

4.2 DETAILS OF USING GPSSP FOR ANCHORED WALL ANALYSES

GPSSP offer a general formulation for determining equilibrium for a soil mass. Some details and advantages of the GPSSP are discussed herein.

The factor of safety in GPSSP is based on the ratio of the soil strength available to the soil strength required for equilibrium. This definition is consistent with the factor of safety with respect to strength (discussed in Chapter 3). The factor of safety is defined mathematically as:

$$FS = \frac{\text{available strength}}{\text{strength required for equilibrium}} \quad \dots [4.1]$$

A general procedure for determining the factor of safety for a soil mass is to construct a trial failure surface through the soil mass and then subdivide the soil above the failure plane into several vertical slices. Subdividing the soil mass into slices allows GPSSP to include effects of soil layering, effects of water pressure, variable geometry, and surface loads (Figure 41). GPSSP require a variety of assumptions to solve equilibrium equations for the soil above a

potential failure surface. Methods available may solve for the factor of safety by requiring force equilibrium ($\Sigma F_x = 0$ and $\Sigma F_y = 0$), or moment equilibrium ($\Sigma M = 0$), or a combination of moment and force equilibrium. If equations of equilibrium are formulated for each slice, there will be $3*n$ equations, where n is the number of slices.

Equilibrium Equations	
n	Moment Equations
n	Forces in X direction
n	Forces in Y direction
Total = $3n$ Equations of Equilibrium	

The unknown quantities for each slice (Figure 41) include the location and magnitude of the normal force (N), the magnitude of the interslice shear force (X), and the magnitude and location of the interslice normal force (E). Unfortunately, the number of equilibrium equations is fewer than the number of unknowns (e.g., the factor of safety and the magnitude and location of forces along the side and base), thus, the system of equations is under-determined. The number of unknowns is quantified below:

Number of Unknowns	
1	Factor of Safety
n	Values of Normal Force (N)
n	Locations of Normal Force
$n-1$	Values of Interslice Shear Force (X)
$n-1$	Values of Interslice Normal Force (E)
$n-1$	Locations for Interslice Force
Total = $5n - 2$ Unknowns	

To make solving for equilibrium a determinate problem, assumptions are required to reduce the number of unknowns to equal the number of equations. Most solution techniques require assumptions with respect to the interslice force angle. General features for some common methods of slices are given in Table 7. Additional information is provided on the assumptions made for interslice forces.

GPSSP allow the use of both circular and non-circular failure surfaces. Algorithms to find the critical failure surface employ a procedural search of trial failure surfaces. Shown in Table 7 is a list of analyses available and their capabilities to accommodate circular and non-circular failure surfaces. Many GPSSP are coded to allow the user to select a specific method of analyses from a list of several methods, such as those listed below.

A key advantage of GPSSP is their ability to compute the factor of safety for a trial failure surface very quickly. This ability allows several trial failure surfaces to be evaluated and

assists greatly in identifying the critical failure surface (the failure surface with the smallest factor of safety).

TABLE 7
Assumptions and Features of Some GPSSP Methods of Analysis

METHOD OF ANALYSES	SHAPE OF FAILURE SURFACE	EQUILIBRIUM EQUATIONS	ASSUMPTIONS FOR INTERSLICE FORCES
Bishop	circular	$\Sigma F_v = 0$ $\Sigma M_{\text{overall}} = 0$	horizontal
Janbu (simplified)	circular, non-circular	$\Sigma F_v = 0$ $\Sigma F_H = 0$	horizontal
Janbu (rigorous)	circular, non-circular	$\Sigma F_v = 0$ $\Sigma F_H = 0$ $\Sigma M = 0$	user-defined line of thrust
Corps of Engineers	circular, non-circular	$\Sigma F_v = 0$ $\Sigma F_H = 0$	user-defined interslice force angle
Lowe and Karafiath	circular, non-circular	$\Sigma F_v = 0$ $\Sigma F_H = 0$	interslice force angle defined by slope of top and bottom of each slice
Spencer	circular, non-circular	$\Sigma F_v = 0$ $\Sigma F_H = 0$ $\Sigma M = 0$	constant interslice force angle
Morgenstern and Price	circular, non-circular	$\Sigma F_v = 0$ $\Sigma F_H = 0$ $\Sigma M = 0$	user-defined variation in interslice force angle.

As indicated above, GPSSP programs make assumptions regarding the interslice forces in order to reduce the unknowns so the equilibrium equations can be solved. Ground anchor forces are applied in the same orientation as the interslice forces, and the simplifying assumptions may affect how the ground anchor force is distributed to the slices or the mass. Therefore, before using a GPSSP to evaluate the internal stability of an anchored wall, the computer code should be verified. One means of checking a program is to see if it will predict failure surfaces and ground anchor loads similar to those determined using the simple force equilibrium method contained in Chapter 3. Hand computations and performing analyses with a different GPSSP also can provide an independent confirmation of the program's accuracy. Estimates based on design charts or apparent earth pressure diagrams can provide additional support for a valid solution.

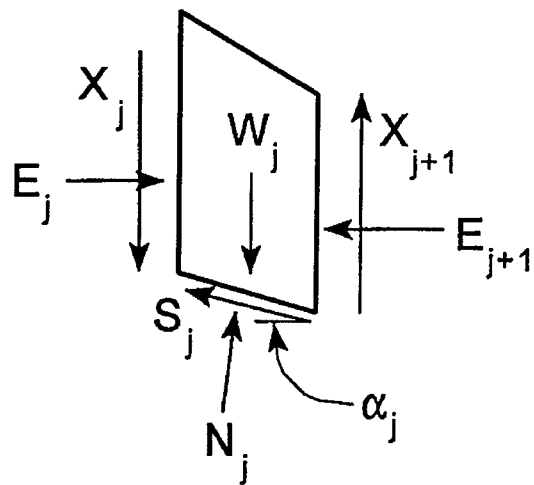
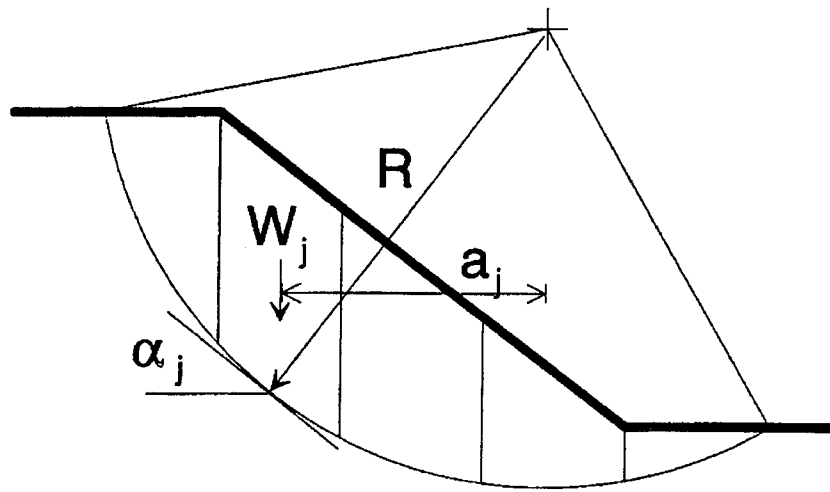


FIGURE 41
Equilibrium Considerations for Method of Slices

4.3 USE OF GPSSP FOR DETERMINING P_{reqd}

GPSSP can be used to determine the force required to meet equilibrium requirements for an anchored wall. Shown in Figure 42a is an anchored wall. A potential failure surface passing through the soil and under the soldier beams is shown in Figure 42b. The failure surface passes in front of the anchor bond zone, therefore, the complete ground anchor load acts as a stabilizing force to the soil mass above the failure plane (Figure 42c). This illustration is the simplest representation of equilibrium considerations. The shaded zone in Figure 42 identifies the area over which failure surfaces may occur. Some failure surfaces may pass under the tip of the soldier beams while other potential failure surfaces are shallower and pass through the soldier beams.

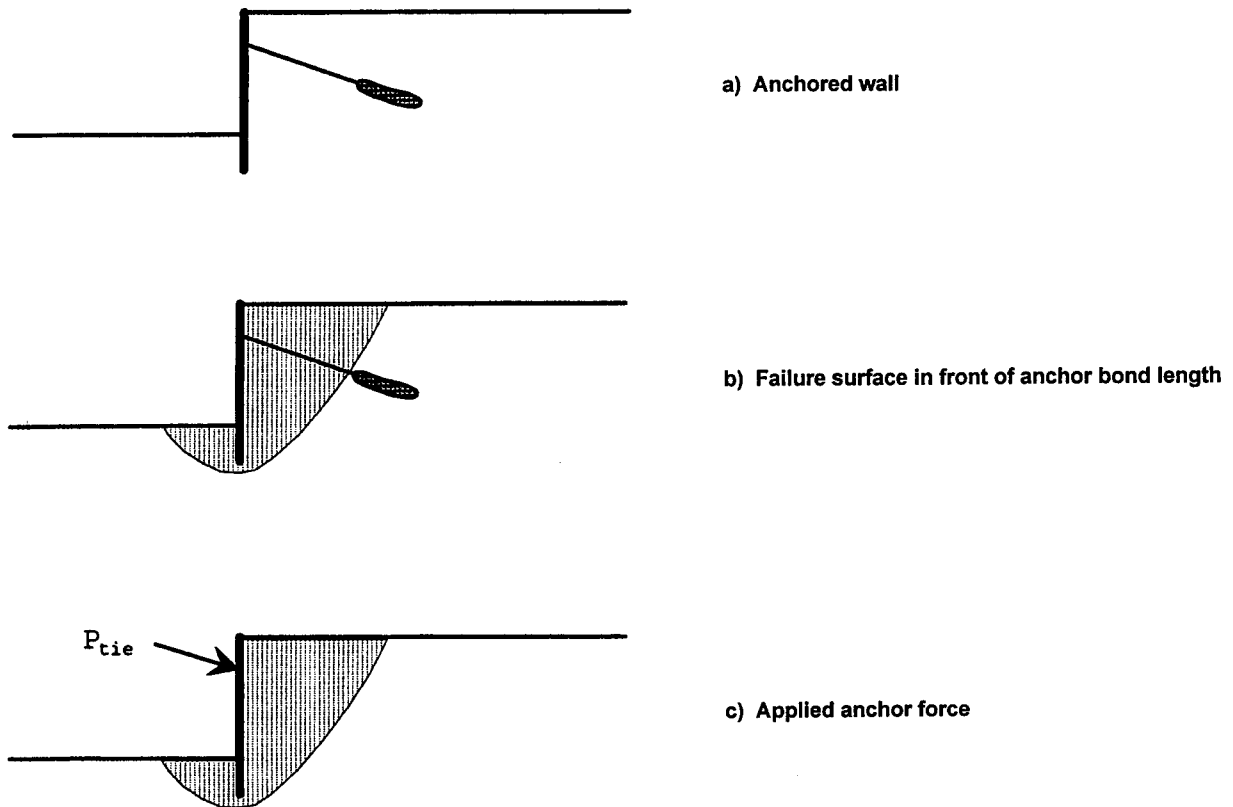


FIGURE 42
Considerations for Stability of Failure Surfaces Passing in Front of the Anchor Bond Length

4.3.1 Analyses Based on the Location of the Failure Surface

When failure surfaces pass through structural components such as the anchor bond zone or the soldier beams, it is necessary to analyze for the forces exerted on the soil mass rather than the forces applied to the structural components. Three cases are presented herein to illustrate methods to obtain the anchor force required for stability of a retained soil mass. The cases include conditions where the potential failure surface passes: (1) through the soldier beam at the level of the excavation, (2) through the soldier beam at a level just below the excavation, and (3) below the tip of the soldier beam.

4.3.1.1 Failure Surfaces Passing Through the Soldier Beam at the Excavation Level

Free-body diagrams for a failure surface passing through the soldier beam and in front of the anchor bond zone are shown in Figure 43. The ground anchor force applied to the wall and the failure surface is illustrated in Figure 43a.

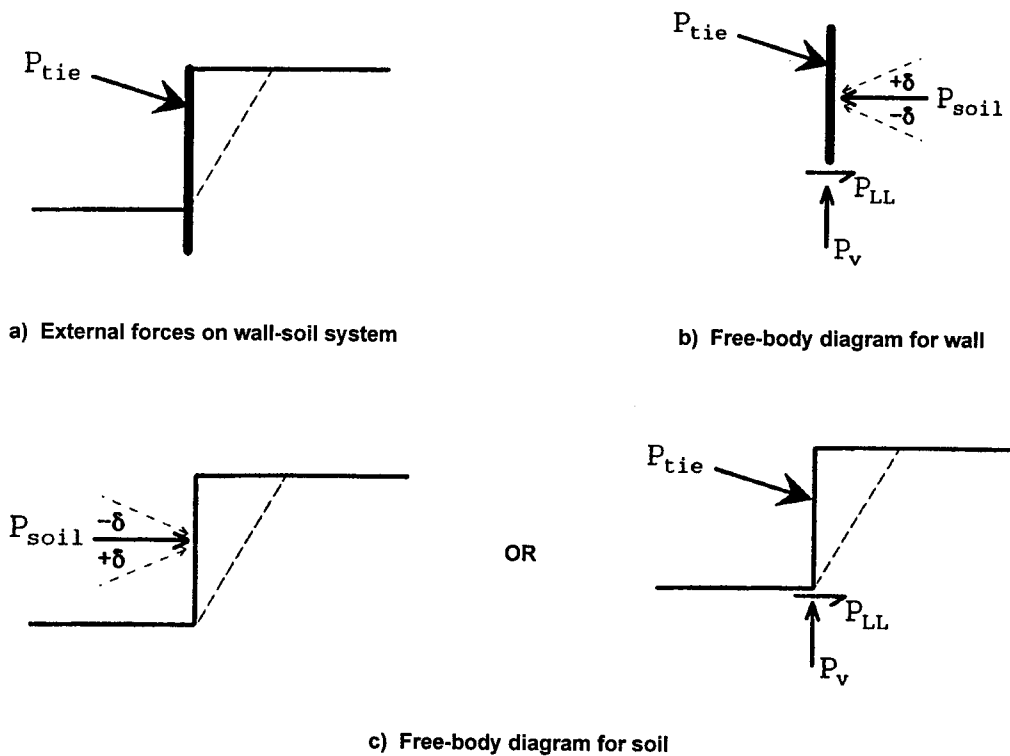


FIGURE 43
Determining the Load Required for Stability of Soil in Front of the Anchor
(potential failure surface passing in front of the anchor length
and through the bottom corner of the excavation)

A free-body diagram for the wall components (soldier beams) above the potential failure surface is illustrated in Figure 43b. If the soil mass moves downward with respect to the movement of the soldier beam, downdrag forces result, and the load exerted by the soil (P_{soil}) is angled downward (at an angle $+\delta$). However, if the wall components settle more than the soil mass, then P_{soil} is directed upward at an angle ($-\delta$). Resistance to lateral and vertical movement of the soldier beam is provided by the portion of the soldier beam embedded below the failure surface. Resistance to lateral movement is quantified as P_{LL} , while resistance to vertical movement is provided by P_V . The specific magnitude, orientation, and location of the force P_{soil} depends on such details as the lateral load (P_{LL}), the relative movement between the wall and the soil, and the anchor force and inclination.

Two free-body diagrams for the soil behind the anchored wall are shown in Figure 43c. The left diagram illustrates the stability in terms of the soil force, P_{soil} , while the right diagram expresses the free-body diagram in terms of the individual forces P_{tie} , P_V , and P_{LL} . These individual forces are applied to the soil by the anchor and the structural components below the failure surface, and their result is equal to P_{soil} .

Since the embedded portion of a soldier beam typically has a vertical capacity greater than the applied vertical load, the soldier beam should settle less than the soil, and the resultant P_{soil} will be oriented at $+\delta$. If effects of wall friction are neglected (a conservative approach if P_{soil} is oriented at $+\delta$), P_{soil} is horizontal. The elevation at which P_{soil} acts is dependent on the interaction between the wall and the soil mass. Based on estimates from full-scale measurements, the elevation is typically between 30 and 55 percent of the wall height (Terzaghi, et al., 1996).

4.3.1.2 Failure Surfaces Passing Through the Soldier Beam Between the Beam Tip and the Bottom of the Excavation

Free-body diagrams for a failure surface passing in front of the anchor bond zone and through the soldier beam at an elevation between the beam tip and the excavation level are shown in Figure 44. The ground anchor force applied to the wall and the failure surface is illustrated in Figure 44a.

A free-body diagram for the wall components (soldier beams and lagging) above the potential failure surface is illustrated in Figure 44b and is very similar to that shown in Figure 43b. If the soil mass moves downward with respect to the soldier beam, downdrag forces result, and the load exerted by the soil (P_{soil}) is angled downward (at an angle $+\delta$). However, if the wall components settle more than the soil mass, then P_{soil} is directed upward at an angle ($-\delta$). Resistance to lateral and vertical movement of the soldier beam is provided by the portion of the soldier beam embedded below the failure surface. Resistance to lateral movement is quantified as P_{LL} , while resistance to vertical movement is provided by P_V . The specific magnitude, orientation, and location of the force P_{soil} depends on such details as the lateral load (P_{LL}), the relative movement between the wall and the soil, and the anchor force and inclination.

Two free-body diagrams for the soil behind the anchored wall are shown in Figure 44c. The left diagram illustrates the stability in terms of the soil force, P_{soil} , while the right diagram expresses the free-body diagram in terms of the individual forces P_{tie} , P_{LL} , and P_v applied to the soil by the anchor and structural components below the failure plane. The result of the individual forces (P_{tie} , P_{LL} , and P_v) equals P_{soil} .

Since the embedded portion of a soldier beam has a vertical capacity greater than the applied vertical load, the soldier beam will settle less than the soil, and the resultant P_{soil} will be oriented at $+\delta$. If the effects of wall friction are neglected (a conservative approach for P_{soil} oriented at $+\delta$), P_{soil} is horizontal. The elevation at which P_{soil} acts is dependent on the interaction between the wall and the soil mass. Based on estimates from full-scale measurements, the elevation is typically between 30 and 55 percent of the wall height (Terzaghi et al., 1996).

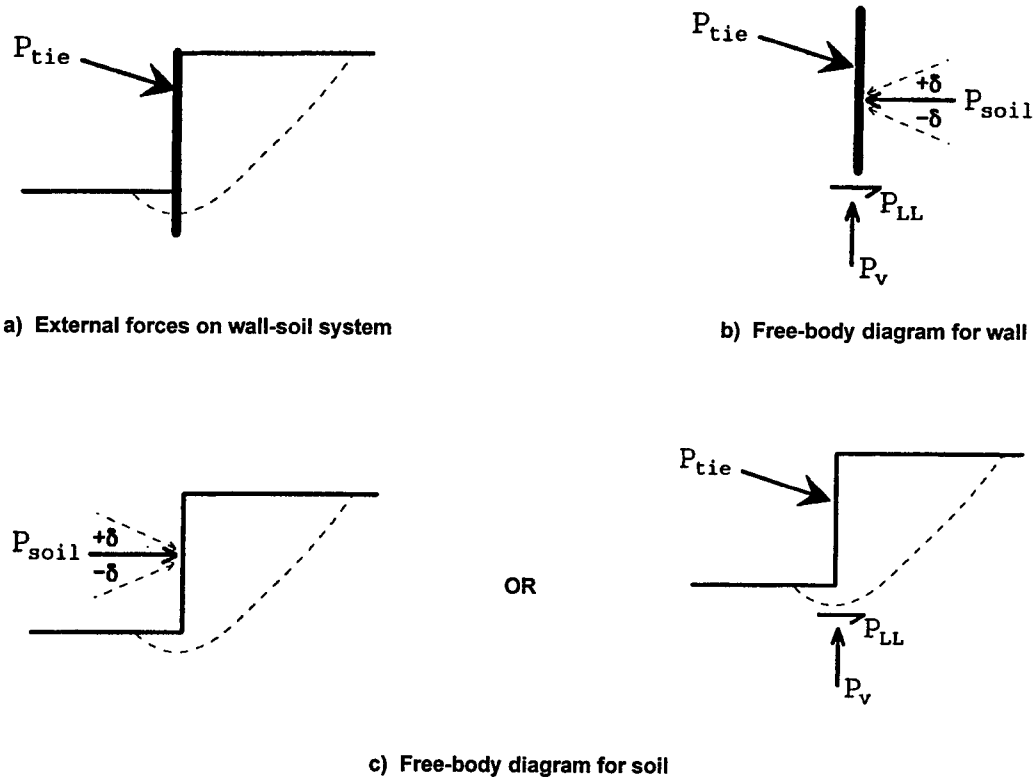


FIGURE 43
Determining the Load Required for Stability of Soil in Front of the Anchor
(potential failure surface passing in front of the anchor length and
between the bottom of the excavation and the soldier beam tip)

4.3.1.3 Failure Surfaces Passing Below the Soldier Beam

Free-body diagrams for a failure surface passing in front of the anchor bond zone and below the tip of the soldier beam are shown in Figure 45. The failure surface and the anchor force applied to the wall are illustrated in Figure 45a.

A free-body diagram for the wall components (soldier beams and lagging) above the potential failure surface is illustrated in Figure 45b. The combination of resistance provided by the soil, P_{soil} , and by end bearing at the beam tip, P_v , is equal and opposite in direction to the applied anchor load.

A free-body diagram for the soil behind the anchored wall is shown in Figure 45c. The diagram illustrates the stability in terms of the external force applied by the anchor, P_{tie} .

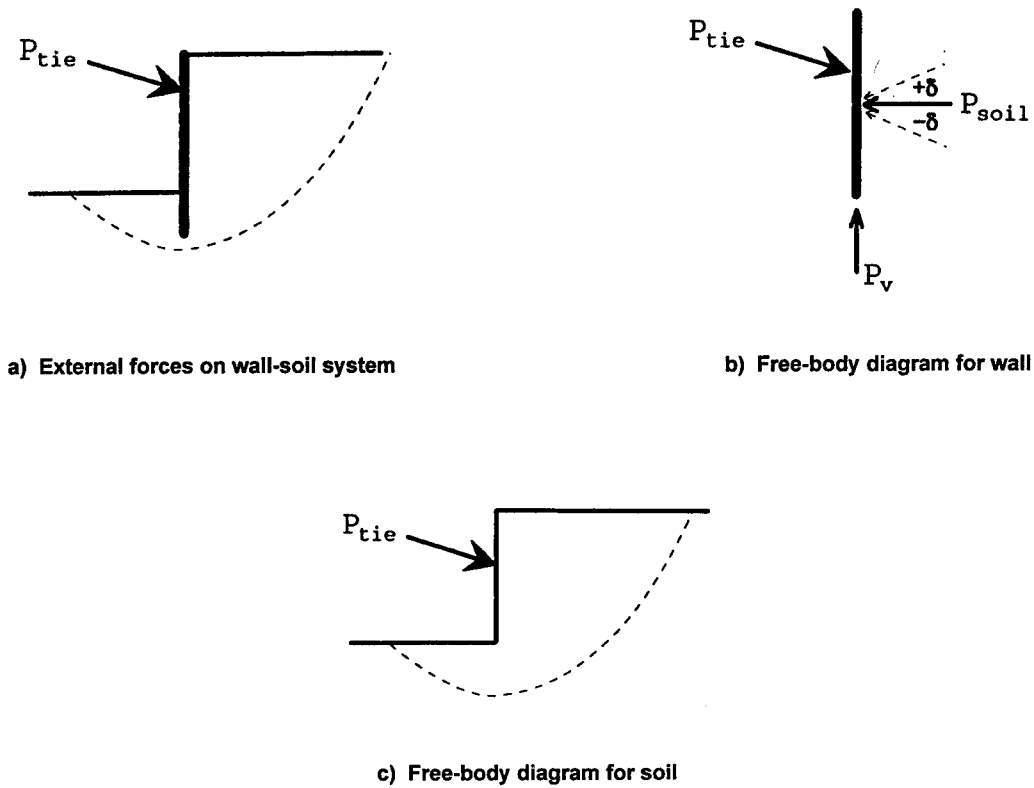


FIGURE 43
Determining the Load Required for Stability of Soil in Front of the Anchor
(potential failure surface passing in front of the anchor length and below the soldier beam)

4.3.2 Simplified Approach for Determining P_{reqd}

The total horizontal load required for the stability of the soil (P_{reqd}) can be estimated using GPSSP. The approach assumes that P_{reqd} includes the load contributed by the ground anchor and by the soldier beams. The location of P_{reqd} is based on results of earth pressure measurements, and typically is selected to be at an elevation of 30 to 50 percent of the wall height. Furthermore, the orientation of P_{reqd} is assumed to be horizontal. The magnitude of P_{reqd} is increased until the minimum acceptable factor of safety is obtained. The magnitude of P_{reqd} represents the total anchor load and the load carried by the soldier beams.

Results of the simple approach using GPSSP are shown in Figure 46 for cuts in sand. GPSSP analyses were performed for several soil strengths (ϕ) using a non-circular failure surface passing through the bottom corner of the excavation. Several analysis methods were used to estimate K_A . The methods of analysis include approximate methods (e.g., Rankine), methods that solve for moment equilibrium only (e.g., log-spiral method), methods that require force equilibrium only (e.g., the Corps of Engineers' method and Lowe and Karafiath's method), and a method that requires moment and force equilibrium (e.g., Spencer's method). Most predictions for P_{reqd} agree except the log-spiral method. The log-spiral method under-predicts the magnitude of P_{reqd} because the log-spiral shape for the failure surface is too restrictive and does not allow the failure surface enough flexibility to assume a shape that would provide less soil resistance.

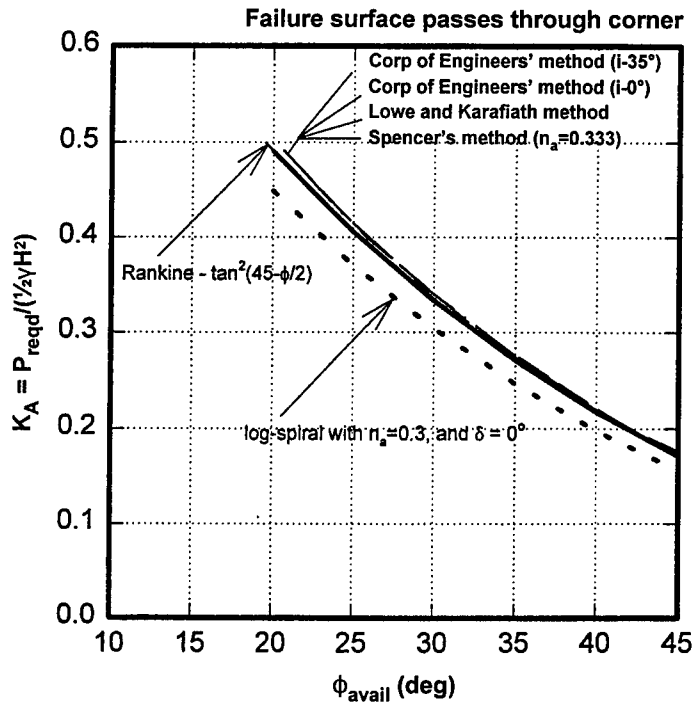


FIGURE 46
Effect of Method of Analysis and Friction Angle on the Magnitude of P_{reqd}

Results of the simple approach using GPSSP for cuts in clay are shown in Figure 47a for failures through the bottom of the excavation and Figure 47b for failures that pass below the bottom of the excavation at a depth of $0.2H$. GPSSP analyses were done for several soil strengths and are reported in non-dimensional form using the normalizing relationship $\gamma H/s_u$, where γ is the total unit weight of the clay, H is the total height of the cut, and s_u is the undrained shear strength of the clay. The three equilibrium methods of analysis used to develop the relationship between P_{reqd} and $\gamma H/s_u$ are Bishop's method, the Corps of Engineers' method, and Spencer's method. The relationships are compared with those predicted using the approximate relationships such as the Rankine and modified Rankine method (Terzaghi, et al., 1996), and Henkel's method (Henkel, 1971).

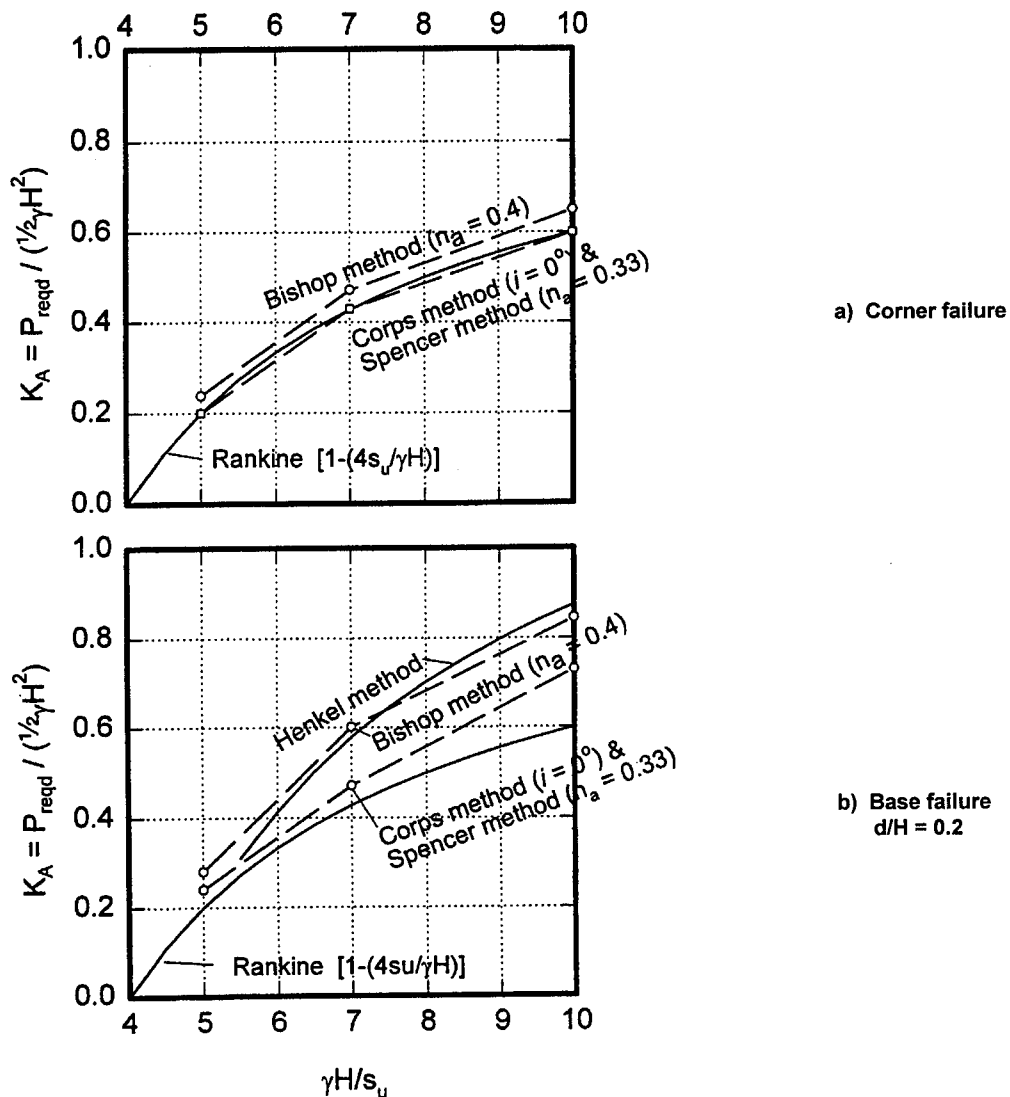


FIGURE 47
Relationship Between K_A and $\gamma H/s_u$ for Different Limiting Equilibrium Methods

Limiting equilibrium methods agree well with Rankine analyses for failure surfaces passing through the bottom corner of the excavation, however, the methods diverge for conditions where the failure surface passes below the bottom of the excavation. For ratios of $\gamma H/s_u$ between 5 and 7, the GPSSP predicts slightly higher values than the Rankine and Henkel models. For ratios of $\gamma H/s_u$ greater than 7, the limiting equilibrium methods are bounded by the Rankine predictions (lower bound) and by predictions using Henkel's method (upper bound). Overall, predictions using the Henkel model agree well with Bishop's method.

4.3.3 Toe Resistance

As the soil above the failure surface attempts to move out, shear resistance is mobilized in the soldier beams. Shear in the soldier beam provides additional resistance to soil movement. Predicting soldier beam shear requires the consideration of three possible failure modes. The failure modes are: (1) Shear of the soldier beam; (2) Flow of the soil between the soldier beams; and (3) Lateral capacity of the soldier beams.

Shear of the soldier beam will seldom control the toe resistance. Toe resistance dependent on flow resistance or lateral capacity of the soldier beams is discussed below.

4.3.3.1 Failure by Soil Flowing Between the Soldier Beams

Figure 48a illustrates how the toe resistance is dependent on the movement of the soil between the soldier beams. This type of failure will be described herein as a "flow-through" failure because the soil above the failure plane moves between the firmly embedded soldier beams. The soldier beams are assumed to be structurally fixed and firmly embedded below the failure surface. Therefore, resistance to failure is provided by the soldier beam cross-section restricting the flow of the soil. Two examples are given in Figure 48a: the left diagram illustrates a case where the soldier beam is firmly socketed into a strong material, while the right diagram illustrates a very long soldier beam that is firmly embedded because of its great length below the failure surface.

The resistance provided by flow-through failure is quantified by determining the resistance to flow caused by the presence of the soldier beams. The resistance to flow (ρ_L) is proportional to the length of the soldier beam and, therefore, exhibits units of force per unit length F/L. A sketch of the soil resistance to flow is shown in Figure 48b. The total resistance exerted by the soldier beam is proportional to the length of the beam over which flow occurs. Therefore, as the depth of the potential failure surface increases, so does the resistance to flow (Figure 48b).

Broms suggests the lateral soil resistance, ρ_{LL} , of a soldier beam at a given depth be equal to

$$\rho_{LL} = 3 \cdot \sigma_v \cdot K_{PR} \cdot b \quad \dots [4.2]$$

where σ_v is the vertical effective stress, K_{PR} is the Rankine passive earth pressure coefficient, and b is the beam width or diameter. The soil resistance, p_{LL} , is expressed in units of force per unit length of soldier beam (F/L). The total resistance provided by the soldier beam to flow of the soil between the beams (P_{LL}) is determined by summing up the soil resistance for the portion of the beam above the potential failure plane. This concept is illustrated in Figure 48b.

Thus, the total resistance provided by the soldier beam considers the potential for flow through the beams. However, the lateral capacity of the portion of the soldier beam embedded below the potential failure surface must be capable of resisting this load. The lateral capacity of the embedded portion of the soldier beam is the subject of the section below.

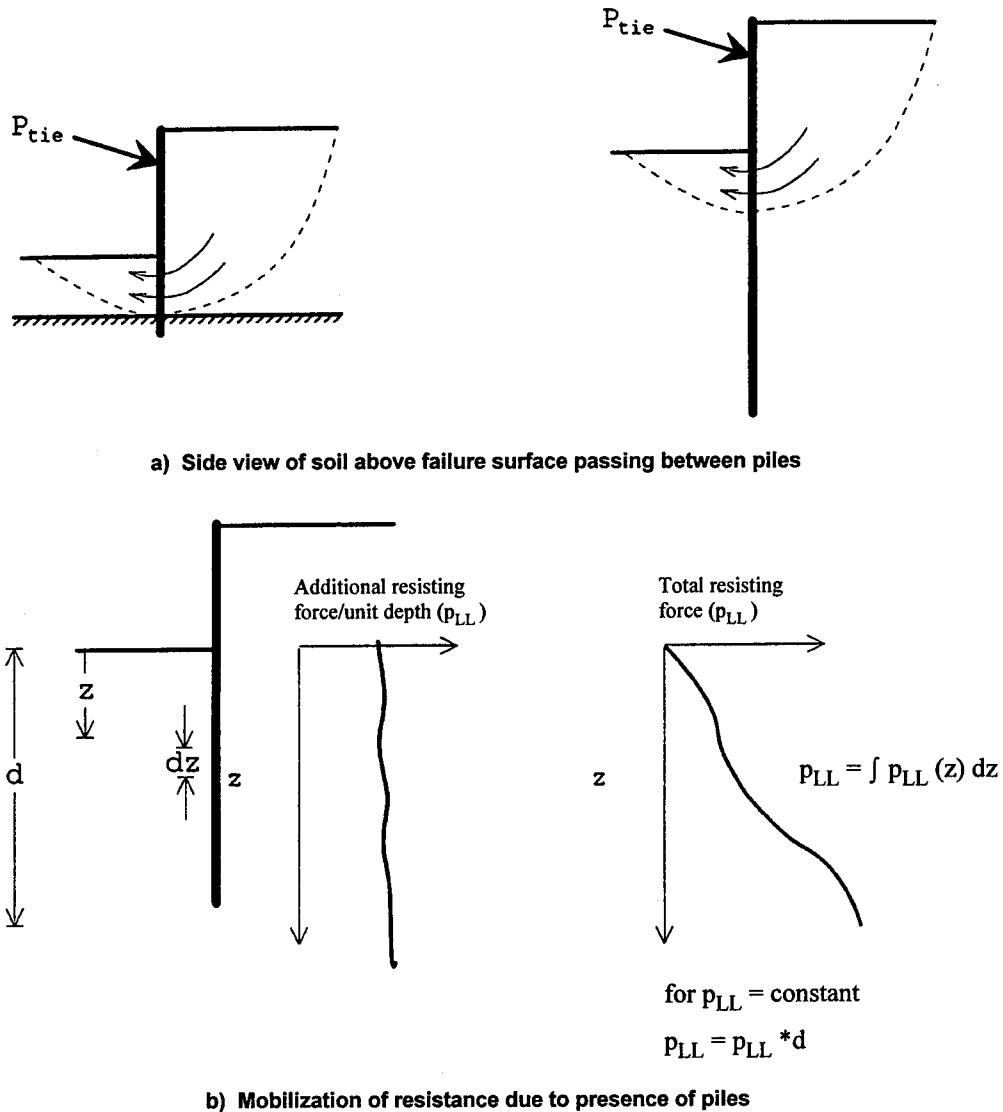


FIGURE 48
Flow Through Resistance Provided by the Soldier Beams

4.3.3.2 Failure by Exceeding the Lateral Capacity of the Soldier Beam Below the Failure Surface

Figure 49a illustrates a condition where the soldier beams move with the soil above the failure plane, and the limiting soldier beam resistance is provided by the portion of the soldier beam embedded below the failure surface. The lateral capacity of the embedded portion of the beam can be determined using Broms' method, or COM624 (Wang and Reese, 1992).

The total resistance provided by the soldier beams can be modeled as a reinforcement with shear resistance. The resistance provided by the soldier beam decreases with depth as the failure surface deepens. Both failure by flow and failure by exceeding the lateral capacity of the embedded portion of the soldier beam should be investigated for each case. The resistance provided by the soldier beam would be the minimum load due to either case. Normally, resistance due to flow between soldier beams greatly exceeds the lateral capacity of the embedded portion of the beams. Flow resistance may control in soft clay soils.

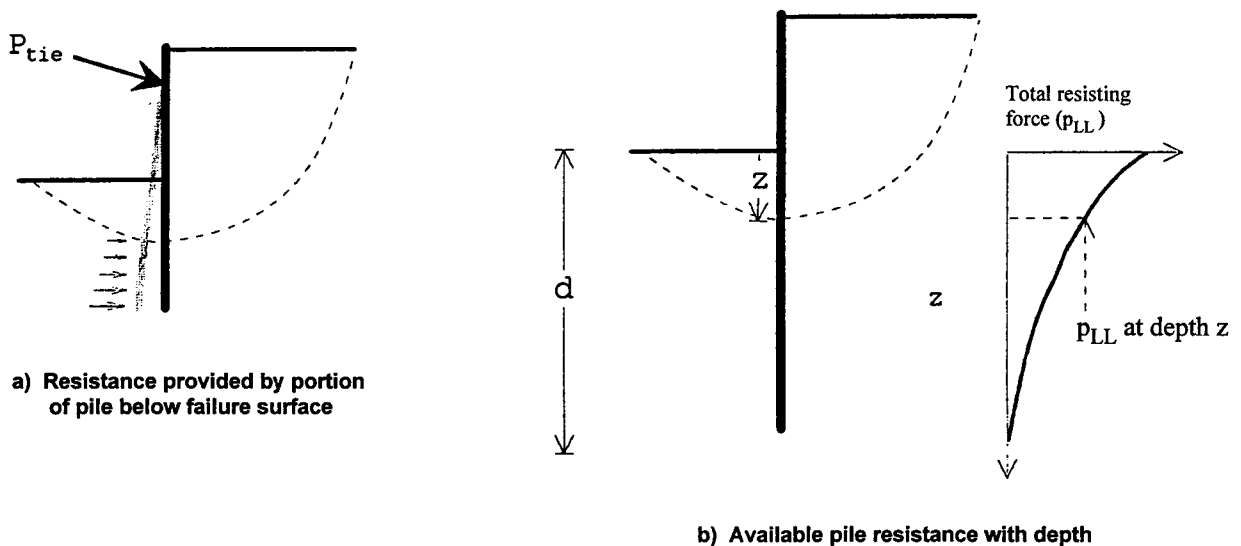


FIGURE 49
Lateral Resistance Provided by the Soldier Beams

4.4 USE OF GPSSP FOR DETERMINING THE POSITION FOR THE BACK OF THE ANCHOR

Limiting equilibrium methods can also be used to determine the position required for the back of an anchor to satisfy external stability requirements. Limiting equilibrium programs allow the user to evaluate the factor of safety for an anchored wall with a specific geometry and ground anchor length. Multiple analyses can be conducted to determine the position required for the back of the anchor to achieve a specific factor of safety.

For a specific anchored wall with a predefined geometry and anchor length, several trial failure surfaces are passed through the back of the anchor to find the critical failure surface and the minimum factor of safety (Figure 50a). If the failure surface intersects the soldier beams, their resistance also can be included in the evaluation for the factor of safety. If the factor of safety is too low, a new position of the anchor can be selected, and the analyses repeated.

Conducting multiple stability analyses for failure surfaces passing through several positions represents a design option for determining the position necessary for the back of the anchor. A grid of points is constructed near the anticipated position for the back of the anchor. Minimum factors of safety are determined for each point (Figure 50b). Contours for factors of safety can be constructed and used to determine the position required for the anchor to achieve a desired factor of safety (Figure 50c). Figure 50c illustrates how the position of the back of the ground anchor affects the factor of safety. This plot can be constructed for a specific site and used to identify the required position for the back of the anchors for cuts in cohesive soils, cohesionless soils, and layered soils.

Several analyses have been conducted with the limiting equilibrium methods to identify the position required for the back of the anchors for a 10-m-high cut in cohesionless soil ($c = 0$). The results of these analyses are shown in Figure 51a for potential failure surface passing through the bottom of the excavation (corner failure), and in Figure 51b for potential failure surfaces passing below the bottom of the excavation (base failure). No resistance from the soldier beams was assumed. Contours are labeled as mobilized friction angles from 20° to 40° . These contours represent a factor of safety equal to one for each mobilized friction angle. The factor of safety for specific site conditions can be determined by varying anchor geometry to determine ϕ_{mob} . The factor of safety is then determined as the ratio of $\tan(\phi_{avail}) / \tan(\phi_{mob})$.

Results of GPSSP are compared with results of the force equilibrium method developed in Chapter 3. The GPSSP employed Spencer's method to determine the factor of safety (and mobilized friction angle). Stability analyses were conducted for failure surfaces passing through points on a grid pattern extending horizontally from 6 m to 20 m from the vertical face of the wall, and from 2 m to 8 m above the bottom of the cut. Contours of mobilized friction angles developed from the stability analyses (using the Spencer's method) are shown with a solid line. Superimposed on the same graph are contours of mobilized friction angles determined from a force equilibrium method (developed in the previous chapter). The shapes and

positions of the two sets of contours compare favorably for failures passing through the bottom of the excavation (Figure 51a). These results suggest that the two methods predict similar requirements for the back of the anchor.

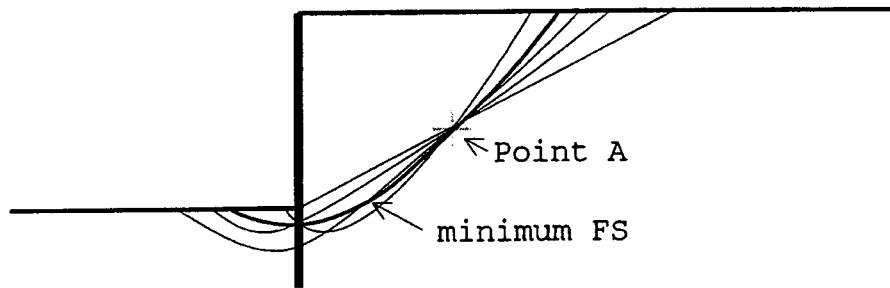
Contours for failure surfaces allowed to develop below the bottom of the excavation (Figure 51b) show similar trends for both the GPSSP and for the force equilibrium method. The agreement between the two methods is very close for mobilized friction angles above 30° , but the GPSSP predicts slightly shorter total anchor lengths for friction angles below 30° . Overall, however, the predictions for anchor length made with the GPSSP and the force equilibrium (Chapter 3) method agree within 0.5 m for soil friction angles above 25° .

Figure 52a–d illustrate the effect of analysis method on the required position of the back of the anchor. Four different equilibrium methods were used with the GPSSP (Corps of Engineers' method, Lowe and Karafiath, Janbu, and Spencer's method, respectively). Predictions were made for a cut in sand, allowing the failure surface to pass beneath the bottom of the cut. Results for each method are shown on separate graphs as solid contour lines for mobilized soil friction angles between 20° and 40° . Also shown on each graph are dotted contour lines that represent results from the force equilibrium method (Chapter 3).

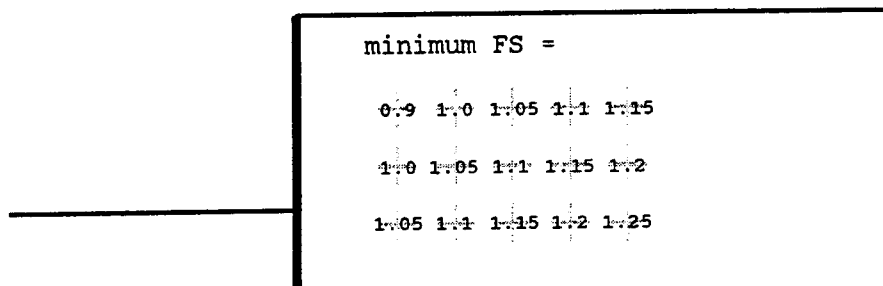
The GPSSP predictions using the Corps of Engineers' method are shown in Figure 52a. The required distance to the back of the anchor is similar for the two prediction methods for ϕ_{mob} of 35° and greater. However, predictions for the two methods disagree as much as 3 m for ϕ_{mob} of 20° . The different predictions are due to differences in assumptions used to solve the equilibrium equations and the difference in the assumed shape of the failure surface. The Corps of Engineers' method assumes a constant inclination for the interslice forces (for this case = 0°) for both the active and passive portions of the potential failure surface and assumes a planar shape for the active and passive portion of the soil, while the force equilibrium method (Chapter 3) uses a log spiral for the shape of the passive wedge and assigns an interslice force angle equal to ϕ_{mob} between the active and passive wedge.

Predictions for determining the distance to the back of the anchor using the GPSSP and the Lowe and Karafiath method (Figure 52b) are similar to results using the Corps of Engineers' method. Predictions between the Lowe and Karafiath method and the force equilibrium method are similar for ϕ_{mob} of 35° and greater, but diverge for ϕ_{mob} less than 30° . The differences between the two predictions result from different assumptions for the passive wedge and for the interslice force angles, as discussed above.

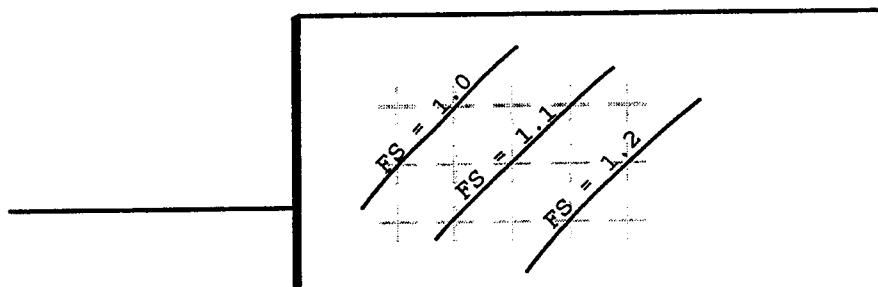
Predictions for distance required for the back of an anchor using the GPSSP and Janbu's method (Figure 52c) are in close agreement with those of the force equilibrium method (Chapter 3) for ϕ_{mob} between 20° and 40° .



a) Search for surface with a minimum factor of safety that passes through Point A



b) Summary of the results from several searches through many points



c) Interpolated contours for factor of safety as a function of the position of the failure surface

FIGURE 50
Determination of the Position Required for the Back of the Anchor to Satisfy External Stability

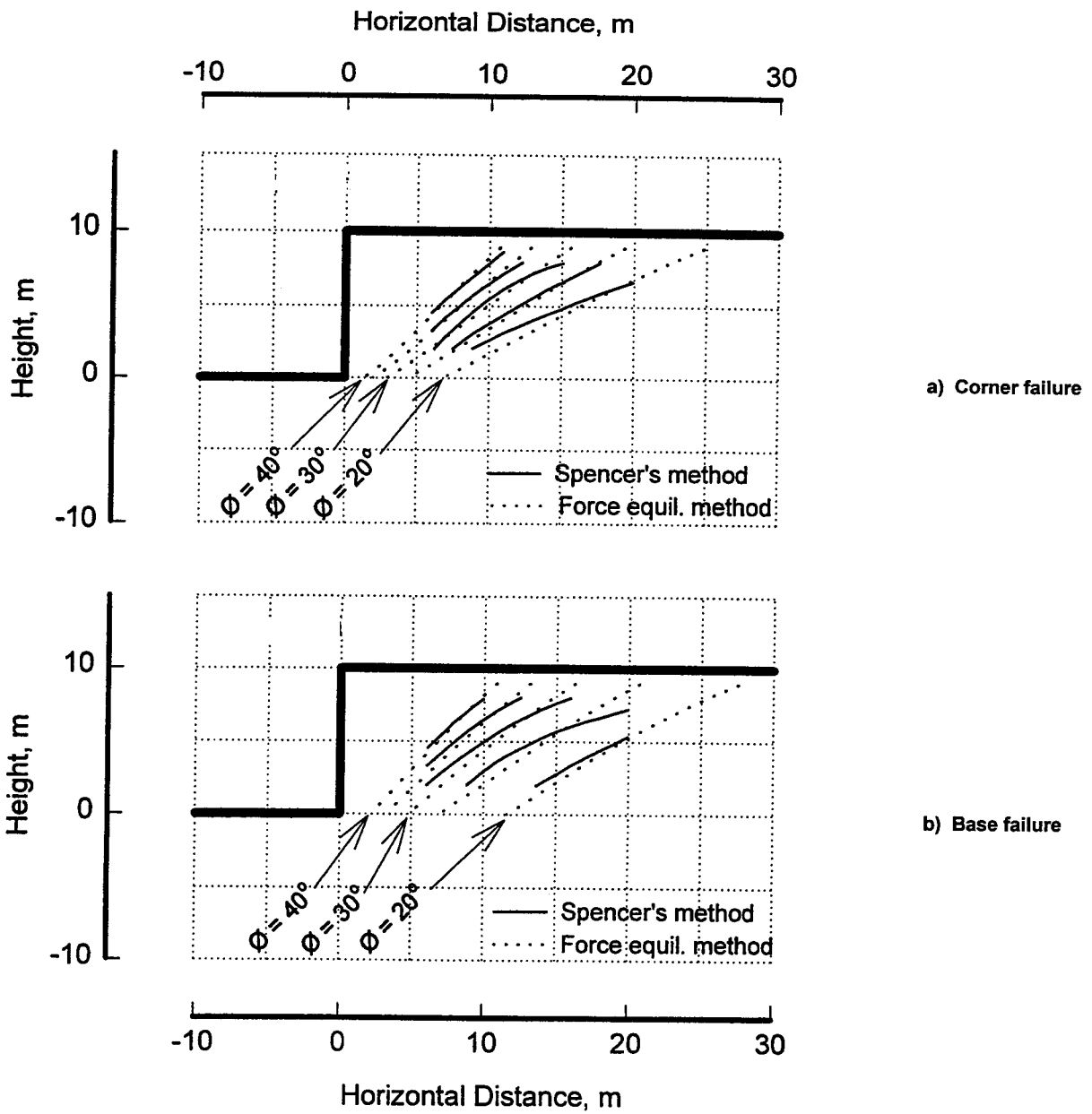


FIGURE 51
Position Required for the Back of the Anchor —
Spencer's Method and Force Equilibrium Method

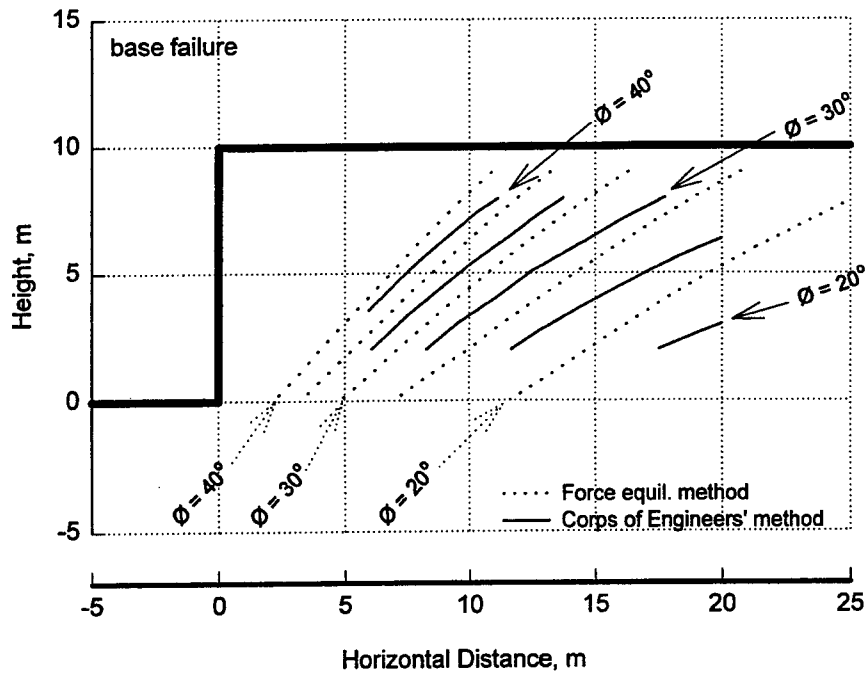


FIGURE 52a
Position Required for Back of the Anchor — Comparison of Corps of Engineers' Method and Force Equilibrium Method

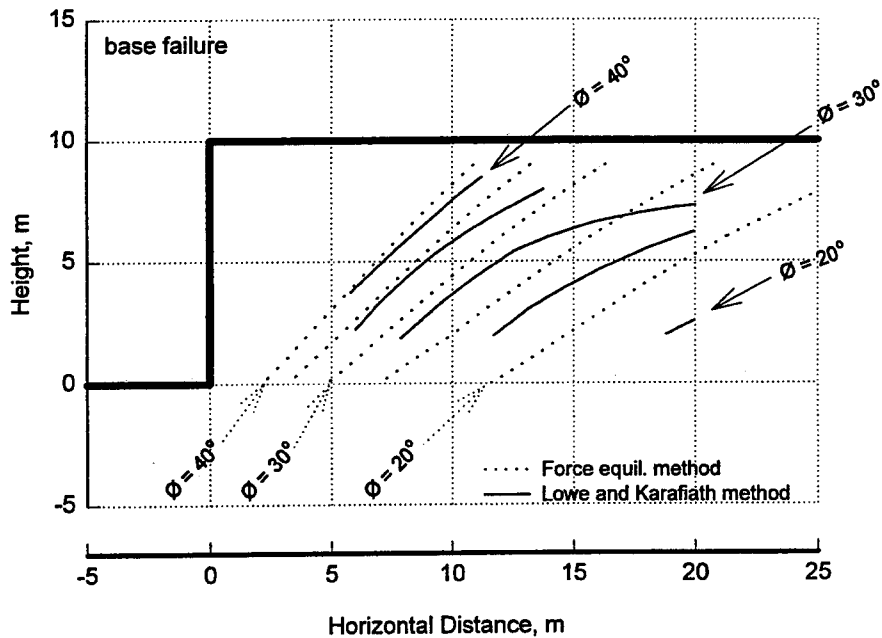


FIGURE 52b
Position Required for Back of the Anchor — Comparison of Lowe and Karafiath Method and Force Equilibrium Method

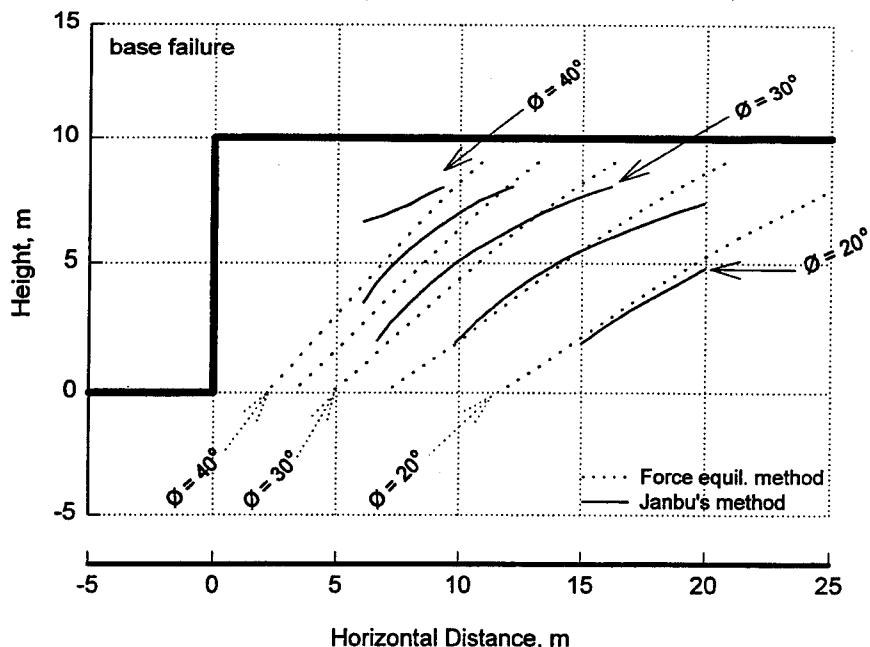


FIGURE 52c
Position Required for Back of the Anchor — Comparison
of Janbu's Method and Force Equilibrium Method

4.5 USE OF GPSSP FOR DETERMINING STABILITY FOR FAILURE SURFACES THROUGH THE ANCHOR BOND LENGTH

Methods for determining the factor of safety for failure surfaces passing in front of and behind the anchor bond zone have been discussed in the previous sections. Discussed herein are details of how GPSSP can be used to determine the factor of safety for failure surfaces passing through the anchor bond length.

The determination of the factor of safety for a failure surface passing through the anchor bond zone requires consideration of load transfer along the ground anchor. Consider the case of a failure surface passing in front of the anchor bond zone. The full ground anchor load contributes to the stability of the wall because the anchor bond zone is behind the failure surface. Conversely, no anchor force contributes to stability if the failure surface passes behind the anchor bond zone because the load at the face of the wall and at the top of the anchor bond zone are equal and opposite (and cancel each other out). However, if the failure surface passes

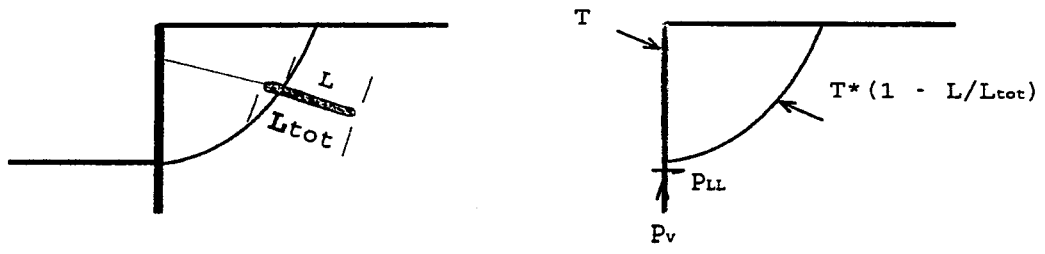
through the anchor bond length, only a portion of the total anchor load will contribute to stability. The portion of the anchor load depends on the length of the anchor bond length that lies beyond the failure surface and its load-transfer characteristics.

4.5.1 Assumptions Necessary for GPSSP Analyses

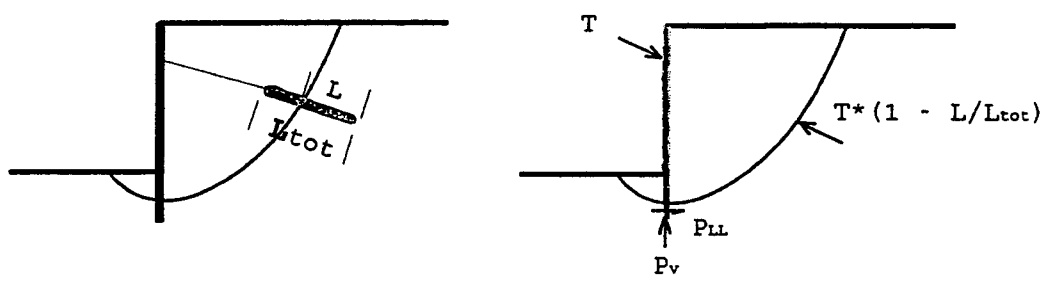
GPSSP can be used to determine the stability of an anchored wall system with the failure surface passing through the anchor bond zone; however, several assumptions are required. The first assumption is used to define load transfer along the anchor bond zone. If the soil provides equal resistance to pullout along the length of the anchor bond zone, then the load in the anchor varies linearly from the anchor load at the front of the anchor, to zero at the back of the anchor. The variation in load along the length can be expressed as equal to $T*(1 - L/L_{tot})$, where L_{tot} is the anchor bond length, L is the length of the anchor behind the failure surface, and T is the total ground anchor load.

The second assumption identifies the lateral load provided by the soldier beams. If the failure surface intersects the soldier beams, their contribution also can be included in the GPSSP analyses. Methods to quantify the contribution due to lateral capacity are identical to those described earlier in this chapter under the section “Toe Resistance.” Three cases are illustrated in Figure 53 where the failure surface passes through the bottom corner of the excavation, below the bottom of the cut, and below the tip of the soldier beam.

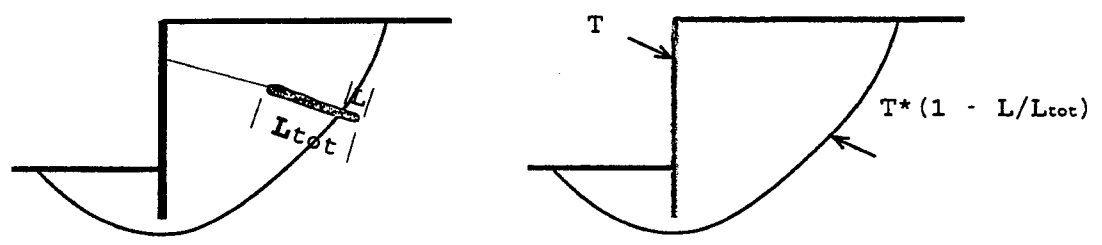
The third assumption requires defining the inclination of the external force supporting the face of the wall. The inclination is difficult to assess and depends on axial load transfer along the wall, below the wall, and at the tip of the soldier beam. If the axial capacity of the beam exceeds the vertical component of the load carried by the soldier beam, then the external force supporting the face will be either horizontal or inclined upward.



a) Failure surface passing through corner



b) Failure surface below corner and above pile tip



c) Failure surface passing below pile tip

FIGURE 53
Failure Surface Passing Through the Anchor Bond Zone

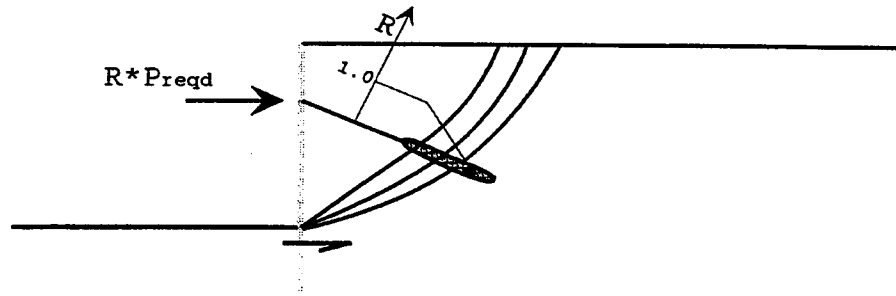
4.5.2 Simplified GPSSP Analyses — Modeling Options

Simplified assumptions are used to conduct GPSSP analyses for failure surfaces passing through the anchor bond length. Many assumptions are identical to those used for GPSSP analyses for failure surfaces passing in front of the anchor bond zone. Three options for modeling the anchored wall and the anchor bond length are given.

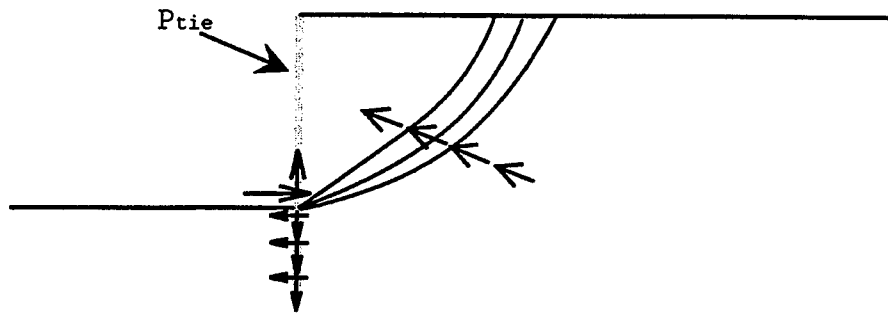
The first method for modeling an anchored wall for analysis with a GPSSP is shown in Figure 54a. The vertical loads along the wall are assumed to oppose each other, so the resultant load on the soil mass is horizontal. Lateral loads from the soldier beams are included if the failure surface intersects them. The horizontal force on the face of the wall is proportional to the location where the failure surface intersects the anchor. A load reduction factor, R , varies linearly from 1.0 at the front of the anchor bond zone to 0.0 at the back of the anchor. Thus, if the failure surface intersects the middle of the anchor bond zone, the factor R is 0.5, and one-half of the anchor force is applied to the wall. This method has the advantage that, as the failure surface approaches the front of the anchor bond zone, the solution will converge with the solution for determining P_{reqd} as presented earlier in this chapter. This method has the disadvantage that few GPSSP methods currently can model a force dependent on the location of the failure surface.

A second means to conduct GPSSP analyses for failure surfaces passing through the anchor bond zone is illustrated in Figure 54b. The anchor force is modeled as a point load on the face of the wall, and the anchor bond zone is modeled as an in-line series of point loads. The soldier beams also are modeled with lateral and axial forces to represent their contribution. The factor of safety is determined for the soil mass above the failure surface. All loads acting on or within the soil mass are considered in the equilibrium of the mass. Many GPSSP include the capability of placing point loads along a face or within the soil mass; however, considerable effort is required to model a wall in this manner. Furthermore, modeling the vertical loads along the wall and along the soldier beams requires knowledge of vertical and lateral load transfer along the beam.

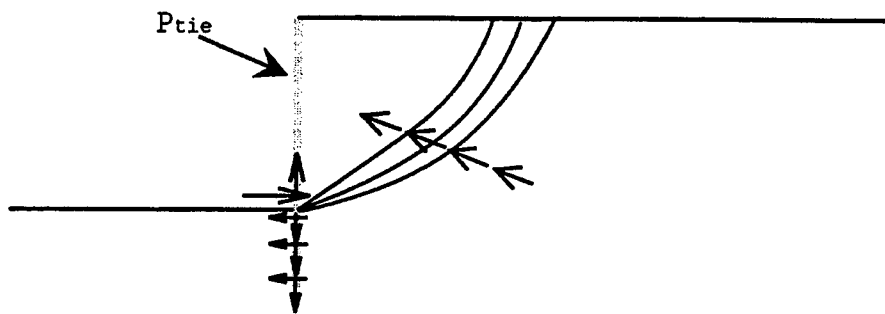
A third way to use a GPSSP to model failure through the anchor bond zone is to consider the anchor force as a high-capacity reinforcement (Figure 54c). The axial anchor force is modeled along the length of the anchor and the anchor bond zone. The axial force in the reinforcement is assumed to vary linearly from the full anchor capacity for all positions in front of the anchor bond zone, to zero force at the end of the reinforcement. Many GPSSP have the capability to include reinforcements in their analyses. Many GPSSP also have the ability to incorporate multiple layers of reinforcements in the analyses. Thus, multiple levels of anchors can be modeled. However, this model has the disadvantage that the reinforcement force is placed at the location of the anchor bond zone, and therefore, does not allow the anchor load to be more widely distributed over the potential failure plane. The resistance provided by the soldier beam also can be modeled as a reinforcement; however, estimates for the vertical and lateral resistances provided by the soldier beam are necessary.



a) Tieback load on wall—magnitude of load proportional to intersection of failure surface with tieback anchor



b) Modeling tieback, anchorage, and pile as opposing forces



c) Modeling tie and anchorage as a reinforcement

FIGURE 54
Means to Analyze Failure Surfaces Passing Through the Anchor Bond Zone

4.5.3 Results

Method 1 (Figure 54a) was used to determine the effect of failure surfaces through the anchor bond length. Analyses were conducted by modifying the FORTRAN code for the program UTEXAS2 (Wright, 1986) to allow the surface load on the vertical face to be proportional to the location where the failure surface intersected the anchor bond zone. Stability was assessed employing Spencer's method.

Analyses were performed for two anchored walls with the same soil properties and wall geometry but with different anchor bond lengths. The back of the anchor was identical for both walls (point C, Figure 55), but the location for the front of the anchor differed. The front of the anchor bond length for the first wall was just behind the critical failure surface (point A, Figure 55). The anchor load (P_{reqd}) and the location for the back of the anchor were adjusted so that the minimum factor of safety was 1.5 for failure at the front of the anchor, and 1.5 for failure at the back of the anchor. The front of the anchor bond length for the second wall was located halfway between the Rankine failure zone and the back of the anchor (point B, Figure 55). In summary, both anchors have identical capacities, but the second anchor developed capacity deeper in the ground over a shorter length.

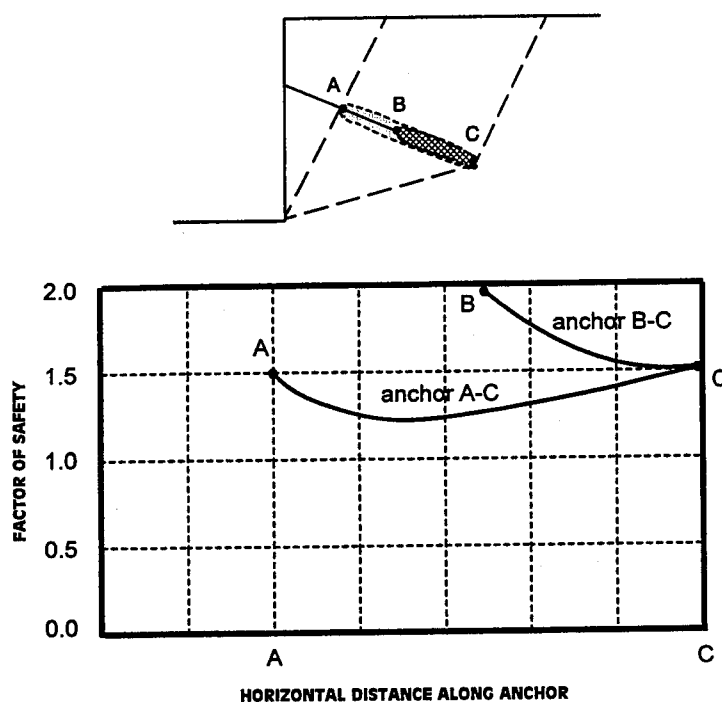


FIGURE 55
Variation of Factor of Safety for Failure Surfaces Passing Through a Long Anchor and a Short Anchor

Factors of safety were determined for specific points along the anchor bond zone for both walls (Figure 55). The factor of safety for the first wall is shown to decrease for failure surfaces that pass through the anchor bond zone. Factors of safety are shown to reduce to values near 1.2. The factor of safety for the second wall is 2.0 at the front of the anchor bond zone and decreases as failure surfaces intersect closer to the back of the anchor. However, the factor of safety never drops below 1.5.

The above analysis uses a load-transfer model that may not be realistic for most ground anchors. Normally the anchor bond length is selected using a working load-transfer rate of 50 percent of the ultimate load-transfer rate, and each anchor is load tested to an overload of 1.33 to verify capacity. As a result, the capacity of the anchor is normally much greater than the anchor design load. However, the study of failure surfaces passing through the anchor bond length shows that anchors that develop their load-carrying capacity near the front of the anchor bond length may not adequately contribute to the overall stability of the wall. In ground where better ground overlies poorer ground, the load-transfer characteristics of the anchors should be estimated, and GPSSP can be used to evaluate the stability of these walls.

4.5.4 Modeling Multiple Anchors with GPSSP

The factor of safety for failure surfaces can be evaluated when more than one row of ground anchors are used to support a wall. Failure surfaces may pass behind the backs of some anchors, in front of other anchors, and through the anchor bond lengths of some of the anchors. Failure surfaces passing through the anchors need some means to quantify the load that the anchors contribute to overall stability. The approach for proportioning the load can follow the same approaches discussed above for the single row of anchors, and illustrated in Figure 54a-c. Current capabilities of GPSSP may allow modeling the anchors as reinforcements, as surface loads, or as internal loads.

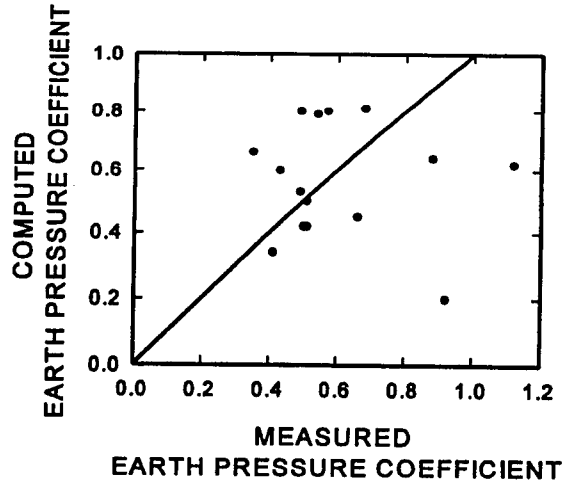
4.6 USE OF GPSSP FOR LATERAL LOADS IN SOFT TO MEDIUM CLAYS

Bishop's method was used to estimate the lateral load required to support the cuts that formed the basis of the soft to medium clay apparent earth pressure diagram (Figures 4 and 17). Cuts with $\gamma H/s_u < 4.5$ were not analyses. Flaate (1966) describes the wall and the soil profile at each cut in detail. A GPSSP was used to perform the limiting equilibrium analyses. The computer program allowed the actual soil profile to be modeled. Low-strength soils extended below the bottom of the excavation for many of the cuts. Factors of safety were determined for failure surfaces that went through the bottom corner of the excavation and through the base. Figure 56 compares the computed earth pressure coefficients from the limiting equilibrium analyses with the measured earth pressure coefficients reported by Flaate (1966). Earth pressure coefficients for limiting equilibrium analyses with a $FS_{strength} = 1$ and coefficients for analyses with a $FS_{strength} = 1.3$ were computed. The steps performed to compute the earth pressure coefficient were as follows:

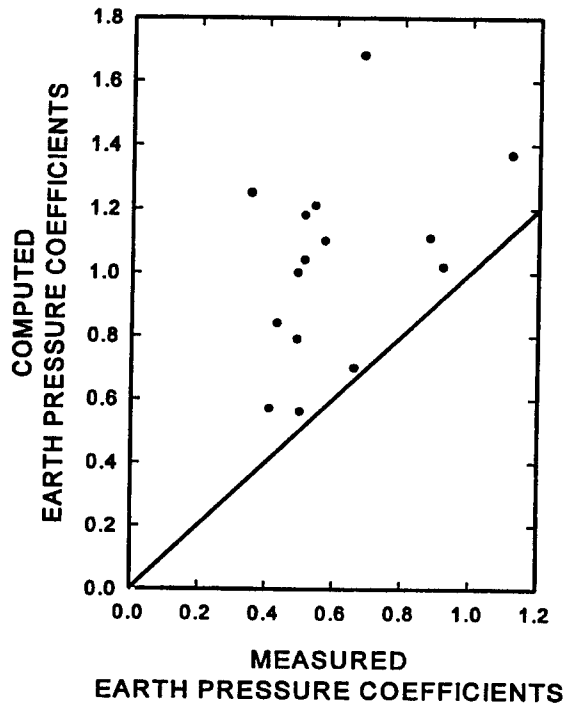
- Determine the lateral load required to support the cut for $FS_{strength} = 1$.
- Compute the earth pressure coefficient for $FS_{strength} = 1$ by dividing the lateral load by $0.5\gamma H^2$.
- Determine the lateral load required to support the cut for $FS_{strength} = 1.3$.
- Compute the earth pressure coefficient for $FS_{strength} = 1.3$ by dividing the lateral load by $0.5\gamma H^2$.

Figure 56a shows the measured and computed earth pressure coefficients for failure surfaces with $FS_{strength} = 1$. Except for four case histories, the lateral loads computed from the limiting equilibrium analyses were approximately equal to or greater than the measured load. The four exceptions were projects in Norway. Flaate (1966) reported that ground freezing probably increased the measured strut loads on two of these projects, and that one other project was flooded for 20 days during construction.

Figure 56b shows the earth pressure coefficients computed from the limiting equilibrium analyses with $FS_{strength} = 1.3$ versus the measured earth pressure coefficients for the cuts. A $FS_{strength} = 1.3$ was selected for these analyses since the limiting equilibrium studies discussed in Sections 3.2.2 and 3.3.4.4 indicated that the total load determined from the apparent earth pressure diagrams had a factor of safety with respect to undrained shear strength of between 1.25 and 1.40. Figure 56b shows that the lateral loads determined using $FS_{strength} = 1.3$ were greater than the measured loads on all the projects, including the four projects in Norway.



a) Limiting Equilibrium FS = 1



b) Limiting Equilibrium FS = 1.3

FIGURE 56
Comparison of Computed Earth Pressure Coefficients from Limiting Equilibrium Analyses with Measured Coefficients for Soft to Medium Clays

Figure 57 compares the computed earth pressure coefficients from the limiting equilibrium analyses ($FS_{strength} = 1.3$) with earth pressure coefficients back-calculated from the total load determined from the soft to medium earth pressure diagram (Figure 4). Earth pressure coefficients computed from the limiting equilibrium analyses are greater than those computed from the apparent earth pressure diagram when the failure surface extended below the bottom of the excavation more than 15 percent of the height of the cut. When the failure surface was near the bottom corner of the excavation, the earth pressure coefficients calculated from the apparent earth pressure diagram were greater than the earth pressure coefficients from the limiting equilibrium analysis. Figure 57 shows that lateral loads estimated using the soft to medium apparent earth pressure diagram include shallow base failures but the diagram does not account for deep base failures. Terzaghi, et al. (1996) recommended that the earth pressure coefficients from the soft to medium clay diagram be increased to account for deep-seated base failures following recommendations by Henkel (1971). Henkel used a limiting equilibrium method to determine the lateral earth pressure coefficient when deep-seated base failures could develop.

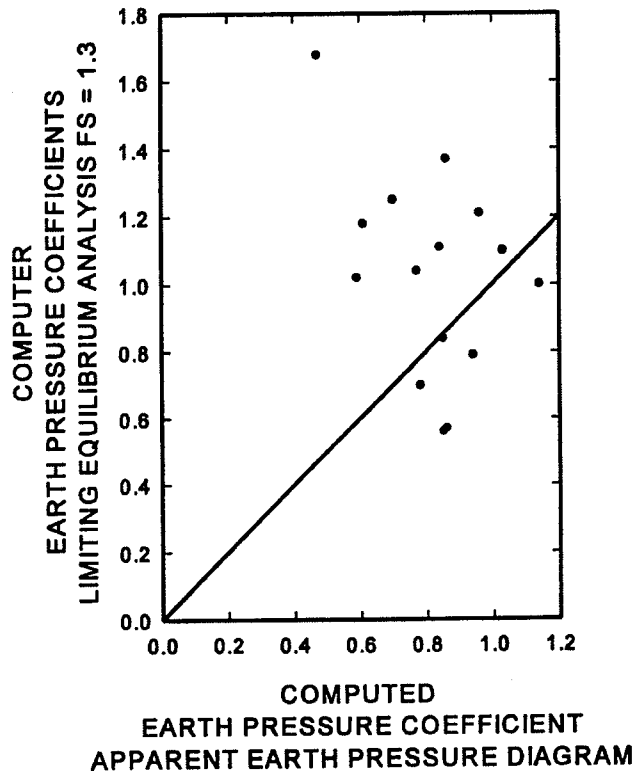


FIGURE 57
Comparison of Completed Earth Pressure Coefficients from Limiting Equilibrium Analyses with Computed Earth Pressure Coefficients from the Apparent Earth Pressure Diagram for Soft to Medium Clays

The limiting equilibrium study of cuts in soft to medium clays shows that:

- Bishop's method implemented in a GPSSP can be used to determine the lateral load required to support the cuts.
- A $FS_{strength} = 1.3$ applied to the undrained shear strength is satisfactory for determining the lateral load for the design of a wall.
- Lateral loads determined from a limiting equilibrium analysis may be less than those determined from the apparent earth pressure diagram if good ground is at the bottom of the excavation.
- GPSSP can determine the lateral loads required to support cuts with deep-base failure surfaces.

4.7 ILLUSTRATION OF SOME EFFECTS WITH GPSSP

An advantage of GPSSP is their general application for solving equilibrium for complicated boundary conditions. For example, by discretizing the soil above a potential failure surface into slices and applying equations of equilibrium, GPSSP can solve equilibrium for layered soils and can include the effects of groundwater, surface loads, internal loads, and seismic events. Circular and non-circular shapes can be used to generate potential failure surfaces. While these realistic conditions can be modeled by many GPSSP available today, these conditions are not directly included in the more empirical approaches for estimating anchor loads and anchor lengths. Thus, GPSSP can be used to determine the extra force or extra anchor length required to support a wall due to seepage toward the excavation. GPSSP can also be used to quantify ground anchor loads required to support cuts through layered soils, such as sand over clay. Finally, analyses can be conducted with circular and non-circular failure surfaces to investigate effect of the shape of the failure surface.

A GPSSP is used to illustrate the effect of two details:

- The effect of the position of the groundwater table (GWT) on stability of an anchored wall.
- The effect of using a circular or non-circular failure surface for estimating the stability of anchored walls.

4.7.1 Effect of Groundwater Table

A GPSSP was used to determine the effect of the position of the GWT on the stability of an anchored wall. Results of the analyses are summarized as contours defining the position required for the back of the anchor for soil strengths ranging from 20° to 40°.

GPSSP analyses were conducted for three positions of the groundwater table:

- A GWT well below the excavation.
- A horizontal GWT at the same elevation as the excavation.
- A GWT that results in seepage toward the wall.

The GWT reaches a height of 7.5 m above the excavation level at a distance of 30 m from the vertical face of the cut. The GWT rises from the excavation as a parabola. The shape for the GWT is based on recommendations by Casagrande (1937). The shapes assumed for the GWT at the excavation level and for the case of seepage toward the wall are shown in Figure 58a.

Stability analyses for the anchored wall were conducted using Spencer's method. Non-circular failure surfaces were used to determine the minimum factor of safety, and failure was allowed to pass either through the bottom corner of the excavation or through the base. Lateral resistance provided by the soldier beam was ignored. Results illustrating the effect of a GWT at the level of the excavation are shown in Figure 58b. Dotted contour lines are drawn for the case where the GWT is at the level of the excavation. Several contour lines are given for soil strengths between 20° and 40°. For comparison, solid line contours are shown to illustrate the required position for the back of the anchor when no GWT is present. The effect of the GWT is quite apparent for soil strengths of 30° and below. The contour lines for the GWT at excavation level require the back of the anchor to be placed at a horizontal distance from the wall greater than for the condition of no GWT.

Results of GPSSP analyses including effects of seepage (Figure 58c) show a significant effect on requirements for the back of the anchor. Horizontal distances required for the back of an anchor are significantly different for soil strengths of 35° and less. For conditions where the mobilized strength is 30° and the groundwater is seeping toward the wall, the back of the anchor must be placed a horizontal distance of 3 m to 6 m further back than if no GWT were present. Consequently, the location of the GWT and seepage can effect the geometry of the wall and of the anchors.

The effect of restricting the failure surface to a corner failure is shown in Figure 58d. Excavations to bedrock or firm strata may restrict the failure surface to pass through the bottom corner of the excavation, rather than allowing the failure surface to pass through the base. Shorter ground anchor lengths are required if a base failure cannot develop.

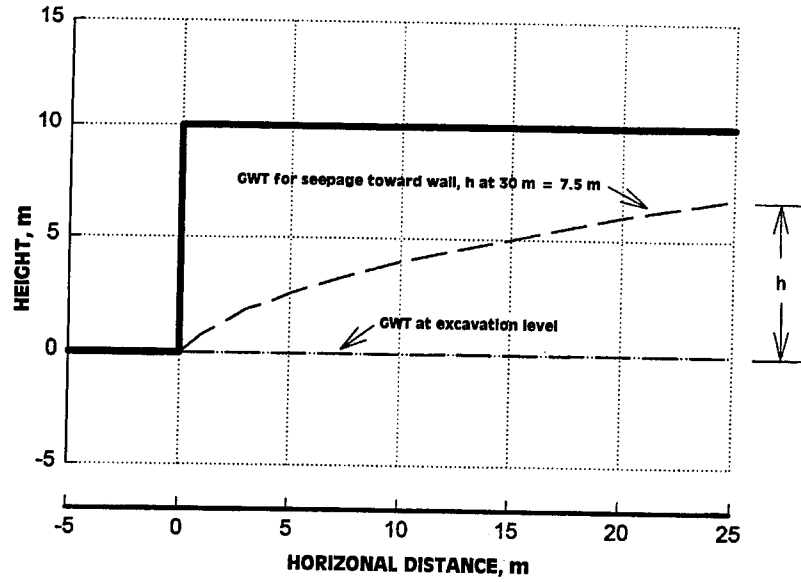


FIGURE 58a
Positions Assumed for the GWT in Stability Analysis

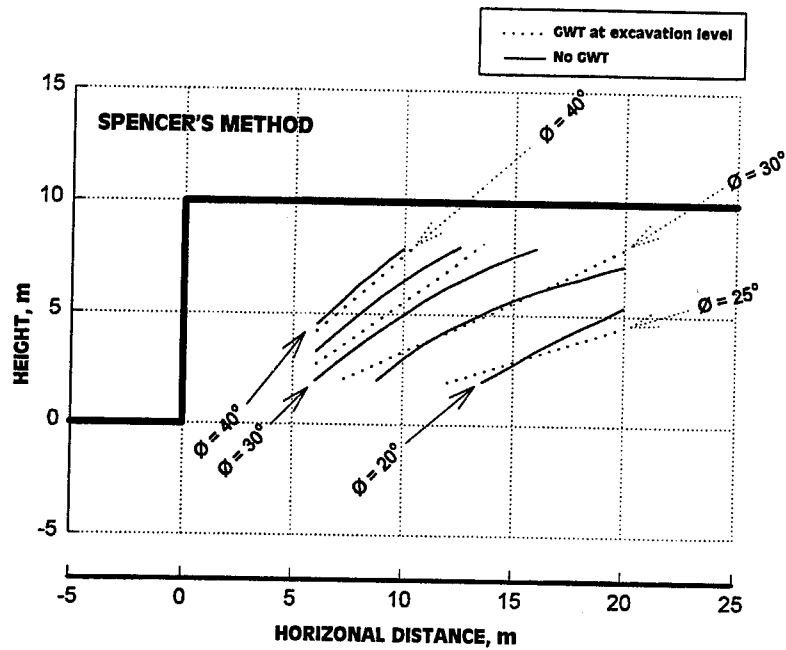


FIGURE 58b
Effect of Mobilized Soil Strength ($FS = 1$) on the Position Required for the Back of an Anchor (base failure) — GWT at Excavation Level

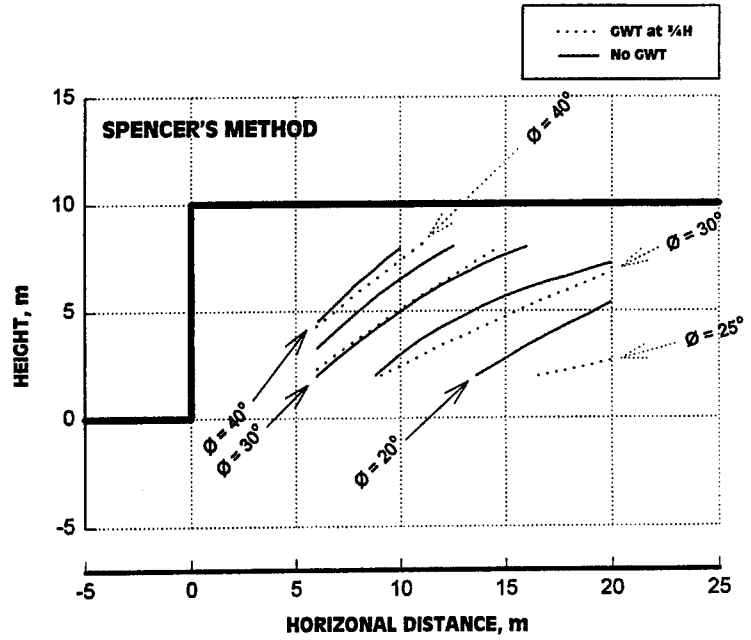


FIGURE 58c
Effect of Mobilized Soil Strength ($F_s = 1$) on the Position Required for the Back of an Anchor (base failure) — Effect of Seepage Toward the Wall

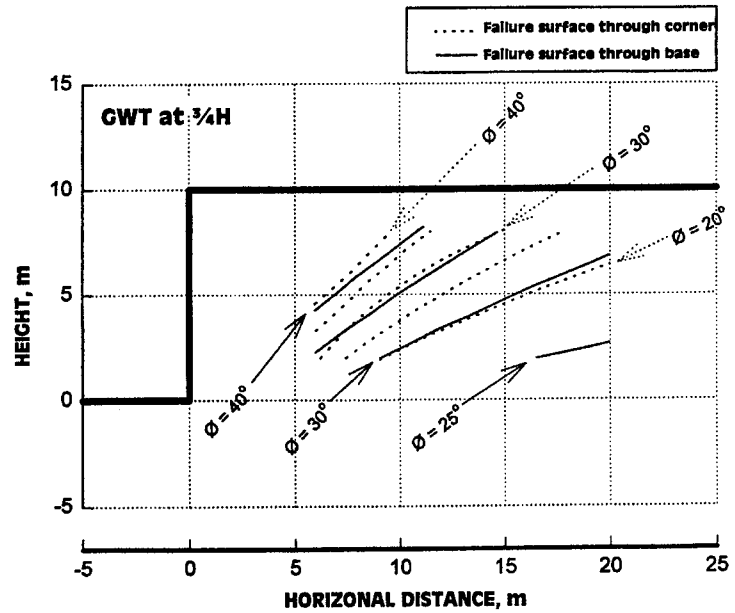


FIGURE 58d
Effect of Mobilized Soil Strength ($F_s = 1$) on the Position Required for the Back of an Anchor — Comparison of Results for Failure Through the Bottom of the Excavation Versus Failure Through Base for Seepage Toward the Wall

4.7.2 Effect of the Shape of the Failure Surface

Most GPSSP allow the user to search for the minimum factor of safety with circular failure surfaces. Many of the GPSSP allow the user to specify non-circular failure surfaces. However, few GPSSP maintain a robust algorithm that conducts a search for the minimum failure surface using a non-circular failure surface.

Non-circular failure surfaces possess some inherent advantages over circular surfaces. The non-circular failure surfaces can bend and distort to find the path of least resistance, and therefore the minimum factor of safety. If a layer is weak, the non-circular failure surface may distort to allow more of the failure surfaces to pass through the weaker layer. If a layer is strong, or a reinforcement is embedded in the soil, the non-circular surface may deform and take a shape to reduce its effect. However, circular failure surfaces are restricted in shape and cannot distort as readily to adapt to weak or strong areas in the soil mass. Thus, it is logical that GPSSP analyses conducted with circular failure surfaces will result in factors of safety greater than GPSSP analyses conducted with non-circular failure surfaces. The difference in results between the two shapes will depend on the specific case. Small differences for homogeneous soils are probable. Nevertheless, significant differences may occur for cases where the soil is heterogeneous and reinforcements (or ground anchors) are present. Shown in Figure 59 are results of GPSSP analyses using circular and non-circular failure surfaces. Analyses with non-circular failure surfaces clearly require the back of the anchor to be located at greater distances behind the wall than analyses with a circular failure surface.

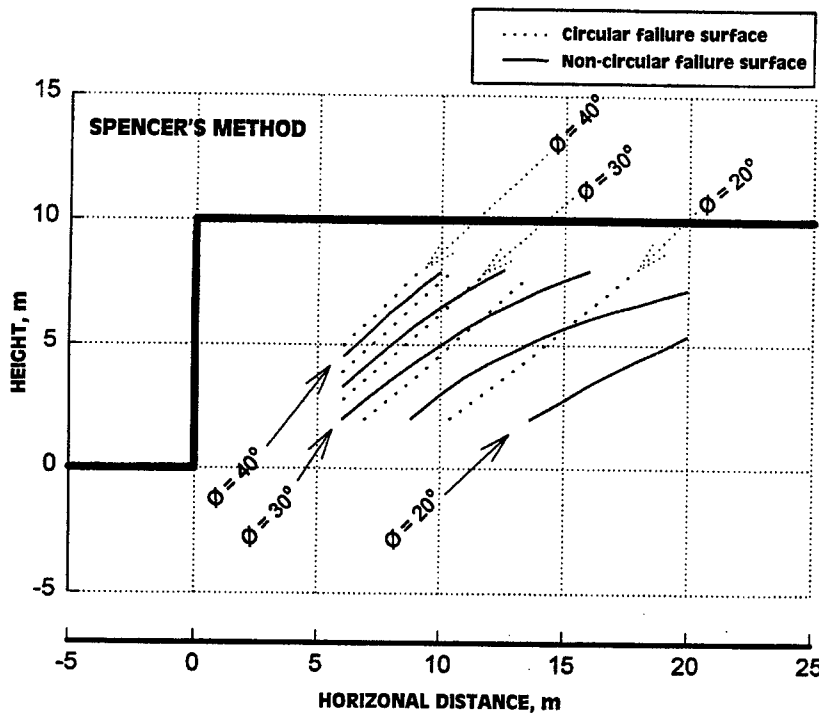


FIGURE 59
Effect of Mobilized Soil Strength ($F_s = 1$) on Position Required for the Back of the Anchor (base failure) — Comparison of Results for Non-circular and Circular Failure Surface

4.8 DISCUSSION

GPSSP are a powerful tool that can be applied to determine equilibrium for a general class of problems. GPSSP can accommodate layered soils, surface and internal loads, multiple groundwater tables, and circular and non-circular failure surfaces. Several methods of analyses are available that can satisfy force equilibrium, moment equilibrium, and overall equilibrium (force and moment equilibrium). Because the GPSSP are such a powerful tool, and because GPSSP have been used extensively for determining the stability of slopes, GPSSP also can be considered a powerful tool for analyzing anchored walls. It has been illustrated that the analyses with GPSSP usually agree with results from empirical methods. These empirical methods are based on simple theoretical relationships adjusted to agree with results measured in the field. However, it also should be stressed that the method of slices and analyses used with GPSSP have been developed for slopes and soil masses without concentrated anchor loads.

An anchored wall is characterized by an anchor and a concentrated load on the wall. The soldier beam interacts with the soil, mobilizing both lateral and vertical resistance. These loads are distributed to the soil mass in ways that cannot always be predicted. Therefore, the user should proceed with caution. While GPSSP have advantages, the results should be inspected to ensure the GPSSP results are reasonable. This may include inspecting the prediction of normal stress along the failure surface, the interslice force angle, the shape of the failure surface, and the location and orientation of the interslice force. Furthermore, results should be checked with current empirical methods or the force equilibrium method.

REFERENCES

- AASHTO-AGC-ARTBA Joint Committee Task Force 27 Report (1990). *Specification for Permanent Ground Anchors*, Washington, DC.
- Broms, B.B. and Bennemark, H. (1968). "Stability of Cohesive Soils behind Vertical Openings in Sheet Pile Walls," Contributions to the *Third Budapest Conference on Soil Mechanics and Foundation Engineering*, Budapest.
- Broms, B.B. (1988). "Design and Construction of Anchored and Strutted Sheet Pile Walls in Soft Clay," *Proceedings Second International Conference on Case Histories in Geotechnical Engineering*, June 1-5, St. Louis, MO, Invited Paper, Vol. 2, pp. 1515-1550.
- Casagrande, Arthur (1937). "Seepage Through Dams," *New England Water Works Assoc.*, Vol. 51, June 1937.
- Christian, J.T. (1989). "Design of Lateral Support Systems," *Proceedings of the Boston Society of Civil Engineers*, Boston.
- Coulomb, C.A. (1776). "Essai sur une application des règles des maximis et minimis à quelques problèmes de statique relatifs à l'architecture", *Mém. acad. roy. Près divers savants*, Vol. 7, Paris, 1776.
- Duncan, J.M. (1992). "State of the Art: Static Stability and Deformation Analysis," *Proceedings, Stability and Performance of Slopes and Embankments - II*, Geotechnical Special Publication No. 31, ASCE, pp. 222-266.
- Flaate, K.S. (1966). "Stresses and Movements in Connection with Braced Cuts in Sand and Clay," Ph.D. Thesis, University of Illinois, Urbana-Champaign, IL, 264 pp.
- Fredlund, D.G. and Krahn, J. (1977). "Comparison of Slope Stability Methods of Analysis," *Canadian Geotechnical Journal*, Vol. 14, No. 3, pp. 429-439.
- Henkel, David J. (1971). "The Calculation of Earth Pressures in Open Cuts in Soft Clays," *The Arup Journal*, Vol. 6, No. 4, pp. 14-15.
- Janbu, N., Bjerrum, L. and Kjaernsli, B. (1956). "Soil Mechanics Applied to Some Engineering Problems," in Norwegian with English summary, *Norwegian Geotechnical Publication 16*.
- Knapp, R.S. and Peck, R.B. (1941). "Open-cut Soil Pressures on Chicago Subway," *Engineering News Record*, Nov. 20, 1941, pp. 87-90.

REFERENCES

(continued)

- Kranz (1953). *Über die Verankerung von Spundwänden*, 2 Auflage, Mitteilungen aus dem Gebiete des Wasserbaues und der Baugrundforschung, Heft 11, Berlin: Wilh, Ernst & Sohn.
- Mueller, C. G., Long, J. H., Weatherby, D. E., Cording, E. J., Power III, W. F., and Briaud, J.L. (1998). *Summary Report of Research on Permanent Ground Anchor Walls*, Volume III Model-scale Wall Tests and Ground Anchor Tests, Report No. FHWA-RD-98-067, Federal Highway Administration, McLean, VA.
- NAVFAC (1982). *Design Manual DM-7.2, Foundations and Earth Structures*, Naval Facilities Engineering Command, Alexandria, VA.
- Ostermayer, H. (1977). "Practice on the Detail Design Application of Anchorages," *A Review of Diaphragm Walls*, Institution of Civil Engineers, London, pp. 55-61.
- Peck, R.B. (1969). "Deep Excavations and Tunneling in Soft Ground, State of Art Report," *7th ICSMFE*, Mexico City, pp. 225-290.
- Peck, R.B., Hanson, W.E., and Thornburn T.H. (1974). *Foundation Engineering*, John Wiley & Sons, New York.
- Ranke, A. and Ostermayer, H. (1968). "A Contribution to the Stability Calculations of Multiple Tiedback Walls" ("Beitrag zur Stabilitäts Untersuchung..."), *Die Bautechnik*, Vol. 45, No. 10, pp. 341-349.
- Schnabel, H.J. (1982). *Tiebacks in Foundation Engineering and Construction*, McGraw-Hill Book Company, New York.
- Taylor, D.W. (1948). *Fundamentals of Soil Mechanics*, John Wiley & Sons, New York.
- Terzaghi, K. and Peck, R.B. (1967). *Soil Mechanics in Engineering Practice*, 3rd Edition, John Wiley & Sons, New York.
- Terzaghi, K., Peck, R.B. and Mesri, G. (1996). *Soil Mechanics in Engineering Practice*, 3rd Edition, John Wiley & Sons, New York.
- Urzua, A. and Weatherby, D.E. (1998). *TB Wall - Anchored Wall Design and Analysis Program for Personal Computers*, Report No. FHWA-RD-98-093, Federal Highway Administration, McLean, VA.

REFERENCES

(continued)

- Wang, S.-T. and Reese, L.C. (1992). *COM624P: Laterally Loaded Pile Analysis Program for the Microcomputer, Version 2.0*, FHWA Report No. SA-91-048, Washington, DC.
- Weatherby, D.E. (1982). *Tiebacks*, Report No. FHWA Report No. RD-82/047, Federal Highway Administration, Washington, DC.
- Weatherby, D.E. (1997). *Design Manual for Permanent Ground Anchor Walls*, Report No. FHWA-RD-97-130, Federal Highway Administration, McLean, VA.
- Weatherby, D.E. (1998). *Summary Report of Research on Permanent Ground Anchor Walls, Volume IV: Conclusions and Recommendations*, Report No. FHWA-RD-98-068, Federal Highway Administration, McLean, VA.
- Weatherby, D.E., Chung, M., Kim, N.-K., and Briaud, J.L. (1998). *Summary Report of Research on Permanent Ground Anchor Walls, Volume II: Full-scale Wall Tests and a Soil-Structure Interaction Model*, Report No. FHWA-RD-98-066, Federal Highway Administration, McLean, VA.
- Wright, S.G., Kulhawy, F.H., and Duncan, J.M. (1973). "Accuracy of Equilibrium Slope Stability Analysis," *Journal of the Soil Mechanics and Foundation Division*, ASCE, Vol. 99, No. 10, pp. 783-791.
- Wright, S.G. (1986). "UTEXAS2 - A Computer Program for Slope Stability Calculations," Geotechnical Engineering Software HS86-1, Geotechnical Engineering Center, Bureau of Engineering Research, The University of Texas at Austin, TX.

